Received: 29 August 2022 | Revised: 13 December 2022 | Accepted: 24 December 2022

DOI: 10.1111/sapm.12560

STUDIES IN APPLIED MATHEMATICS WILEY

ORIGINAL ARTICLE

Nonconstant steady states and pattern formations of generalized 1D cross-diffusion systems with prey-taxis

Demou Luo[1,2] | **Qiru Wang**[1] | **Li Chen**[2]

[1]School of Mathematics, Sun Yat-sen University, Guangzhou, Guangdong, China

[2]School of Business Informatics and Mathematics, University of Mannheim, Mannheim, Baden-Württemberg, Germany

Correspondence
Li Chen, School of Business Informatics and Mathematics, University of Mannheim, Mannheim 68131, Baden-Württemberg, Germany.
Email: chen@math.uni-mannheim.de

Funding information
National Natural Science Foundation of China, Grant/Award Number: 12071491

Abstract

Cross-diffusion effects and tactic interactions are the processes that preys move away from the highest density of predators preferentially, or vice versa. It is renowned that these effects have played significant roles in ecology and biology, which are also essential to the maintenance of diversity of species. To simulate the stability of systems and illustrate their spatial distributions, we consider positive nonconstant steady states of a generalized cross-diffusion model with prey-taxis and general functional responses in one dimension. By applying linear stability theory, we analyze the stability of the interior equilibrium and show that even in the case of negative cross-diffusion rate, which appeared in many models, the corresponding cross-diffusion model has opportunity to achieve its stability. Meanwhile, in addition to the cross-diffusion effect, tactic interactions can also destabilize the homogeneity of predator–prey systems if the tactic interaction coefficient is negative. Otherwise, taxis effects can stabilize the homogeneity.

KEYWORDS
1D cross-diffusion systems with prey-taxis, general functional responses, nonconstant steady states, pattern formations

1 | INTRODUCTION

In mathematical biology and mathematical ecology, one of the significant topics is to discuss the long-term coexistence between two or more species. Particularly, it is important to study the long-term coexistence of predator–prey systems. It is renowned that biological diversity has become increasingly important at present such as reducing the risk of natural hazard, safeguarding natural resource (timber, water, and coal) security, and so on. Cross-diffusion systems in the last few decades have received the best treatment to simulate the spatial-temporal patterns by the scientists in many fields. In this work, we study the following strongly coupled cross-diffusion system without self-diffusion:

$$\begin{cases} \partial_t u = D_1 \partial_{xx}(u + duv) + F(u,v), & x \in (0,L),\ t > 0, \\ \partial_t v = \partial_x(D_2 \partial_x v - \chi \phi(u,v)\partial_x u) + G(u,v), & x \in (0,L),\ t > 0, \\ \partial_x u(x,t) = \partial_x v(x,t) = 0, & x = 0, L,\ t > 0, \\ u(x,0) = u_0(x),\ v(x,0) = v_0(x), & x \in (0,L). \end{cases} \tag{1}$$

The population densities of prey and predator are denoted by $u(x,t)$ and $v(x,t)$, respectively. D_1 and D_2 are both positive constants and stand for the diffusion rates of prey and predator. χ is a prey-taxis parameter. The reaction functions are given by F and G. The main purpose of this paper is to study the bifurcation analysis with respect to d and χ constants.

In this paper, we assume that $F(u,v)$, $G(u,v)$, and $\phi(u,v)$ fulfill $F, G \in C^4(\mathbb{R}\times\mathbb{R};\mathbb{R})$, $\phi \in C^3(\mathbb{R}\times\mathbb{R};\mathbb{R})$, and satisfy the following hypotheses:

(H1) $F(u^*,v^*) = G(u^*,v^*) = 0$ for some $u^* > 0$, $v^* > 0$: system (1) always possesses an interior (positive) constant equilibrium (u^*,v^*);
(H2) $F_u^* < 0\ G_v^* < 0$: the effect of crowding since the carrying capacity of environment is limited;
(H3) $F_v^* < 0\ G_u^* > 0$: the dynamical behavior of population since predators hunt preys,

where we use notations

$$F_u^* = \frac{\partial F}{\partial u}(u^*,v^*),\ F_v^* = \frac{\partial F}{\partial v}(u^*,v^*),\ F_{uv}^* = \frac{\partial^2 F}{\partial v \partial u}(u^*,v^*),\ \cdots \tag{2}$$

as the partial derivatives of F evaluated at (u^*,v^*) and the same for G, which are also applicable throughout the rest of this work.

Our main theoretical contribution utilizes for model (1) in its general form, and our numerical tests are delivered for this model comprising double Beddington–DeAngelis functional responses

or Beddington–DeAngelis and Tanner functional responses, that is,

$$F(u,v)=u-u^2-\frac{uv}{1+\alpha u+\beta v},\ \ G(u,v)=-dv+\frac{cuv}{1+\alpha u+\beta v},$$

or

$$F(u,v)=r_1u-bu^2-\frac{\delta uv}{1+\alpha u+\beta v},\ \ G(u,v)=r_2v-\frac{v^2}{\gamma u}. \tag{3}$$

Here, b, c, d, r_1, r_2, α, β, γ, and δ are all positive constants.

The multidimensional version of (1) reads

$$\begin{cases}\partial_t u=D_1\Delta(u+duv)+F(u,v), & x\in\Omega,\ t>0,\\ \partial_t v=\nabla\cdot(D_2\nabla v-\chi\phi(u,v)\nabla u)+G(u,v), & x\in\Omega,\ t>0,\\ \partial_{\mathbf{n}}u(x,t)=\partial_{\mathbf{n}}v(x,t)=0, & x\in\partial\Omega,\ t>0,\\ u(x,0)=u_0(x),\ v(x,0)=v_0(x), & x\in\Omega,\end{cases} \tag{4}$$

where Ω denotes a bounded domain in $\mathbb{R}^n(n\geq 1)$ with C^3 boundary $\partial\Omega$. The divergence operator can be described by $\nabla=(\frac{\partial}{\partial x_1},\frac{\partial}{\partial x_2},\dots,\frac{\partial}{\partial x_n})$ and the Laplace operator can be defined by $\Delta=\sum_{i=1}^{n}\frac{\partial^2}{\partial x_i^2}$. The outer normal derivative can be regarded as $\partial_{\mathbf{n}}$.

Model (4) can be utilized to model the temporal and spatial evolution process of population densities of predator and prey in a higher-dimensional space. It simulates the ecological case that predator species diffuse by a combination of advection and pure diffusion and prey species diffuse by cross-diffusion. Here, the advection is along the gradient of prey population density. Accordingly, when predator forages prey prey-tactically, we can term this directed movement as prey-taxis. D_1 and D_2 are two measurements which illustrate the tendency of random dispersals of prey and predator; the positive constant χ reflects the rate of intrinsic tactic interaction, and the bivariate function $\phi(u,v)$ describes the strength of tactic interaction with respect to u and v. Local kinetics functions $F(u,v)$ and $G(u,v)$ proposed by (3) are of the Beddington–DeAngelis and Tanner type functional responses which were introduced by Beddington,[1] DeAngelis,[2] and Tanner[3] almost simultaneously. Biologically speaking, the homogeneous Neumann boundary condition is applicable when and only when the habitat is hermitic; thus, the population migration across $\partial\Omega$ is impossible. The remaining coefficients in (4) possess the following meanings in biology or ecology: r_1 and r_2 are the intrinsic growth rates of prey and predator, respectively; α can be regarded as the degree of saturation for an alternative prey; β can illustrate the interference of predator; γ can be treated as the carrying capacity of natural environment for the predator with respect to food quality provided by prey; δ measures the consumption rate. We refer the reader to Ref. 4 and the references therein for further studies for Beddington–DeAngelis and Tanner systems and the model coefficients.

Without loss of generality for our theoretical research, we consider nonconstant steady states of system (1) in 1D comprising abstract kinetics functions, though our main results carry over to a higher-dimensional space. Particularly, we perform the numerical results of model (1) with Beddington–DeAngelis and Tanner functional responses (3). In addition, it is obvious via a direct

calculation that model (1) possesses a unique positive equilibrium (u^*, v^*), where

$$u^* = \frac{[r_1\alpha - b + r_2\gamma(r_1\beta - \delta)] + \sqrt{[r_1\alpha - b + r_2\gamma(r_1\beta - \delta)]^2 + 4br_1(\alpha + r_2\beta\gamma)}}{2b(\alpha + r_2\beta\gamma)}, \quad v^* = r_2\gamma u^*,$$

or

$$u^* = \frac{\alpha d + \beta c - c + \sqrt{(\alpha d + \beta c - c)^2 + 4\beta c d}}{2\beta c}, \quad v^* = \frac{c(1 - u^*)u^*}{d}. \tag{5}$$

In Section 5, we, for double Beddington–DeAngelis functional responses, still postulate that

$$c > d(1 + \alpha), \tag{6}$$

which is necessary for ensuring $u^* < 1$ and $v^* > 0$, that is, the existence of a positive equilibrium.

1.1 | Systems without cross-diffusion and prey-taxis

For planar differential systems (two-component predator–prey ordinary differential equation (ODE) models), if they possess a unique interior equilibrium, we generally postulate that global stability and local stability of these equilibria are equivalent. As proved by Hsu and Huang,[5] this hypothesis can be valid for the corresponding ODE model. In 2018, Luo [6] constructed a transformation $w = \frac{y}{x}$ to prove the global stability of the equilibrium by utilizing scalar parabolic techniques such as comparison principle and iteration method. Unfortunately, it is verified in Ref. 7 that global stability and local stability are not equivalent generally for the corresponding ODE model. It is spectacular that the researchers in Ref. 7 proposed a detailed bifurcation analysis, that is, the presence of branch G of two limit cycles embracing the interior equilibrium which possesses local stability and presence of a bifurcating branch S of semistable limit cycles. In 1988, two mathematicians and an ecologist considered a temperature-dependent model for predator–prey mite outbreak interactions on fruit trees,[8] and their numerical tests have been confirmed due to the coexistence of persistent oscillations and stable equilibrium. For further bifurcation analysis, the reader can refer to Refs. 9, 10 and the references therein.

If $d = \chi = 0$, model (4) degenerates to the corresponding pure reaction–diffusion model

$$\begin{cases} \partial_t u = D_1\Delta u + F(u, v), & x \in \Omega,\ t > 0, \\ \partial_t v = D_2\Delta v + G(u, v), & x \in \Omega,\ t > 0, \\ \partial_{\mathbf{n}} u(x, t) = \partial_{\mathbf{n}} v(x, t) = 0, & x \in \partial\Omega\ t > 0, \\ u(x, 0) = u_0(x),\ v(x, 0) = v_0(x), & x \in \Omega, \end{cases} \tag{7}$$

and it has been widely investigated by many biologists, ecologists, and mathematicians. As previously mentioned, the global asymptotic stability has been proved by Luo [6] under the circumstance of multidimensional bounded region. In addition, the permanence of two-component system is

possible due to the persistence of unique positive equilibrium.[4] The nonexistence and existence of nonconstant steady states can be derived by utilizing energy technique and degree approach and involving a priori estimates. In 2005, Peng and Wang [11] have demonstrated that model (7) with $F(u,v) = r_1u - bu^2 - \frac{\delta uv}{1+\alpha u+\beta v}$, $G(u,v) = r_2v - \frac{v^2}{\gamma u}$, and $\beta = 0$ (the renowned Holling–Tanner system) possesses no interior nonconstant steady states if one of the following situations can be satisfied: D_1 is large or δ is small, or D_2 is large and $r_2\gamma < \frac{1}{\delta}$ or $\frac{1}{\delta} = r_2\gamma > r_1$. Nevertheless, system (7) with $\beta = 0$ exists positive nonconstant steady states if D_2 is large enough and the remaining coefficients must be controlled within a reasonable scope. It is easy to expand these parameter conditions in parallel for the discussion of (7). Two years later, they also proposed that the homogeneous equilibrium (u^*, v^*) of (7) with $\beta = 0$ has locally asymptotic stability when

$$\left(\frac{1}{\delta}\right)^2 + \frac{2(r_1 + r_2\gamma)}{\delta} + r_1^2 - 2r_1r_2\gamma \geq 0 \tag{8}$$

and it possesses global stability when the rest of parameters have been selected in a suitable interval. By applying an interesting iterative method, the global stability theorem has been improved by Qi and Zhu.[12] More precisely, Theorem 1 in Ref. 12 claims that the positive equilibrium possesses globally asymptotic stability when $d = d(x,t)$ is strictly continuous, bounded and positive in $\overline{\Omega} \times [0,\infty)$ and $\frac{r_1\gamma\delta}{r_1\delta+1} < 1$. Accordingly, under these circumstances, the nonexistence of nonconstant steady states has been proved. Hopf bifurcation and Turing instability of both partial differential equation (PDE) and ODE systems have been studied by Li et al.[13] A step further, they obtain presuppositions to guarantee the stability of the bifurcating periodic solution and decide the direction of bifurcation. In addition, bifurcation analysis, such as Hopf bifurcation and steady-state bifurcation, has been described by Ma and Li.[14] Traveling-wave analysis of (7) with $\beta = 0$ in 1D is released by Ghazaryan et al,[15] where fronts are structured by applying the theory of rotated vector fields and geometric singular perturbation theory. Finally, by utilizing a recent generalization of the entry–exit function, they have also constructed periodic traveling waves of relaxation oscillation type. We must point that there are abundant works on reaction–diffusion predator–prey models.

When $\beta > 0$, it means that the mutual interferences from predator will be considered. Consequently, we are convinced that it is useful and profound to simulate system (7) since it contains the former simulations and extends them.

1.2 | Cross-diffusion models with prey-taxis

With the fast developments of modern sciences, pure reaction–diffusion models could not meet demands to rapid renewal of techniques. There are numerous researches focus on other kinds of diffusive models to beyond traditional reaction–diffusion processes such as the well-known prey-taxis, Shigesada–Kawasaki–Teramoto (SKT) cross-diffusion[16] and advection in bio-mathematics. The general SKT cross-diffusion system is described by

$$\begin{cases} \partial_t u = \Delta[(D_1 + d_{11}u + d_{12}v)u] + F(u,v), \\ \partial_t v = \Delta[(D_2 + d_{21}u + d_{22}v)v] + G(u,v), \end{cases} \tag{9}$$

where D_i $(i = 1, 2)$ stand for the diffusion rates of species u or v; d_{ii} $(i = 1, 2)$ are the self-diffusion rates of species u and v, respectively; d_{12} and d_{21} are the cross-diffusion rates of species u and v, respectively. $F(u, v)$ and $G(u, v)$ can be treated as two local kinetics functions. $u(x, t)$ and $v(x, t)$ are the population densities of preys and predators in location x and at time t. At first, it was proposed in 1979 and utilized to simulate spatial segregation mechanisms of creatures in dynamics of population. Cross-diffusion effect illustrates the species flux generated by mutual interferences. From a particle standpoint, d_{12} and d_{21} may be negative and positive. In the same way, the population moves toward higher density of another population if the cross-diffusion rate is negative and the species tends to lower density of another species if the cross-diffusion rate is positive. Unfortunately, nearly all researches in biomathematics have a confusing hypothesis that $d > 0$ for convenience of discussion or realistic principle in biology.[17–23] Therefore, their models cannot illustrate various phenomena in a precise way. If all creatures are profit and avoid loss, then why there exist suicide phenomena? Profiting and avoiding loss is to survive, which contradicts suicide, and suicide is not a rare phenomenon. "The survival of the fittest," proposed by the renowned British biologist Darwin, is a slogan that virtually preempted all debate. Biologically speaking, death means elimination, particularly for the weak. For instance, walruses or lemmings would plan to kill themselves, which is termed as suicide clusters phenomena. In light of this, $d < 0$ can be used to explain abnormal or extreme phenomena in biology and ecology.[17,24]

Another apparent ecological property of predator is their capacity of detecting the distribution in space of prey, and then hunting their food in high density via taxis mechanism. In 1987, Kareiva and Odell [25] have first introduce the prey-taxis model. This complicated phenomenon is renowned to be significant in natural cybernetics. Sapoukhina et al [26] pointed out that prey can be obtained by predator under a lower level economic threshold. One significant theoretical issue in predator–prey relationship is to determine circumstances on the distributions in space and coexistence of predator and prey, especially for heterogeneous patterns. We need to indicate that taxis mechanism does not lie solely in predator–prey model. It also exists in chemotaxis, quantum physics, and so on. Chemotactically speaking, biological cells move along or against the concentration gradient of chemicals. The generalized reaction–diffusion model comprising prey-taxis can be performed as

$$\begin{cases} \dfrac{\partial u}{\partial t} = D_1 \Delta u + \chi_1 \nabla \cdot (u \nabla v) + F(u, v), \\ \dfrac{\partial v}{\partial t} = D_2 \Delta v - \chi_2 \nabla \cdot (v \nabla u) + G(u, v), \end{cases} \tag{10}$$

where $\chi_i > 0$ are the taxis coefficients of prey $(i = 1)$ and predator $(i = 2)$, respectively. The other coefficients or functions are the same as in SKT model (9). Mathematical researches and numerical simulations of these models have been proposing and improving quickly during the past two decades. From a mathematical standpoint, spread or directional migration of population can be simulated by cross-diffusion model or advection system by comprising prey's density gradient. In 1987, two American zoologists [25] introduced a mechanistic method, simulated as partial differential equations comprising advection effect and spatial diffusion, to describe and understand that the aggregation of predator can be impacted by restricted searching area. A great number of reaction–diffusion models have been introduced and studied to simulate predator–prey interactions with taxis effect from then on. For instance, by comprising different kinetic functions, systems with prey-taxis in the form of (4) have been discussed by several researchers (see Refs. 27–32). The researchers of these literatures devote to global existence, bifurcation

analysis, traveling waves, and pattern formations. Predator–prey cross-diffusion systems have been studied extensively by Refs. 33–37. There also exist numerous articles on two species chemotaxis systems,[38–40] three species (two-prey and one-predator, or one-prey and two-predator) systems with prey-taxis [32] and without prey-taxis.[41–44]

Consequently, it is theoretically significant and ecologically realistic to research the pattern formation of (4) in view of cross-diffusion effect and prey-taxis interaction, especially for the development course and pattern structure of the corresponding coexistent interior steady states which reveal fascinating spatial patterns. Furthermore, we will exhibit in Section 5 that cross-diffusion models with prey-taxis possess abundant patterns as indicated by Refs. 17, 45, 46 (chemotaxis systems with logistic growth). For more detailed references about chemotaxis, we refer readers to the review papers.[47, 48] To sum up, we need to take various factors into consideration when studying and simulating these biomathematical models.

1.3 | Volume-filling and group defense

The binary function $\phi(u, v)$ can illustrate the intension of tactic interaction, and it also acts a significant role in the spatial pattern formations of (1). In 2009, Lee et al[30] shows that positive spatial patterns generated by homogeneous solution will be inhibited by tactic interaction for $\phi^* = (u^*, v^*) > 0$. Recently, Wang et al[49] further demonstrates that patterns can be supported by tactic interaction for $\phi^* < 0$. It simulates an unambiguous type of naturally realistic predator–prey interactions of prey's swarm defense or volume–filling (avoiding chronic overcrowding) in predators. Volume-filling can be regarded as the hypothesis that predators would not move toward high-density regions. Accordingly, it avoids overcrowded situation. From a living organisms standpoint, readers are advised to refer to the relative works of Hillen and Painter[50, 51] and the references cited therein. To simulate this impact, we have to propose the following two assumptions:

(1) For any $v > 0$, we have $\phi(0, v) > 0$;
(2) For all $u > M_1$, $\phi(u, v) < 0$, where M_1 is a positive constant.

That is remarkable when compared with the simplest prey-taxis term $\chi\nabla \cdot (v\nabla u)$ (see Refs. 10, 17, 28, 52).

Another significant property of predator–prey models is the power of preys' group defense. It certainly depends on the large amount of them. Preys will be attacked by predator if the number of prey is not enough, but going overboard is kind of a turn off. Preys can also attack predators for keeping predators away from their area if the amount of predators is not enough. It means that the relationship between predator and prey is relative, that is, their statuses can be converted each other under certain conditions. To model this relationship, we need to suppose d can be negative. This defense behavior depends on population density may result in a transformation to repulsive effect at high population density by intuition. For group defense mechanism, readers are advised to refer to the relative works[53, 54] and the references cited therein. To illustrate this mechanism, we have to introduce the following two assumptions:

(3) For any $u > 0$, we have $\phi(u, 0) = 0$;
(4) For all $v > M_2$, $\phi(u, v) < 0$, where M_2 is a positive constant.

We need to indicate that it is sufficient to postulate that $\phi^* < 0$ since we consider group defense or volume-filling for theoretical analysis. In addition, spatial-temporal patterns will occur and form one of positive solutions if the tactic effect is negative and strong. In Section 5, by setting $\phi(u, v) = uv(M - u)$, we describe the spatial-temporal pattern formations of our numerical examples.

1.4 | Structure of the paper and main results

The main results of this work are the existence and stability of positive nonconstant steady states of (1) under hypotheses (H1)–(H3). More precisely, we studied the influences of d on the χ bifurcation, which is explicitly given in Section 5.2, and vice versa χ for d bifurcation. The organization of the paper are as follows. First, we introduce linear stability of the unique interior equilibrium (u^*, v^*) corresponding to (1) in Section 2. This theoretical analysis points out that cross-diffusion effect can also stabilize the positive equilibrium when the cross-diffusion is repulsive ($d > 0$) or attractive ($d < 0$). This contains and extends the work of Li,[17] where the positivity of d is needed. In addition, if $d = 0$, we can observe that taxis interactions also have similar influence generated from swarm defense of prey and volume-filling of predator, that is, prey-taxis destabilizes the positive equilibrium if $\chi\phi(u, v) < 0$ (prey-taxis is repulsive), and taxis effect stabilizes predator–prey interaction (see Ref. 30) if $\chi\phi(u, v) > 0$ (prey-taxis is attractive). This contains and extends the research of Lee et al.[29] In Section 3, we conduct the bifurcation analysis and obtain the existence of nonconstant steady states of (1) by treating d and χ as a bifurcation parameter. Section 4 gives a detailed analysis about stability of those positive bifurcating solutions. Section 5 proposes several numerical examples of (1) with Beddington–DeAngelis and Tanner functional responses to describe and verify our main results. Finally, we give a conclusion of the current theoretical results and propose discussions for future research projects.

2 | LINEARIZED INSTABILITY DRIVEN BY CROSS-DIFFUSION AND PREY-TAXIS

For studying the spatial-temporal pattern formations of generalized 1D system (1), we utilize a technique which is originally applied to analyze the homogeneous solutions' stability. By the transformation $(U, V) = (u - u^*, v - v^*)$, one gets the approximative system

$$\begin{cases} U_t \approx D_1(1 + dv^*)U_{xx} + D_1 du^* V_{xx} + F_u^* U + F_v^* V, & x \in (0, L),\ t > 0, \\ V_t \approx D_2 V_{xx} - \chi\phi^* U_{xx} + G_u^* U + G_v^* V, & x \in (0, L),\ t > 0, \\ U_x(x, t) = V_x(x, t) = 0, & x = 0, L,\ t > 0. \end{cases} \tag{11}$$

Here and throughout the rest part of this work, we define $\phi^* = \phi(u^*, v^*)$ for convenience. Accordingly, we can derive the stability matrices via (11) as follows:

$$M_k = \begin{pmatrix} -D_1(1 + dv^*)\left(\frac{k\pi}{L}\right)^2 + F_u^* & -D_1 du^*\left(\frac{k\pi}{L}\right)^2 + F_v^* \\ \chi\phi^*\left(\frac{k\pi}{L}\right)^2 + G_u^* & -D_2\left(\frac{k\pi}{L}\right)^2 + G_v^* \end{pmatrix}, \quad k \in \mathbb{N}, \tag{12}$$

and the homologous characteristic equation for μ can be performed as

$$\mu^2 - \mathrm{Tr}(M_k)\mu + \mathrm{Det}(M_k) = 0. \tag{13}$$

Here,

$$\mathrm{Tr}(M_k) = -[D_1(1+dv^*)+D_2]\left(\frac{k\pi}{L}\right)^2 + F_u^* + G_v^*, \tag{14}$$

and

$$\begin{aligned}\mathrm{Det}(M_k) =& \left(D_1(1+dv^*)\left(\frac{k\pi}{L}\right)^2 - F_u^*\right)\left(D_2\left(\frac{k\pi}{L}\right)^2 - G_v^*\right) + \left(D_1 du^*\left(\frac{k\pi}{L}\right)^2 - F_v^*\right)\\ &\left(\chi\phi^*\left(\frac{k\pi}{L}\right)^2 + G_u^*\right)\\ =& D_1D_2(1+dv^*)\left(\frac{k\pi}{L}\right)^4 - D_1(1+dv^*)G_v^*\left(\frac{k\pi}{L}\right)^2 - D_2F_u^*\left(\frac{k\pi}{L}\right)^2 + F_u^*G_v^*\\ &+ D_1du^*\chi\phi^*\left(\frac{k\pi}{L}\right)^4 + D_1du^*G_u^*\left(\frac{k\pi}{L}\right)^2 - \chi\phi^*F_v^*\left(\frac{k\pi}{L}\right)^2 - F_v^*G_u^*.\end{aligned} \tag{15}$$

Thanks to the hypothesis (H2), we can notice that $\mathrm{Tr}(M_k) < 0$ for each $k \in \mathbb{N}$ when $d > \frac{-(D_1+D_2)}{v^*D_1}$. Consequently, M_k possesses an eigenvalue $\mu(k)$ and $\mathrm{Re}(\mu(k)) > 0$ if and only if $\mathrm{Det}(M_k) < 0$.

Remark 1. From the condition $d > \frac{-(D_1+D_2)}{v^*D_1}$, we can discover that our work is entirely different from the present studies about cross-diffusion system. Almost all the existing literatures in mathematical biology have postulated that the cross-diffusion coefficient d is positive.[17, 24] Actually, in many of the models negative d is allowed to describe the aggregation effects.

It is well-known that the eigenvalues of (12) can determine the stability of (u^*, v^*). Then one gets the corresponding lemma.

Lemma 1. *Postulate the hypotheses (**H1**)–(**H3**) hold and $d \geq 0$. Define*

$$\chi_k = \frac{\left(D_1(1+dv^*)\left(\frac{k\pi}{L}\right)^2 - F_u^*\right)\left(D_2\left(\frac{k\pi}{L}\right)^2 - G_v^*\right) + \left(D_1du^*\left(\frac{k\pi}{L}\right)^2 - F_v^*\right)G_u^*}{\left(F_v^* - D_1du^*\left(\frac{k\pi}{L}\right)^2\right)\phi^*\left(\frac{k\pi}{L}\right)^2}, \quad k \in \mathbb{N}_+. \tag{16}$$

Then the following cases hold:

(1) *When $\phi(u^*, v^*) = 0$, the positive equilibrium (u^*, v^*) has local asymptotic stability;*

(2) *When $\phi(u^*, v^*) < 0$, the positive equilibrium (u^*, v^*) possesses local asymptotic stability for $\chi < \min_{k\in\mathbb{N}_+} \chi_k$ and it is unstable for $\chi > \min_{k\in\mathbb{N}_+} \chi_k$;*

(3) *When $\phi(u^*, v^*) > 0$, the positive equilibrium (u^*, v^*) possesses local asymptotic stability for $\chi > \max_{k\in\mathbb{N}_+} \chi_k$ and it is unstable for $\chi < \max_{k\in\mathbb{N}_+} \chi_k$.*

Proof. If both eigenvalues of (12) possess a negative real part for each $k \in \mathbb{N}_+$, then the positive equilibrium (u^*, v^*), with respect to (1), is stable. Conversely, if there exists a $k_0 \in \mathbb{N}_+$ to guarantee M_{k_0} having an eigenvalue with positive real part, then the positive equilibrium (u^*, v^*), with respect to (1), is unstable. $\mathrm{Det}(M_k)$ can be treated as a linear function with respect to χ for each $k \in \mathbb{N}_+$. Thus, we can perform $\mathrm{Det}(M_k)$ as

$$\mathrm{Det}(M_k) = \left(F_v^* - D_1 d u^* \left(\frac{k\pi}{L}\right)^2\right)\phi^* \left(\frac{k\pi}{L}\right)^2 (\chi_k - \chi). \tag{17}$$

We only need to prove case (3) since (1) and (2) can be regarded as the same discussion. Thanks to (H3), we have $F_v^* - D_1 d u^* (\frac{k\pi}{L})^2 < 0$ due to $d \geq 0$. By $\phi(u^*, v^*) > 0$ in case (3), we can obtain at once that the real part of one eigenvalue of M_k is positive if $\mathrm{Det}(M_k) < 0$. Let us put it another way, it means that $\chi_k - \chi > 0$. The proof is completed now. ■

Due to $F_v^* < 0$, we have that the cases $d > 0$ and $d = 0$ can be discussed together. Meanwhile, $\min_{k\in\mathbb{N}_+} \chi_k$ of case (2) and $\max_{k\in\mathbb{N}_+} \chi_k$ of case (3) are well-defined. $\phi(u^*, v^*) > 0$ is widely appreciated by researchers as pointed out by the widely appreciated work of Lee et al,[30] that is, the positive equilibrium can be stabilized by tactic interaction, which can also inhibit the spatial pattern formations. On the contrary, $\phi(u^*, v^*) < 0$ means that the positive equilibrium is destabilized by prey-taxis; accordingly, there is reason to believe that tactic interaction plays a significant role in the nontrivial pattern formation. Furthermore, we hope we can reveal the attractive effect ($\chi_k > 0$), the repulsive effect ($\chi_k < 0$) and their different impacts to system (1). Meanwhile, we note that the case $\chi_k \phi(u^*, v^*) < 0$ exists in both two situations, and consequently, the positive solution will be unstable if this situation occurs.

If $\chi_k < 0$ for each $k \in \mathbb{N}_+$, (u^*, v^*) always possesses asymptotic stability and $\phi(u^*, v^*) > 0$, we hope spatial-temporal patterns of system (1) can be formulated only when $\chi < 0$, which can be utilized to explain how the population density of prey affects the diffusion of predator. It is obvious that the repulsion of prey-taxis, case (2) or (3) in Lemma 1, favors the nonexistence or existence of nonconstant steady states. To sum up, the retreat of predator is closely related to the nontrivial pattern formations in predator–prey models from the point of view of advection interaction.[55]

As previously mentioned, when the cross-diffusion rate d is negative, system (1) also has its great relevance. For $d < 0$, we have the following lemma.

Lemma 2. *Postulate the hypotheses (**H1**)–(**H3**) hold. If $d < 0$ and $F_v^* > D_1 d u^* (\frac{\pi}{L})^2$, we have:*

(1) *When $\phi(u^*, v^*) = 0$, the positive equilibrium (u^*, v^*) has local asymptotic stability;*

(2) *When $\phi(u^*, v^*) < 0$, the positive equilibrium (u^*, v^*) possesses local asymptotic stability for $\chi > \max_{k\in\mathbb{N}_+} \chi_k$ and it is unstable for $\chi < \max_{k\in\mathbb{N}_+} \chi_k$;*

(3) *When $\phi(u^*, v^*) > 0$, the positive equilibrium (u^*, v^*) possesses local asymptotic stability for $\chi < \min_{k\in\mathbb{N}_+} \chi_k$ and it is unstable for $\chi > \min_{k\in\mathbb{N}_+} \chi_k$.*

Proof. The proof is similar to that of Lemma 1 and is omitted here. ■

Due to $D_1 du^*(\frac{\pi}{L})^2 = \max_{k\in\mathbb{N}_+} D_1 du^*(\frac{k\pi}{L})^2$ for $d < 0$, we have $F_v^* - D_1 du^*(\frac{k\pi}{L}) > 0$ for each $k \in \mathbb{N}_+$. It is essential to postulate that $F_v^* > D_1 du^*(\frac{\pi}{L})^2$ in Lemma 2 for the sign-preserving property of $\mathrm{Det}(M_k)$. Lemma 2 tells us that the dynamical behavior of preys is also a significant factor for the nontrivial pattern formations of predator–prey models. The cross-diffusion term $\partial_{xx}(duv)$ is termed attractive for $d < 0$, otherwise it is called repulsive ($d > 0$). From the point of view of biology, it is meaningful and interesting that the dynamics of prey is also impacted by the pressure of population densities from other species. It is easy to understand that d illustrates the tendency that the prey keeps away from the predator when it is positive. Conversely, $d < 0$ means that the prey tends to the predator for the stability of their system.

Based on the above arguments, we have reason to believe that the cross-diffusion rate d can be also used to discuss the spatial distributions of predator–prey models. Denote

$$d_k = \frac{-D_1 D_2\left(\frac{k\pi}{L}\right)^4 + (D_1 G_v^* + D_2 F_u^* + \chi\phi^* F_v^*)\left(\frac{k\pi}{L}\right)^2 - (F_u^* G_v^* - F_v^* G_u^*)}{(D_1 D_2 v^* + D_1 u^* \chi\phi^*)\left(\frac{k\pi}{L}\right)^4 - (D_1 v^* G_v^* - D_1 u^* G_u^*)\left(\frac{k\pi}{L}\right)^2}, \quad k \in \mathbb{N}_+. \tag{18}$$

We can derive the following two lemmas.

Lemma 3. *Assume the hypotheses (**H1**)–(**H3**) hold and $\chi > 0$. Then the following cases hold:*

(1) *When $\phi(u^*, v^*) = 0$, the positive equilibrium (u^*, v^*) has local asymptotic stability;*

(2) *When $\phi(u^*, v^*) < \frac{-D_2 v^*}{u^*\chi}$, the positive equilibrium (u^*, v^*) possesses local asymptotic stability for $d > \max_{k\in\mathbb{N}_+} d_k$ and it is unstable for $d < \max_{k\in\mathbb{N}_+} d_k$ if and only if $(D_2 v^* + u^*\chi\phi^*)(\frac{\pi}{L})^2 < (v^* G_v^* - u^* G_u^*)$;*

(3) *When $\phi(u^*, v^*) > \frac{-D_2 v^*}{u^*\chi}$, the positive equilibrium (u^*, v^*) possesses local asymptotic stability for $d < \min_{k\in\mathbb{N}_+} d_k$ and it is unstable for $d > \min_{k\in\mathbb{N}_+} d_k$.*

If $\chi = 0$ or $\phi(u^*, v^*) = \frac{-D_2 v^*}{u^*\chi}$, we obtain that the positive equilibrium (u^*, v^*) possesses local asymptotic stability for $d < \min_{k\in\mathbb{N}_+} d_k$ and it is unstable for $d > \min_{k\in\mathbb{N}_+} d_k$.

Proof. Suppose that both eigenvalues of (12) have a negative real part for each $k \in \mathbb{N}_+$. Then the interior equilibrium (u^*, v^*) with respect to (1) has stability. On the contrary, if there exists a $k_0 \in \mathbb{N}_+$ such that M_{k_0} has an eigenvalue and its real part is positive, then the interior equilibrium (u^*, v^*) with respect to (1), is unstable. $\mathrm{Det}(M_k)$ can be treated as a linear function with respect to d for each $k \in \mathbb{N}_+$. Thus, we can perform $\mathrm{Det}(M_k)$ as

$$\mathrm{Det}(M_k) = \left[(D_2 v^* + u^*\chi\phi^*)\left(\frac{k\pi}{L}\right)^2 + (u^* G_u^* - v^* G_v^*)\right] D_1\left(\frac{k\pi}{L}\right)^2 (d_k - d). \tag{19}$$

We only need to prove case (3) since (1) and (2) can be treated as the same consideration. Based on (H2) and (H3), we have $u^*G_u^* - v^*G_v^* > 0$. By $\phi(u^*, v^*) > \frac{-D_2 v^*}{u^*\chi}$ in case (3), we can obtain at once that the real part of one eigenvalue of M_k is positive if $\mathrm{Det}(M_k) < 0$. Let us put it another way, it means that $d_k - d > 0$. The proof is completed. ■

Lemma 4. *Suppose the hypotheses (**H1**)–(**H3**) hold and $\chi < 0$. Then, the following cases hold:*

(1) *When $\phi(u^*, v^*) = 0$, the positive equilibrium (u^*, v^*) has local asymptotic stability;*

(2) *When $\phi(u^*, v^*) < \frac{-D_2 v^*}{u^*\chi}$, the positive equilibrium (u^*, v^*) possesses local asymptotic stability for $d < \min\limits_{k\in\mathbb{N}_+} d_k$ and it is unstable for $d > \min\limits_{k\in\mathbb{N}_+} d_k$;*

(3) *When $\phi(u^*, v^*) > \frac{-D_2 v^*}{u^*\chi}$, the positive equilibrium (u^*, v^*) possesses local asymptotic stability for $d > \max\limits_{k\in\mathbb{N}_+} d_k$ and it is unstable for $d < \max\limits_{k\in\mathbb{N}_+} d_k$ when and only when $(D_2 v^* + u^*\chi\phi^*)(\frac{\pi}{L})^2 < (v^*G_v^* - u^*G_u^*)$.*

Proof. The proof is similar to that of Lemma 3. Hence we omit it. ■

3 | EXISTENCE OF NONCONSTANT POSITIVE STEADY STATES

By Crandall–Rabinowitz bifurcation theory[56] and its user-friendly version,[57] we discuss the existence of nonnegative nonconstant steady states for model (1).

3.1 | Local bifurcation around the positive constant steady state

More precisely, we consider interior nonconstant solutions of the undermentioned general model

$$\begin{cases} D_1(u + duv)'' + F(u, v) = 0, & x \in (0, L), \\ (D_2 v' - \chi\phi(u, v)u')' + G(u, v) = 0, & x \in (0, L), \\ u'(x) = v'(x) = 0, & x = 0, L. \end{cases} \tag{20}$$

Throughout the rest part of this paper, $\}'''$ refers specifically to the differentiation with respect to location x. By treating d and χ as bifurcation parameters, we discuss the impacts of cross-diffusion mechanism or tactic interaction on the formation of spatial-temporal patterns and perform (20) as the undermentioned form

$$\mathbf{F}(u, v, d, \chi) = 0,\ (u, v, d, \chi) \in \mathbb{X} \times \mathbb{X} \times \mathbb{R} \times \mathbb{R}, \tag{21}$$

where

$$\mathbf{F}(u, v, d, \chi) = \begin{pmatrix} D_1(u + duv)'' + F(u, v) \\ (D_2 v' - \chi\phi(u, v)u')' + G(u, v) \end{pmatrix} \tag{22}$$

and

$$\mathbb{X} = \{w \in H^2(0,L) | w'(0) = w'(L) = 0\}. \tag{23}$$

For χ fixed, we use the notation $\mathbf{F}_d(u,v,d) = \mathbf{F}(u,v,d,\chi)$ and $\mathbf{F}_\chi(u,v,\chi) = \mathbf{F}(u,v,d,\chi)$ for fixed d. In (23), $w = u$ or v. Some facts are collected as follows:

- $\mathbf{F}_d$ and $\mathbf{F}_\chi$ are two continuously differentiable mapping from $\mathbb{X}\times\mathbb{X}\times\mathbb{R}$ to $\mathbb{Y}\times\mathbb{Y}$, $\mathbb{Y} = L^2(0,L)$;
- $\mathbf{F}_d(u^*,v^*,d) = 0$ and $\mathbf{F}_\chi(u^*,v^*,\chi) = 0$ for any $d \in \mathbb{R}$ and $\chi \in \mathbb{R}$;
- It is obvious via a direct computation that, for any fixed $(\tilde{u},\tilde{v}) \in \mathbb{X}\times\mathbb{X}$, the Fréchet derivative of $\mathbf{F}_d$ or $\mathbf{F}_\chi$ is performed as

$$D_{(u,v)}\mathbf{F}_d(\tilde{u},\tilde{v},d) = D_{(u,v)}\mathbf{F}_\chi(\tilde{u},\tilde{v},\chi) = \begin{pmatrix} D_1(1+d\tilde{v})u'' + D_1 d\tilde{u}v'' + \tilde{F}_u u + \tilde{F}_v v \\ D_2 v'' - \chi(\tilde{\phi}u' + \tilde{u}'(\tilde{\phi}_u u + \tilde{\phi}_v v))' + \tilde{G}_u u + \tilde{G}_v v \end{pmatrix}, \tag{24}$$

where we utilize the tilde mark to define the value of the function achieved at $(\tilde{u},\tilde{v})$.

Define $\mathbf{e} = (u,v)^T$ and perform (24) into

$$D_{(u,v)}\mathbf{F}_d(\tilde{u},\tilde{v},d)(u,v) = D_{(u,v)}\mathbf{F}_\chi(\tilde{u},\tilde{v},\chi)(u,v) = \mathcal{M}_0\mathbf{e}'' + \mathcal{F}_0(x,\mathbf{e},\mathbf{e}'), \tag{25}$$

where

$$\mathcal{M}_0 = \begin{pmatrix} D_1(1+d\tilde{v}) & D_1 d\tilde{u} \\ -\chi\tilde{\phi} & D_2 \end{pmatrix}, \tag{26}$$

and

$$\mathcal{F}_0 = \begin{pmatrix} \tilde{F}_u u + \tilde{F}_v v \\ -\chi(\tilde{\phi}'u' + (\tilde{u}'(\tilde{\phi}_u u + \tilde{\phi}_v v))') + \tilde{G}_u u + \tilde{G}_v v \end{pmatrix}. \tag{27}$$

The operator in (24) is strictly elliptic if and only if $\mathcal{M}_0$ is positive-definite, that is,

$$\mathrm{Tr}(\mathcal{M}_0) = D_1(1+d\tilde{v}) + D_2 > 0 \ \text{ and } \ \mathrm{Det}(\mathcal{M}_0) = D_1 D_2(1+d\tilde{v}) + D_1\chi\tilde{\phi}d\tilde{u} > 0. \tag{28}$$

Moreover, Agmon's condition is satisfied with $\theta \in [-\frac{\pi}{2},\frac{\pi}{2}]$ in view of Remark 2.5 (case 2) in Ref. 57. Together with Theorem 3.3 and Remark 3.4 in Ref. 57, $D_{(u,v)}\mathbf{F}_d(\tilde{u},\tilde{v},d)$ or $D_{(u,v)}\mathbf{F}_\chi(\tilde{u},\tilde{v},d)$ stands for a Fredholm operator with index zero.

Now, we search for possible bifurcation values by verifying necessary conditions proposed by Crandall and Rabinowitz,[56] that is,

$$\mathbb{Z}(D_{(u,v)}\mathbf{F}_d(u^*,v^*,d)) \neq \{\mathbf{0}\} \ \text{ or } \ \mathbb{Z}(D_{(u,v)}\mathbf{F}_\chi(u^*,v^*,d)) \neq \{\mathbf{0}\}, \tag{29}$$

where $\mathbb{Z}$ means the null space of the corresponding linear operator. First, by setting $(\tilde{u}, \tilde{v}) = (u^*, v^*)$ in (24), one gets

$$D_{(u,v)}\mathbf{F}_d(u^*, v^*, d)(u, v) = D_{(u,v)}\mathbf{F}_\chi(u^*, v^*, \chi)(u, v) = \begin{pmatrix} D_1(1 + dv^*)u'' + D_1 du^* v'' + F_u^* u + F_v^* v \\ D_2 v'' - \chi\phi^* u'' + G_u^* u + G_v^* v \end{pmatrix}. \tag{30}$$

Thus, the above null space contains solutions to the following model:

$$\begin{cases} D_1(1 + dv^*)u'' + D_1 du^* v'' + F_u^* u + F_v^* v = 0, & x \in (0, L), \\ D_2 v'' - \chi\phi^* u'' + G_u^* u + G_v^* v = 0, & x \in (0, L), \\ u'(x) = v'(x) = 0, & x = 0, L. \end{cases} \tag{31}$$

To check the necessary conditions mentioned above, we denote $(u(x), v(x))$ as a solution of (31) and perform it into the eigen-expansions

$$u = \sum_{k=0}^{\infty} a_k \cos\frac{k\pi x}{L}, \quad v = \sum_{k=0}^{\infty} b_k \cos\frac{k\pi x}{L}, \tag{32}$$

where a_k and b_k are coefficients to be determined. To prove (29), it is equivalent to find nontrivial (a_k, b_k) such that

$$\begin{pmatrix} -D_1(1 + dv^*)\left(\frac{k\pi}{L}\right)^2 + F_u^* & -D_1 du^*\left(\frac{k\pi}{L}\right)^2 + F_v^* \\ \chi\phi^*\left(\frac{k\pi}{L}\right)^2 + G_u^* & -D_2\left(\frac{k\pi}{L}\right)^2 + G_v^* \end{pmatrix}\begin{pmatrix} a_k \\ b_k \end{pmatrix} = \begin{pmatrix} 0 \\ 0 \end{pmatrix}, \ k \in \mathbb{N}. \tag{33}$$

We obtain that the value of determinant corresponding to the coefficient matrix in (33) equals to zero. We notice that $k = 0$, thanks to (H2) and (H3), can be effortlessly ruled out due to $F_u^* G_v^* - F_v^* G_u^* \neq 0$. We get from direct computation that (29) is satisfied at $\chi = \chi_k$ (or $d = d_k$) for any positive integer k and

$$\chi_k = \frac{\left(D_1(1 + dv^*)\left(\frac{k\pi}{L}\right)^2 - F_u^*\right)\left(D_2\left(\frac{k\pi}{L}\right)^2 - G_v^*\right) + \left(D_1 du^*\left(\frac{k\pi}{L}\right)^2 - F_v^*\right)G_u^*}{\left(F_v^* - D_1 du^*\left(\frac{k\pi}{L}\right)^2\right)\phi^*\left(\frac{k\pi}{L}\right)^2}$$

or

$$d_k = \frac{-D_1 D_2\left(\frac{k\pi}{L}\right)^4 + (D_1 G_v^* + D_2 F_u^* + \chi\phi^* F_v^*)\left(\frac{k\pi}{L}\right)^2 - (F_u^* G_v^* - F_v^* G_u^*)}{(D_1 D_2 v^* + D_1 u^* \chi\phi^*)\left(\frac{k\pi}{L}\right)^4 - (D_1 v^* G_v^* - D_1 u^* G_u^*)\left(\frac{k\pi}{L}\right)^2}. \tag{34}$$

Note that (34) is equivalent to (16) or (18). Furthermore, it is obvious that $\dim(\mathbb{Z}(D_{(u,v)}\mathbf{F}_d(u^*,v^*,d_k))) = \dim(\mathbb{Z}(D_{(u,v)}\mathbf{F}_\chi(u^*,v^*,\chi_k))) = 1$ and $\mathbb{Z}(D_{(u,v)}\mathbf{F}_d(u^*,v^*,d_k)) = \mathbb{Z}(D_{(u,v)}\mathbf{F}_\chi(u^*,v^*,\chi_k)) = \text{span}\{(u_k^*,v_k^*)\}$, where

$$d:(u_k^*,v_k^*)=\left(\frac{D_2\left(\frac{k\pi}{L}\right)^2-G_v^*}{\chi\phi^*\left(\frac{k\pi}{L}\right)^2+G_u^*},1\right)\cos\frac{k\pi x}{L}\triangleq(Q_k,1)\cos\frac{k\pi x}{L},$$
$$\chi:(u_k^*,v_k^*)=\left(1,\frac{D_1(1+dv^*)\left(\frac{k\pi}{L}\right)^2-F_u^*}{F_v^*-D_1du^*\left(\frac{k\pi}{L}\right)^2}\right)\cos\frac{k\pi x}{L}\triangleq(1,P_k)\cos\frac{k\pi x}{L}, \tag{35}$$

where we use $d:$ and $\chi:$ for the case that d and χ are treated as bifurcation parameters, respectively. The possible bifurcation value can be found out by (34) (the formulas of χ_k and d_k). Now, we deliver our first theoretical result of this work which claims that the local bifurcation does appear at (u^*,v^*,d_k) or (u^*,v^*,χ_k) for each $k\in\mathbb{N}_+$.

Theorem 1. *Assume that, besides the bifurcation parameters d and χ, all the other coefficients in system (20) are positive and hypotheses (**H1**)–(**H3**) are satisfied. Postulate that*

$$\{[D_1D_2(1+dv^*)F_v^*\phi^*]+D_1du^*\phi^*[D_1du^*G_u^*-D_1(1+dv^*)G_v^*-D_2F_u^*]\}j^2k^2\left(\frac{\pi}{L}\right)^4$$
$$+D_1du^*\phi^*(F_u^*G_v^*-F_v^*G_u^*)(j^2+k^2)\left(\frac{\pi}{L}\right)^2\neq F_v^*\phi^*(F_u^*G_v^*-F_v^*G_u^*)$$

or

$$[D_1D_2(D_1v^*G_v^*-D_1u^*G_u^*)-(D_1G_v^*+D_2F_u^*+\chi\phi^*F_v^*)(D_1D_2v^*+D_1u^*\chi\phi^*)]j^2k^2\left(\frac{\pi}{L}\right)^4$$
$$+(D_1D_2v^*+D_1u^*\chi\phi^*)(F_u^*G_v^*-F_v^*G_u^*)(j^2+k^2)\left(\frac{\pi}{L}\right)^2\neq(D_1v^*G_v^*-D_1u^*G_u^*)(F_u^*G_v^*-F_v^*G_u^*). \tag{36}$$

Then, for any $k\in\mathbb{N}_+$, there exists a positive constant ϵ to guarantee system (20) possesses positive nonconstant solutions $(u_k(s,x),v_k(s,x),d_k(s))$ or $(u_k(s,x),v_k(s,x),\chi_k(s))$ for $s\in(-\epsilon,\epsilon)$, which bifurcates from (u^*,v^*,d_k) or (u^*,v^*,χ_k). Here, $d_k(s)\in\mathbb{R}$ (or $\chi_k(s)\in\mathbb{R}$) and $(u_k(s,x),v_k(s,x))\in\mathbb{X}\times\mathbb{X}$ are smooth functions with respect to s. Meanwhile, around (u^*,v^*,d_k), the bifurcating branch can be parameterized as

$$\Upsilon_{d_k}(s)=\{(u_k(s,x),v_k(s,x),d_k(s))|s\in(-\epsilon,\epsilon)\}\ \text{or}\ \Upsilon_{\chi_k}(s)=\{(u_k(s,x),v_k(s,x),\chi_k(s))|s\in(-\epsilon,\epsilon)\} \tag{37}$$

with

$$\begin{cases} d : (u_k(s,k), v_k(s,k)) = (u^*, v^*) + s(Q_k, 1)\cos\dfrac{k\pi x}{L} + s(\xi_{1k}(s,x), \xi_{2k}(s,x)), \\ d : d_k(s) = d_k + sC_1 + s^2C_2 + O(s^3), \\ \chi : (u_k(s,k), v_k(s,k)) = (u^*, v^*) + s(1, P_k)\cos\dfrac{k\pi x}{L} + s(\zeta_{1k}(s,x), \zeta_{2k}(s,x)), \\ \chi : \chi_k(s) = \chi_k + sC_3 + s^2C_4 + O(s^3), \end{cases} \tag{38}$$

where C_1, C_2, C_3, and C_4 are constants, $(\xi_{1k}(s,x), \xi_{2k}(s,x))$ and $(\zeta_{1k}(s,x), \zeta_{2k}(s,x))$ are two elements in a closed complement $\mathbb{W}_k$ of $\mathbb{Z}(D_{(u,v)}\mathbf{F}_d(u^*, v^*, d_k))$ and $\mathbb{Z}(D_{(u,v)}\mathbf{F}_\chi(u^*, v^*, \chi_k))$, respectively, in $\mathbb{X}\times\mathbb{X}$ with

$$(\xi_{1k}(0,x), \xi_{2k}(0,x)) = (0,0) \text{ or } (\zeta_{1k}(0,x), \zeta_{2k}(0,x)) = (0,0), \tag{39}$$

$$\mathbb{W}_k = \left\{ (u,v) \in \mathbb{X}\times\mathbb{X} \middle| \int_0^L u_k^* u + v_k^* v dx = 0 \right\}, \tag{40}$$

and (u_k^*, v_k^*) described in (35). Moreover, $(u_k(s,x), v_k(s,x), d_k(s))$ (or $(u_k(s,x), v_k(s,x), \chi_k(s))$) is a solution of model (20) and all positive nonconstant solutions of model (20) around (u^*, v^*, d_k) have to stay on the curve $\mathrm{Y}_{d_k}(s)$ (or $\mathrm{Y}_{\chi_k}(s)$).

Proof. By applying the bifurcation theory of Crandall–Rabinowitz,[56] we only need to verify the following transversality condition:

$$\begin{aligned} &\frac{d}{d\chi} D_{(u,v)}\mathbf{F}_\chi(u^*, v^*, \chi)(u_k^*, v_k^*)\Big|_{\chi=\chi_k} \notin \mathfrak{R}_\chi(D_{(u,v)}\mathbf{F}_\chi(u^*, v^*, \chi_k)) \\ &\text{or} \\ &\frac{d}{dd} D_{(u,v)}\mathbf{F}_d(u^*, v^*, d)(u_k^*, v_k^*)\Big|_{d=d_k} \notin \mathfrak{R}_d(D_{(u,v)}\mathbf{F}_d(u^*, v^*, d_k)), \end{aligned} \tag{41}$$

where $\mathfrak{R}_\chi$ and $\mathfrak{R}_d$ are two ranges of $D_{(u,v)}\mathbf{F}_\chi(u^*, v^*, \chi_k)$ and $D_{(u,v)}\mathbf{F}_d(u^*, v^*, d_k)$, respectively. In addition,

$$\frac{d}{d\chi} D_{(u,v)}\mathbf{F}_\chi(u^*, v^*, \chi)(u_k^*, v_k^*)\Big|_{\chi=\chi_k} = \begin{pmatrix} 0 \\ -\phi^* u_k^{*\prime\prime} \end{pmatrix} \tag{42}$$

and

$$\frac{d}{dd} D_{(u,v)}\mathbf{F}_d(u^*, v^*, d)(u_k^*, v_k^*)\Big|_{d=d_k} = \begin{pmatrix} -D_1 v^* u_k^{*\prime\prime} - D_1 u^* v_k^{*\prime\prime} \\ 0 \end{pmatrix}. \tag{43}$$

If (41) does not hold, there exists a nontrivial pair $(\bar{u}, \bar{v})$, which fulfills-

$$\begin{pmatrix} D_1(1+dv^*)\bar{u}'' + D_1 du^* \bar{v}'' + F_u^* \bar{u} + F_v^* \bar{v} \\ D_2 \bar{v}'' - \chi \phi^* \bar{u}'' + G_u^* \bar{u} + G_v^* \bar{v} \end{pmatrix} = \begin{pmatrix} 0 \\ -\phi^* u_k^{*''} \end{pmatrix} \tag{44}$$

or

$$\begin{pmatrix} D_1(1+dv^*)\bar{u}'' + D_1 du^* \bar{v}'' + F_u^* \bar{u} + F_v^* \bar{v} \\ D_2 \bar{v}'' - \chi \phi^* \bar{u}'' + G_u^* \bar{u} + G_v^* \bar{v} \end{pmatrix} = \begin{pmatrix} -D_1 v^* u_k^{*''} - D_1 u^* v_k^{*''} \\ 0 \end{pmatrix}. \tag{45}$$

Plugging

$$\bar{u} = \sum_{k=0}^{\infty} \bar{a}_k \cos \frac{k\pi x}{L}, \quad \bar{v} = \sum_{k=0}^{\infty} \bar{b}_k \cos \frac{k\pi x}{L}, \tag{46}$$

into the last equations yields

$$\begin{pmatrix} -D_1(1+dv^*)\left(\frac{k\pi}{L}\right)^2 + F_u^* & -D_1 du^* \left(\frac{k\pi}{L}\right)^2 + F_v^* \\ \chi\phi^* \left(\frac{k\pi}{L}\right)^2 + G_u^* & -D_2 \left(\frac{k\pi}{L}\right)^2 + G_v^* \end{pmatrix} \begin{pmatrix} \bar{a}_k \\ \bar{b}_k \end{pmatrix} = \begin{pmatrix} 0 \\ \phi^* \left(\frac{k\pi}{L}\right)^2 \end{pmatrix} \tag{47}$$

or

$$\begin{pmatrix} -D_1(1+dv^*)\left(\frac{k\pi}{L}\right)^2 + F_u^* & -D_1 du^* \left(\frac{k\pi}{L}\right)^2 + F_v^* \\ \chi\phi^* \left(\frac{k\pi}{L}\right)^2 + G_u^* & -D_2 \left(\frac{k\pi}{L}\right)^2 + G_v^* \end{pmatrix} \begin{pmatrix} \bar{a}_k \\ \bar{b}_k \end{pmatrix} = \begin{pmatrix} D_1 v^* \left(\frac{k\pi}{L}\right)^2 + D_1 u^* \left(\frac{k\pi}{L}\right)^2 \\ 0 \end{pmatrix}. \tag{48}$$

Together with two formulas of χ_k and d_k in (34), we check immediately that the coefficient matrices in (47) and (48) are singular. However, the right-hand side of the equation is nonzero. Accordingly, this contradiction guarantees that the transversality condition has been checked. Consequently, the theory of bifurcation from simple eigenvalues proposed by Crandall and Rabinowitz can verify the statements of this theorem. In the end, we need to request $\chi_k \neq \chi_j$ for each $k \neq j$ $(k \in \mathbb{N}_+)$ for the applicability of the bifurcation theory from simple eigenvalue. In light of

direct computation, one obtains

$$\frac{D_1D_2(1+dv^*)\left(\frac{k\pi}{L}\right)^4+[D_1du^*G_u^*-D_1(1+dv^*)G_v^*-D_2F_u^*]\left(\frac{k\pi}{L}\right)^2+F_u^*G_v^*-F_v^*G_u^*}{-D_1du^*\phi^*\left(\frac{k\pi}{L}\right)^4+F_v^*\phi^*\left(\frac{k\pi}{L}\right)^2}$$

$$\neq\frac{D_1D_2(1+dv^*)\left(\frac{j\pi}{L}\right)^4+[D_1du^*G_u^*-D_1(1+dv^*)G_v^*-D_2F_u^*]\left(\frac{j\pi}{L}\right)^2+F_u^*G_v^*-F_v^*G_u^*}{-D_1du^*\phi^*\left(\frac{j\pi}{L}\right)^4+F_v^*\phi^*\left(\frac{j\pi}{L}\right)^2}$$

or (49)

$$\frac{-D_1D_2\left(\frac{k\pi}{L}\right)^4+(D_1G_v^*+D_2F_u^*+\chi\phi^*F_v^*)\left(\frac{k\pi}{L}\right)^2-(F_u^*G_v^*-F_v^*G_u^*)}{(D_1D_2v^*+D_1u^*\chi\phi^*)\left(\frac{k\pi}{L}\right)^4-(D_1v^*G_v^*-D_1u^*G_u^*)\left(\frac{k\pi}{L}\right)^2}$$

$$\neq\frac{-D_1D_2\left(\frac{j\pi}{L}\right)^4+(D_1G_v^*+D_2F_u^*+\chi\phi^*F_v^*)\left(\frac{j\pi}{L}\right)^2-(F_u^*G_v^*-F_v^*G_u^*)}{(D_1D_2v^*+D_1u^*\chi\phi^*)\left(\frac{j\pi}{L}\right)^4-(D_1v^*G_v^*-D_1u^*G_u^*)\left(\frac{j\pi}{L}\right)^2}.$$

It is equivalent to (36). The proof is completed now. ■

Thanks to Lemmas 1–4 and Theorem 1, steady-state bifurcation appears at an accurate position where the positive equilibrium (u^*, v^*) loses its stability and shifts to nontrivial spacial patterns since the cross-diffusion rate d or the prey-taxis parameter χ crosses their critical bifurcation values. Obviously, the occurrence of those nontrivial positive solutions is due to the impacts of the value of d or χ.

Remark 2. The main theoretical results in this section are also applicable to high-dimensional cases, but the structures of Neumann eigenvalues are not as clean as in the one dimension situation.

3.2 | Global bifurcation analysis for multidimensional case in (4)

Throughout the entire paper, we suppose that the model (1) always exist a positive constant solution $\mathbf{e}^* = (u^*, v^*)$. In addition, we regard the parameter of cross-diffusion or nonlinear prey-taxis $\bullet$ as a bifurcation parameter, where $\bullet = d$ or χ. Consequently, we derive the following lemma in view of the original Crandall–Rabinowitz bifurcation theory[56] and its user-friendly version.[57]

Lemma 5 (Theorem 4.3 in Ref. 57). *Let X and Y be real Banach spaces. Postulate that W represents an open connected set in $\mathcal{R}\times X$ and $(\bullet_0, \mathbf{e}^*)\in W$ and $\mathbf{F}$ stands for a continuously differentiable mapping from W into Y. Assume that*

(1) *For all $(\bullet, \mathbf{e}^*)\in W$, $\mathbf{F}(\bullet, \mathbf{e}^*) = 0$;*
(2) *The partial derivative $D_{\mathbf{e}}\mathbf{F}(\bullet, \mathbf{e})$ exists and is continuous in $(\bullet, \mathbf{e})$ near $(\bullet_0, \mathbf{e}^*)$;*

(3) $\mathcal{R}(D_{\mathbf{e}}\mathbf{F}(\bullet_0, \mathbf{e}^*))$ *is closed,* $\dim\mathrm{Ker}(D_{\mathbf{e}}\mathbf{F}(\bullet_0, \mathbf{e}^*)) = 1$ *and* $\mathrm{codim}\mathcal{R}(D_{\mathbf{e}}\mathbf{F}(\bullet_0, \mathbf{e}^*)) = 1$ *for some* $(\bullet_0, \mathbf{e}^*) \in W$*;*

(4) $D_{\bullet_{\mathbf{e}}}\mathbf{F}(\bullet_0, \mathbf{e}^*)\mathbf{e}_0 \notin \mathcal{R}(D_{\mathbf{e}}\mathbf{F}(\bullet_0, \mathbf{e}^*))$*, where* $\mathbf{e}_0 \in X$ *spans* $\mathrm{Ker}(D_{\mathbf{e}}\mathbf{F}(\bullet_0, \mathbf{e}^*))$.

Let z be any closed complement of $\mathrm{span}\{\mathbf{e}_0\}$ *in Y. Then, there exist an open interval $I_0 = (-\varepsilon, \varepsilon)$ and continuously differentiable functions $\chi : I_0 \to \mathcal{R}$ and $\varphi : I_0 \to z$ such that $\bullet(0) = \bullet_0$, $\varphi(0) = 0$, and if $\mathbf{e}(s) = \mathbf{e}^* + s\mathbf{e}_0 + s\varphi(s)$ for $s \in I_0$ then*

$$\mathbf{F}(\bullet(s), \mathbf{e}(s)) = 0. \tag{50}$$

In addition, in any sufficiently small neighborhood of $(\bullet, \mathbf{e}^*)$ in W, the entire solution set for $\mathbf{F}(\chi, \mathbf{e}) = 0$ consist of the line $(\bullet, \mathrm{e}^*)$ and the curve $(\bullet(s), \mathbf{e}(s))$. Furthermore, if

(5) $D_{\mathbf{e}}\mathbf{F}(\bullet, \mathbf{e})$ *is a Fredholm operator for all $(\bullet, \mathbf{e}) \in W$, then the curve $(\bullet(s), \mathbf{e}(s))$ is contained in C, which represents a connected component of $\overline{S}$, where $S = \{(\bullet, \mathbf{e}) \in W, \mathbf{F}(\lambda, \mathbf{e}) = 0, \mathbf{e} \neq \mathbf{e}^*\}$ and either C is not compact in W or C contains a point $(\bullet^*, \mathbf{e}^*)$ with $\bullet^* \neq \bullet_0$.*

Let us stipulate that

$$\mathbf{F}(\bullet, \mathbf{e}) = \begin{pmatrix} \Delta(u + duv) + F(u, v) \\ \Delta v - \chi\nabla(v\nabla u) + G(u, v) \end{pmatrix}, \tag{51}$$

where $\mathbf{e} = (u, v)$. Throughout the entire paper, $\bullet = d$ or χ. Therefore, the solutions of the following elliptic system of (1):

$$\begin{cases} \mathbf{F}(\bullet, \mathbf{e}) = 0, \quad x \in \Omega, \\ \dfrac{\partial u}{\partial \nu} = \dfrac{\partial v}{\partial \nu} = 0, \quad x \in \partial\Omega \end{cases} \tag{52}$$

can represent the positive steady states of system (1).

In this section, we will deduce the global bifurcation theorems when we regard the cross-diffusion rate d or the coefficient of nonlinear prey-taxis χ as a bifurcation parameter. First, we have to check that all hypotheses introduced by Lemma 5 are fulfilled for the system (20) under some suitable cases. Assume that $\lambda > 0$ stands for a simple eigenvalue of the following elliptic model:

$$\begin{cases} -\Delta v = \lambda v, & x \in \Omega, \\ \dfrac{\partial v}{\partial \nu} = 0, & x \in \partial\Omega. \end{cases} \tag{53}$$

We need to provide some notations which will be utilized in our proof.

$$\begin{aligned}
\mathbb{X} =&\left\{(u,v)\in[W^{2,r}(\Omega)]^2\middle|\frac{\partial u}{\partial \nu}=\frac{\partial v}{\partial \nu}=0, x\in\partial\Omega\right\},\\
\mathbb{W}_d =&\{(d,u,v)\in\mathcal{R}\times\mathbb{X}|d\neq 0,u>0,v>0\},\\
\mathbb{W}_\chi =&\{(\chi,u,v)\in\mathcal{R}\times\mathbb{X}|\chi\neq 0,u>0,v>0\},\\
\mathbb{Y} =&[L^r(\Omega)]^2,\\
\mathbb{Z}_d =&\left\{(u,v)\in\mathbb{X}\middle|\int_\Omega[((1+dv^*)\lambda-F_u(u^*,v^*))u+(du^*\lambda-F_v(u^*,v^*))v]\varphi=0\right\},\\
\mathbb{Z}_\chi =&\left\{(u,v)\in\mathbb{X}\middle|\int_\Omega[(\chi v^*\lambda+G_u(u^*,v^*))u+(-\lambda+G_v(u^*,v^*))v]\psi=0\right\},
\end{aligned}\tag{54}$$

where $r>n$ and φ is termed as a normalize eigenfunction with respect to λ.

For convenience, we denote that

$$\Theta=1+d_0v^*+d_0\chi u^*v^*\neq 0,\tag{55}$$

where

$$d_0=\frac{[F_u(u^*,v^*)-\lambda][\lambda-G_v(u^*,v^*)]+F_v(u^*,v^*)[\chi v^*\lambda+G_u(u^*,v^*)]}{u^*\lambda[\chi v^*\lambda+G_u(u^*,v^*)]-v^*\lambda[-\lambda+G_v(u^*,v^*)]}.\tag{56}$$

Theorem 2. *Suppose that*

(i) $\lambda>0$ *can be regarded as a simple eigenvalue of (53).*
(ii) (u,v) *is any nonnegative solution of multidimensional version stationary problem of (20) and there exists a constant* $C>0$ *which is independent of* u *and* v *to guarantee* $\|u\|_{L^\infty}\leq C$ *and* $\|v\|_{L^\infty}\leq C$.
(iii) d *and* χ *can satisfy the following condition* $\frac{1+dv^*}{\Theta}+\frac{d\chi u^*v^*}{\Theta^2}>0$.

Then, we have

(I) *When* $d=d_0\neq 0$ *and*

$$\lambda\neq\sqrt{\left(\frac{1+dv^*}{\Theta}+\frac{d\chi u^*v^*}{\Theta^2}\right)[F_u(u^*,v^*)G_v(u^*,v^*)-G_u(u^*,v^*)F_v(u^*,v^*)]},\tag{57}$$

then for the positive equilibrium (u^*,v^*)*, a bifurcation of nonconstant solution of multidimensional version stationary problem of (20) will bifurcate at* $d=d_0$*. In a neighborhood of the bifurcation point,*

$$(d,u,v)=(d(s),u(s)+s[(1+d_v^*)\lambda-F_u(u^*,v^*)]\varphi+s\zeta_1(s),v(s)+s[du^*\lambda-F_v(u^*,v^*)]\varphi+s\zeta_2(s)).\tag{58}$$

can parameterize the bifurcating branch, where (ζ_1, ζ_2) *belongs to* $\mathbb{Z}_d$ *and* $d(0) = d_0$, $u(0) = u^*$, $v(0) = v^*$, $(\zeta_1(0), \zeta_2(0)) = (0, 0)$.

(II) *Meanwhile, the bifurcating branch can be regarded as a part of a connected component* C_0 *of the set* $\overline{\mathbb{S}_d}$, *where*

$$\mathbb{S}_d = \{(d, u, v) | (d, u - u^*, v - v^*) \in \mathbb{W}_d, \mathbf{F}(d, u - u^*, v - v^*) = 0, (u, v) \neq (u^*, v^*)\}, \quad (59)$$

and C_0 *either includes a point* (d, u, v), *where* $(d, u - u^*, v - v^*) \in \partial\mathbb{W}_d$, *or is unbounded in* d.

(III) *Finally,* C_0 *is unbounded in* d *when* $d > 0$ *or* $d < 0$ *and*

(i) $\lambda \neq F_u(\hat{u}, 0) > 0$ *and* $\frac{F_v(\hat{u},0)}{d\hat{u}} > 0$ *for all semitrivial equilibria* $(\hat{u}, 0)$ *and* $(\hat{v}, 0)$;

(ii) $G_u(\hat{u}, 0) \neq 0$ *or* $\lambda \neq G_v(\hat{u}, 0) > 0$.

Proof. In view of the traditional version of Crandall–Rabinowitz bifurcation theory, it can only be utilized when d_0 is a monotone function for λ. Motivated by Ref. 57, we discover that the user-friendly version (Lemma 5) can solve this problem.

First, we need to linearize $\mathbf{F}(d, u, v)$ with corresponding (u, v) at $\mathbf{e}^*$, and get

$$D_{(u,v)}\mathbf{F}(d, u^*, v^*)(u, v) = \begin{pmatrix} (1 + dv^*)\Delta u + du^*\Delta v + F_u(u^*, v^*)u + F_v(u^*, v^*)v \\ -\chi v^*\Delta u + \Delta v + G_u(u^*, v^*)u + G_v(u^*, v^*)v \end{pmatrix}. \quad (60)$$

It is obvious by a direct computation that the derived function $D_d\mathbf{F}(d, u, v)$ possesses continuity and differentiability with corresponding d, u, and v in $\mathbb{W}_d$. Next, we need to obtain the possible global bifurcation point with a remarkable rate d. To achieve this aim, we must point out that we cannot apply the implicit function theorem if $d \neq 0$. Let us put it another way, it means that the corresponding elliptic model

$$\begin{cases} (1 + dv^*)\Delta u + du^*\Delta v + F_u(u^*, v^*)u + F_v(u^*, v^*)v = 0, & x \in \Omega, \\ -\chi v^*\Delta u + \Delta v + G_u(u^*, v^*)u + G_v(u^*, v^*)v = 0, & x \in \Omega, \\ \dfrac{\partial u}{\partial \nu} = \dfrac{\partial v}{\partial \nu} = 0, & x \in \partial\Omega \end{cases} \quad (61)$$

has a nontrivial solution, that is, we can get a nontrivial solution to satisfy $D_{(u,v)}\mathbf{F}(d, u^*, v^*)(u, v) = 0$.

Any pair of functions in $\mathbb{X}$ will be defined by (u, v). Hence, series of mutually orthogonal eigenfunctions of model (53) with constant vector multipliers can be used to expand u and v for $(u, v) \in \mathbb{Y}$. In addition, when (u, v) is nonzero, one of these eigenfunctions in these expansions is at least nonzero. Postulate that φ with respect to λ represents such a normalized eigenfunction and $\int_\Omega \varphi^2 dx = 1$.

For abbreviation, we stipulate that $\mathbf{U}$ and $\mathbf{V}$ will be applied to replace $\int_\Omega u\varphi$ and $\int_\Omega v\varphi$. By the homogeneous Neumann boundary conditions, multiplying the equations of u and v in the last equations by φ and integrating on Ω by parts, the following system with respect to $\mathbf{U}$ and $\mathbf{V}$

$$\begin{pmatrix} -(1 + dv^*)\lambda + F_u(u^*, v^*) & -du^*\lambda + F_v(u^*, v^*) \\ \chi v^*\lambda + G_u(u^*, v^*) & -\lambda + G_v(u^*, v^*) \end{pmatrix} \begin{pmatrix} \mathbf{U} \\ \mathbf{V} \end{pmatrix} = 0 \quad (62)$$

is derived. Model (62) possesses nontrivial solutions when and only when

$$\begin{vmatrix} -(1+dv^*)\lambda + F_u(u^*,v^*) & -du^*\lambda + F_v(u^*,v^*) \\ \chi v^*\lambda + G_u(u^*,v^*) & -\lambda + G_v(u^*,v^*) \end{vmatrix} = 0, \tag{63}$$

which means that

$$d = d_0 = \frac{[F_u(u^*,v^*)-\lambda][\lambda - G_v(u^*,v^*)] + F_v(u^*,v^*)[\chi v^*\lambda + G_u(u^*,v^*)]}{u^*\lambda[\chi v^*\lambda + G_u(u^*,v^*)] - v^*\lambda[-\lambda + G_v(u^*,v^*)]}. \tag{64}$$

In what follows, we need to deduce that all the hypotheses of the user-friendly version of the Crandall–Rabinowitz theorem are fulfilled if the conditions of Theorem 4 hold when $d = d_0$. It is easy to validate that condition (1) can be satisfied. Now, the proof can be divided into three steps.

Step 1: *The validation of condition* **(5)** *of Lemma* 5.

We denote

$$M_1(d,\mathbf{e}) = \begin{pmatrix} 1+dv & du \\ -\chi v & 1 \end{pmatrix}, \quad f(d,\mathbf{e},\nabla\mathbf{e}) = \begin{pmatrix} 2d\nabla v\cdot\nabla u + F(u,v) \\ -\chi\nabla v\cdot\nabla u + G(u,v) \end{pmatrix} \tag{65}$$

for $\mathbf{e} = (u,v)^T$. Thus, system (51) can be described as

$$\mathcal{F}(d,\mathbf{e}) = -M_1(d,\mathbf{e})[\Delta\mathbf{e}]^T + f(d,\mathbf{e},\nabla\mathbf{e}) = 0. \tag{66}$$

It is easy to perform the linearization of $\mathcal{F}(d,\mathbf{e})$ at $\mathbf{e}$ as

$$D_{\mathbf{e}}\mathcal{F}(d,\mathbf{e})\mathbf{u} = -M_1(\mathbf{e})\Delta\mathbf{u} - M_2(\mathbf{u})\Delta\mathbf{e} - M_3(\nabla\mathbf{e})\cdot\nabla\mathbf{u} - J(\mathbf{e})\mathbf{u}, \tag{67}$$

where $\mathbf{u} = (u_1,u_2)$,

$$M_2(\mathbf{u}) = \begin{pmatrix} d_1u_1 & d_1u_2 \\ -\chi u_1 & 0 \end{pmatrix}, \quad M_3(\nabla\mathbf{e}) = \begin{pmatrix} 2d\nabla u & 2d\nabla v \\ -\chi\nabla u & -\chi\nabla v \end{pmatrix} \tag{68}$$

and $J(\mathbf{e})$ can be treated as the Jacobian matrix

$$J(\mathbf{e}) = \begin{pmatrix} F_u(u,v) & F_v(u,v) \\ G_u(u,v) & G_v(u,v) \end{pmatrix}. \tag{69}$$

Now, we need to consider the value range of d and χ to guarantee $\mathrm{tr}(M_1(d,\mathbf{e})) > 0$ and $\det(M_1(d,\mathbf{e})) > 0$. We obtain the following condition:

$$\frac{1+dv^*}{\Theta} + \frac{d\chi u^*v^*}{\Theta^2} > 0. \tag{70}$$

Consequently, $M_1(d,\mathbf{e})$ satisfies the Assumption (2.6) in Ref. 57. Meanwhile, Agmon's lemma can be satisfied with $\theta \in [-\frac{\pi}{2},\frac{\pi}{2}]$ in view of Remark 2.5 (case 3) in Ref. 57. Therefore, based on Corollary 2.11 of Ref. 57, $D_{\mathbf{e}}\mathcal{F}(d,\mathbf{e})$ stands for a Fredholm operator with index 0 which means that the validation of condition (5) of Lemma 5 is completed.

Step 2: *The validation of condition* **(3)** *of Lemma* 5.

In this step, we need to validate that condition (3) of Lemma 5 can be satisfied according to the hypotheses of Lemma 5 and Theorem 2. Based on (61), we can get

$$\begin{pmatrix}\Delta u\\ \Delta v\end{pmatrix}+M_4\begin{pmatrix}u\\ v\end{pmatrix}=0,\ x\in\Omega,\ \ \frac{\partial u}{\partial \nu}=\frac{\partial v}{\partial \nu}=0,\ x\in\partial\Omega. \tag{71}$$

Here,

$$M_4=\begin{pmatrix}\dfrac{F_u(u^*,v^*)}{\Theta}-\dfrac{du^*G_u(u^*,v^*)}{\Theta} & \dfrac{F_v(u^*,v^*)}{\Theta}-\dfrac{du^*G_v(u^*,v^*)}{\Theta}\\ \dfrac{\chi v^*}{\Theta}F_u(u^*,v^*)+(1+dv^*)G_u(u^*,v^*) & \dfrac{\chi v^*}{\Theta}F_v(u^*,v^*)+(1+dv^*)G_v(u^*,v^*)\end{pmatrix}. \tag{72}$$

It is clear by a direct computation that

$$\begin{aligned}\det(M_4)=&\frac{\chi v^*}{\Theta^2}F_u(u^*,v^*)F_v(u^*,v^*)-\frac{d\chi u^*v^*}{\Theta^2}G_u(u^*,v^*)F_v(u^*,v^*)+\frac{1+dv^*}{\Theta}F_u(u^*,v^*)G_v(u^*,v^*)\\ &-\frac{du^*(1+dv^*)}{\Theta}G_u(u^*,v^*)G_v(u^*,v^*)-\frac{\chi v^*}{\Theta^2}F_u(u^*,v^*)F_v(u^*,v^*)+\frac{d\chi u^*v^*}{\Theta^2}F_u(u^*,v^*)G_v(u^*,v^*)\\ &-\frac{1+dv^*}{\Theta}G_u(u^*,v^*)F_v(u^*,v^*)+\frac{du^*(1+dv^*)}{\Theta}G_u(u^*,v^*)G_v(u^*,v^*)\\ =&\left(\frac{1+dv^*}{\Theta}+\frac{d\chi u^*v^*}{\Theta^2}\right)[F_u(u^*,v^*)G_v(u^*,v^*)-G_u(u^*,v^*)F_v(u^*,v^*)]\\ >&0.\end{aligned} \tag{73}$$

Now, we consider the eigenvalues of the matrix M_4. It is easy to obtain the characteristic equation of the matrix M_4 as follows:

$$\begin{vmatrix}-\mu+\dfrac{F_u(u^*,v^*)}{\Theta}-\dfrac{du^*G_u(u^*,v^*)}{\Theta} & \dfrac{F_v(u^*,v^*)}{\Theta}-\dfrac{du^*G_v(u^*,v^*)}{\Theta}\\ \dfrac{\chi v^*}{\Theta}F_u(u^*,v^*)+(1+dv^*)G_u(u^*,v^*) & -\mu+\dfrac{\chi v^*}{\Theta}F_v(u^*,v^*)+(1+dv^*)G_v(u^*,v^*)\end{vmatrix}=0. \tag{74}$$

Clearly, we can regard $\sigma_1=\lambda>0$ as one of the eigenvalues of M_4. Thus,

$$\sigma_2=\frac{1}{\lambda}\left(\frac{1+dv^*}{\Theta}+\frac{d\chi u^*v^*}{\Theta^2}\right)[F_u(u^*,v^*)G_v(u^*,v^*)-G_u(u^*,v^*)F_v(u^*,v^*)] \tag{75}$$

can be defined as another eigenvalue of M_4. Hence, if

$$\lambda\neq\sqrt{\underbrace{\left(\frac{1+dv^*}{\Theta}+\frac{d\chi u^*v^*}{\Theta^2}\right)}_{Diffusion\ part}\underbrace{[F_u(u^*,v^*)G_v(u^*,v^*)-G_u(u^*,v^*)F_v(u^*,v^*)]}_{ODE\ part}}, \tag{76}$$

then M_4 possesses two positive different eigenvalues $\sigma_1=\lambda>0$ and

$$\sigma_2=\frac{1}{\lambda}\left(\frac{1+dv^*}{\Theta}+\frac{d\chi u^*v^*}{\Theta^2}\right)[F_u(u^*,v^*)G_v(u^*,v^*)-G_u(u^*,v^*)F_v(u^*,v^*)]. \tag{77}$$

By (71) and reversible transformation, we deduce that

$$\begin{pmatrix}\Delta U\\ \Delta V\end{pmatrix}+\begin{pmatrix}\sigma_1 & 0\\ 0 & \sigma_2\end{pmatrix}\begin{pmatrix}U\\ V\end{pmatrix}=0,\ x\in\Omega,\ \ \frac{\partial U}{\partial \nu}=\frac{\partial V}{\partial \nu}=0,\ x\in\partial\Omega. \tag{78}$$

Consequently, if σ_2 cannot be treated as an eigenvalue of (53), we can get that $U=0$ and $V=c\varphi$, where c stands for a constant, and $\sigma_1=\lambda$ represents an eigenvalue of (53). In view of the reversibility of transformation, one gets $u=c_1\varphi$ and $v=c_2\varphi$, where c_1 and c_2 are all constants. Therefore, we get $\dim\ker(D_{\mathbf{e}}\mathbf{F}(d_0,\mathbf{e}^*))=1$. By (62), we obtain

$$\ker(D_{\mathbf{e}}\mathbf{F}(d_0,\mathbf{e}^*))=\operatorname{span}\{[(1+dv^*)\lambda-F_u(u^*,v^*)]\varphi,(du^*\lambda-F_v(u^*,v^*))\varphi\}. \tag{79}$$

It is obvious via a simple verification that $\mathcal{R}(D_{\mathbf{e}}\mathbf{F}(d_0,\mathbf{e}^*))=1$ since $D_{\mathbf{e}}\mathbf{F}(d,\mathbf{e})$ stands for a Fredholm operator with index 0. Thus, the check of condition (3) is completed. We synchronously finish the proof of (I) of this theorem.

Step 3: *The validation of conditions* **(2)** *and* **(4)** *of Lemma* 5.

Define

$$U_0=\begin{pmatrix}[(1+dv^*)\lambda-F_u(u^*,v^*)]\varphi\\ [du^*\lambda-F_v(u^*,v^*)]\varphi\end{pmatrix}. \tag{80}$$

Based on (60), one gets

$$D_{d(u,v)}\mathbf{F}(d,u,v)(u,v)=\begin{pmatrix}u\Delta v+v\Delta u\\ 0\end{pmatrix}. \tag{81}$$

In addition, $D_{d(u,v)}\mathbf{F}(d,u,v)$ possesses continuity. It implies that the check of condition (2) is completed. Plugging u^* and v^* into the above equality yields

$$D_{d(u,v)}\mathbf{F}(d,u^*,v^*)(u,v)=\begin{pmatrix}u^*\Delta v+v^*\Delta u\\ 0\end{pmatrix}, \tag{82}$$

which means that

$$D_{d(u,v)}\mathbf{F}(d_0,u^*,v^*)(u,v)U_0=\begin{pmatrix}-\lambda v^*[(1+dv^*)\lambda-F_u(u^*,v^*)]-\lambda u^*[du^*\lambda-F_v(u^*,v^*)]\\ 0\end{pmatrix}\varphi. \tag{83}$$

Assume that

$$D_{d(u,v)}\mathbf{F}(d_0,u^*,v^*)U_0\in\mathcal{R}(D_{(u,v)}\mathbf{F}(d_0,u^*,v^*)), \tag{84}$$

then we can find some particular u and v such that

$$D_{(u,v)}\mathbf{F}(d_0,u^*,v^*)(u,v)=D_{d(u,v)}\mathbf{F}(d_0,u^*,v^*)U_0. \tag{85}$$

It follows that

$$\begin{cases} (1+dv^*)\Delta u + du^*\Delta v + F_u(u^*,v^*)u + F_v(u^*,v^*)v \\ = -\lambda v^*[(1+dv^*)\lambda - F_u(u^*,v^*)]\varphi - \lambda u^*[du^*\lambda - F_v(u^*,v^*)]\varphi,\ x\in\Omega, \\ -\chi v^*\Delta u + \Delta v + G_u(u^*,v^*)u + G_v(u^*,v^*)v = 0,\ x\in\Omega, \\ \dfrac{\partial u}{\partial \nu} = \dfrac{\partial v}{\partial \nu} = 0,\ x\in\partial\Omega. \end{cases} \tag{86}$$

By the same form of (62), we can immediately obtain

$$\begin{aligned} &\begin{pmatrix} -(1+dv^*)\lambda + F_u(u^*,v^*) & -du^*\lambda + F_v(u^*,v^*) \\ \chi v^*\lambda + G_u(u^*,v^*) & -\lambda + G_v(u^*,v^*) \end{pmatrix}\begin{pmatrix} \mathbf{U} \\ \mathbf{V} \end{pmatrix} \\ &= \begin{pmatrix} -\lambda v^*[(1+dv^*)\lambda - F_u(u^*,v^*)] - \lambda u^*[du^*\lambda - F_v(u^*,v^*)] \\ 0 \end{pmatrix}. \end{aligned} \tag{87}$$

Obviously, it is impossible because the corresponding determinant of the coefficient matrix on the left-hand side is 0 based on (63). Consequently, we obtain a contradiction and derive that

$$D_{d(u,v)}\mathbf{F}(d_0,u^*,v^*)U_0 \notin \mathcal{R}(D_{(u,v)}\mathbf{F}(d_0,u^*,v^*)), \tag{88}$$

which illustrates that the validation of condition (4) of Lemma 5 is completed.

Having said all of above, we see immediately that all conditions of Lemma 5 have been validated to be satisfactory, which deduces that $\mathcal{C}_0$ have to fulfill one of the following three cases:

(i) $\mathcal{C}_0$ has a point (d^*,u^*,v^*) with $d^*\neq d_0$.
(ii) $\mathcal{C}_0$ has a point with $(d,u-u^*,v-v^*)\in\partial\mathbb{W}_d$.
(iii) $\mathcal{C}_0$ is unbounded (joints to ∞) in $\mathcal{R}\times\mathbb{X}$.

Note that interior (positive) solutions of the corresponding elliptic system (20) will bifurcate from (d,u^*,v^*) if $d=d_0$. Consequently, (i) can be excluded immediately. The semitrivial equilibria are denoted by

$$(\hat{u},0)\ \text{ and }\ (0,\hat{v}). \tag{89}$$

Evaluating at $(\hat{u},0)$ yields

$$D_{(u,v)}\mathbf{F}(d,\hat{u},0)(u,v) = \begin{pmatrix} \Delta u + d\hat{u}\Delta v + F_u(\hat{u},0)u + F_v(\hat{u},0)v \\ \Delta v + G_u(\hat{u},0)u + G_v(\hat{u},0)v \end{pmatrix}. \tag{90}$$

By combining with implicit function theorem, we can immediately obtain that the nondegeneracy of $(\hat{u},0)$ if and only if the following two cases are occur:

(i) $\lambda\neq F_u(\hat{u},0)>0$ and $\frac{F_v(\hat{u},0)}{d\hat{u}}>0$.
(ii) $G_u(\hat{u},0)\neq 0$ or $\lambda\neq G_v(\hat{u},0)>0$.

The similar discussion can be derived for $(0, \hat{v})$. Consequently, (ii) can also be excluded immediately. By the condition of Theorem 2, we see at once that any positive solution (u, v) for system (20) possesses boundedness in the norm of $L^\infty(\Omega) \times L^\infty(\Omega)$. We obtain at once that $u, v \in C^{2+\alpha}(\Omega)$ for some $\alpha \in (0, 1)$ in view of the Schauder estimates. Together with the Sobolev embedding theorem, we derive at once that any positive solution (u, v) of system (20) is bounded in the norm of $\mathbb{X}$. To sum up, C_0 possesses boundedness in d, which describes that the validation of condition (2) of Lemma 5 is finished. In the meantime, the proofs of (II) and (III) of Theorem 2 are finished too. The proof of Theorem 2 is completed now. ■

For convenience, we also define that

$$\Lambda = 1 + dv^* + d\chi_0 u^* v^* \neq 0, \tag{91}$$

where

$$\begin{aligned}\chi_0 =& \frac{(1+dv^*)\lambda^2}{v^*\lambda(F_v(u^*,v^*) - du^*\lambda)} + \frac{\{d[u^*G_u(u^*,v^*) - v^*G_v(u^*,v^*)] - [F_u(u^*,v^*) + G_v(u^*,v^*)]\}\lambda}{v^*\lambda(F_v(u^*,v^*) - du^*\lambda)} \\ &+ \frac{F_u(u^*,v^*)G_v(u^*,v^*) - F_v(u^*,v^*)G_u(u^*,v^*)}{v^*\lambda(F_v(u^*,v^*) - du^*\lambda)}.\end{aligned} \tag{92}$$

If we choose χ as a bifurcation parameter, then we have the following theorem by the same method.

Theorem 3. *Assume that*

(i) $\lambda > 0$ *can be regarded as a simple eigenvalue of (53).*
(ii) (u, v) *is any nonnegative solution of multidimensional version stationary problem of (20) and there exists a constant* $C > 0$ *which is independent of* u *and* v *to guarantee* $\|u\|_{L^\infty} \leq C$ *and* $\|v\|_{L^\infty} \leq C$.
(iii) In addition, d *and* χ *can satisfy the following condition* $\frac{1+dv^*}{\Lambda} + \frac{d\chi u^* v^*}{\Lambda^2} > 0$.

Then, we have

(I) *When* $\chi = \chi_0 \neq 0$ *and*

$$\lambda \neq \sqrt{\left(\frac{1+dv^*}{\Lambda} + \frac{d\chi u^* v^*}{\Lambda^2}\right)[F_u(u^*,v^*)G_v(u^*,v^*) - G_u(u^*,v^*)F_v(u^*,v^*)]}, \tag{93}$$

then for the positive equilibrium (u^*, v^*)*, a bifurcation of nonconstant solution of multidimensional version stationary problem of (20) will bifurcate at* $\chi = \chi_0$*. In a neighborhood of the bifurcation point,*

$$(\chi, u, v) = (\chi(s), u(s) + s[-\chi v^*\lambda - G_u(u^*,v^*)]\psi + s\xi_1(s), v(s) + s[\lambda - G_v(u^*,v^*)]\psi + s\xi_2(s)). \tag{94}$$

can parameterize the bifurcating branch, where (ξ_1, ξ_2) *belongs to* $\mathbb{Z}_\chi$ *and* $\chi(0) = \chi_0$, $u(0) = u^*$, $v(0) = v^*$, $(\xi_1(0), \xi_2(0)) = (0, 0)$.

(II) *Meanwhile, the bifurcating branch can be regarded as a part of a connected component* C_0 *of the set* $\overline{\mathbb{S}_\chi}$, *where*

$$\mathbb{S}_\chi = \left\{(\chi, u, v) | (\chi, u - u^*, v - v^*) \in \mathbb{W}_\chi, \mathbf{F}(\chi, u - u^*, v - v^*) = 0, (u, v) \neq (u^*, v^*)\right\}, \quad (95)$$

and C_0 *either includes a point* (χ, u, v), *where* $(\chi, u - u^*, v - v^*) \in \partial\mathbb{W}_\chi$, *or is unbounded in* χ. *Furthermore,* C_0 *is unbounded in* χ *when* $\chi \neq 0$.

4 | STABILITY OF NONCONSTANT POSITIVE STEADY STATES

In this section, the instability and stability of the spatially nonconstant steady states are obtained by Theorem 1. Under the general functional responses, we will offer exact formulas and criteria to get the stability of the bifurcating solutions and the direction of steady-state bifurcations of (1). Employing classical analysis from Ref. 58, our results focus on the linear stability of perturbations with a study of the spectral analysis of (20).

For this purpose, we have the following approach. Based on $\phi(u, v) \in C^3$, $F(u, v) \in C^4$, $G(u, v) \in C^4$, and (u_k, v_k, d_k) (or (u_k, v_k, χ_k)) represent C^3-smooth functions with respect to s, and accordingly, in view of Theorem 1.18 in Ref. 56, $u_k(s, x)$ and $v_k(s, x)$ can be expanded as follows:

$$\begin{cases} d : u_k(s,k) = u^* + sQ_k \cos\dfrac{k\pi x}{L} + s^2\Phi_1(x) + s^3\Phi_2(x) + O(s^3), \\ d : v_k(s,k) = v^* + s\cos\dfrac{k\pi x}{L} + s^2\Psi_1(x) + s^3\Psi_2(x) + O(s^3), \\ \chi : u_k(s,k) = u^* + s\cos\dfrac{k\pi x}{L} + s^2\Phi_3(x) + s^3\Phi_4(x) + O(s^3), \\ \chi : v_k(s,k) = v^* + sP_k\cos\dfrac{k\pi x}{L} + s^2\Psi_3(x) + s^3\Psi_4(x) + O(s^3), \end{cases} \quad (96)$$

where P_k and Q_k are introduced by (35), $(\Phi_i, \Psi_i) \in \mathbb{W}$ for $i = 1, 2, 3, 4$, and the high-order terms $O(s^3)$ in $u_k(s, x)$ and $v_k(s, x)$ are assumed in H^2-norm. Accordingly, one gets

$$\begin{cases} d : D_1u_k''(s,k) = sD_1Q_k\cos''\dfrac{k\pi x}{L} + s^2D_1\Phi_1''(x) + s^3D_1\Phi_2''(x) + O(s^3), \\ d : D_2v_k''(s,k) = sD_2\cos''\dfrac{k\pi x}{L} + s^2D_2\Psi_1''(x) + s^3D_2\Psi_2''(x) + O(s^3), \\ \chi : D_1u_k''(s,k) = sD_1\cos''\dfrac{k\pi x}{L} + s^2D_1\Phi_3''(x) + s^3D_1\Phi_4''(x) + O(s^3), \\ \chi : D_2v_k''(s,k) = sD_2P_k\cos''\dfrac{k\pi x}{L} + s^2D_2\Psi_3''(x) + s^3D_2\Psi_4''(x) + O(s^3). \end{cases} \quad (97)$$

Furthermore, by the Taylor's expansion functions of two variables, we obtain

$$
\begin{cases}
d:F(u_k(s,x),v_k(s,x)) = F^* + s\left[(F_u^*Q_k + F_v^*)\cos\dfrac{k\pi x}{L}\right] \\
\qquad + s^2\left[F_u^*\Phi_1 + F_v^*\Psi_1 + \dfrac{1}{2}(F_{uu}^*Q_k^2 + 2F_{uv}^*Q_k + F_{vv}^*)\cos^2\dfrac{k\pi x}{L}\right] \\
\qquad + s^3\left[F_u^*\Phi_2 + F_v^*\Psi_2 + (F_{uu}^*Q_k + F_{uv}^*)\Phi_1\cos\dfrac{k\pi x}{L} + (F_{uv}^*Q_k + F_{vv}^*)\Psi_1\cos\dfrac{k\pi x}{L}\right. \\
\qquad \left. + \dfrac{1}{6}(F_{uuu}^*Q_k^3 + 3F_{uuv}^*Q_k^2 + 3F_{uvv}^*Q_k + F_{vvv})\cos^3\dfrac{k\pi x}{L}\right] + O(s^3), \\
\chi:G(u_k(s,x),v_k(s,x)) = G^* + s\left[(G_u^* + G_v^*P_k)\cos\dfrac{k\pi x}{L}\right] \\
\qquad + s^2\left[G_u^*\Phi_3 + G_v^*\Psi_3 + \dfrac{1}{2}(G_{uu}^* + 2G_{uv}^*P_k + G_{vv}^*P_k^2)\cos^2\dfrac{k\pi x}{L}\right] \\
\qquad + s^3\left[G_u^*\Phi_4 + G_v^*\Psi_4 + (G_{uu}^* + G_{uv}^*P_k)\Phi_3\cos\dfrac{k\pi x}{L} + (G_{uv}^* + G_{vv}^*P_k)\Psi_3\cos\dfrac{k\pi x}{L}\right. \\
\qquad \left. + \dfrac{1}{6}(G_{uuu}^* + 3G_{uuv}^*P_k + 3G_{uvv}^*P_k^2 + G_{vvv}P_k^3)\cos^3\dfrac{k\pi x}{L}\right] + O(s^3),
\end{cases}
\tag{98}
$$

$$
\begin{cases}
(u_k'(s,x)v_k(s,x))' = sv^*\cos''\dfrac{k\pi x}{L} + s^2\left[v^*\Phi_1'' + P_k\left(\cos\dfrac{k\pi x}{L}\cos'\dfrac{k\pi x}{L}\right)'\right] \\
\qquad + s^3\left[v^*\Phi_2'' + P_k\left(\Phi_1'\cos\dfrac{k\pi x}{L}\right)' + \left(\Psi_1\cos'\dfrac{k\pi x}{L}\right)'\right] + O(s^3), \\
(u_k(s,x)v_k'(s,x))' = su^*\cos''\dfrac{k\pi x}{L} + s^2\left[u^*\Psi_1'' + Q_k\left(\cos\dfrac{k\pi x}{L}\cos'\dfrac{k\pi x}{L}\right)'\right] \\
\qquad + s^3\left[u^*\Psi_2'' + Q_k\left(\Psi_1'\cos\dfrac{k\pi x}{L}\right)' + \left(\Phi_1\cos'\dfrac{k\pi x}{L}\right)'\right] + O(s^3),
\end{cases}
\tag{99}
$$

and

$$
\begin{aligned}
(\phi(u_k(s,x),v_k(s,x))u_k'(s,x))' = {} & s\phi^*\cos''\frac{k\pi x}{L} + s^2\left[\phi^*\Phi_3'' + (\phi_u^* + \phi_v^*P_k)\left(\cos\frac{k\pi x}{L}\cos'\frac{k\pi x}{L}\right)'\right] \\
& + s^3\left[\phi^*\Phi_4'' + (\phi_u^* + \phi_v^*P_k)\left(\Phi_3'\cos\frac{k\pi x}{L}\right)' + \phi_u^*\left(\Phi_3\cos'\frac{k\pi x}{L}\right)'\right. \\
& \left. + \phi_v^*\left(\Psi_3\cos'\frac{k\pi x}{L}\right)' + \frac{1}{2}(\phi_{uu}^* + 2\phi_{uv}^*P_k + \phi_{vv}^*P_k^2)\left(\cos^2\frac{k\pi x}{L}\cos'\frac{k\pi x}{L}\right)'\right] \\
& + O(s^3).
\end{aligned}
\tag{100}
$$

In the following, we show that $\Upsilon_{d_k}(s)$ (or $\Upsilon_{\chi_k}(s)$) is pitchfork bifurcation if $C_1 = C_3 = 0$.

Lemma 6. *Postulate that all hypotheses in Theorem 1 are satisfied. Then for any $k \in \mathbb{N}_+$, $C_1 = C_3 = 0$ and two bifurcation branches $\Upsilon_{d_k}(s)$ and $\Upsilon_{\chi_k}(s)$ around (u^*, v^*, d_k) and (u^*, v^*, χ_k), respectively, are pitchfork.*

Proof. Plugging (96)–(100) and (38) into the first and second equations in (20), respectively, and combining their s^2-terms, one gets

$$\begin{aligned}
&-D_1\Phi_1'' - \left[F_u^*\Phi_1 + F_v^*\Psi_1 + \frac{1}{2}(F_{uu}^*Q_k^2 + 2F_{uv}^*Q_k + F_{vv}^*)\cos^2\frac{k\pi x}{L}\right]\\
&= C_1(u^* + v^*)\cos''\frac{k\pi x}{L} + d_kD_1\left[(v^*\Phi_1'' + u^*\Psi_1'') + (1+Q_k)\left(\cos\frac{k\pi x}{L}\cos'\frac{k\pi x}{L}\right)'\right],
\end{aligned}$$

and (101)

$$\begin{aligned}
&D_2\Psi_3'' + G_u^*\Phi_3 + G_v^*\Psi_3 + \frac{1}{2}(G_{uu}^* + 2G_{uv}^*P_k + G_{vv}^*P_k^2)\cos^2\frac{k\pi x}{L}\\
&= C_3\phi^*\cos''\frac{k\pi x}{L} + \chi_k\left[\phi^*\Phi_3'' + (\phi_u^* + \phi_v^*P_k)\left(\cos\frac{k\pi x}{L}\cos'\frac{k\pi x}{L}\right)'\right].
\end{aligned}$$

Multiplying the last equality by $\cos\frac{k\pi x}{L}$ and integrating from 0 to L yields

$$\begin{aligned}
C_1 = &-\frac{2L}{(k\pi)^2\phi^*}\left\{\left[-D_1(1+d_kv^*)\left(\frac{k\pi}{L}\right)^2 + F_u^*\right]\int_0^L\Phi_1\cos\frac{k\pi x}{L}dx\right.\\
&\left.+\left[-D_1d_ku^*\left(\frac{k\pi}{L}\right)^2 + F_v^*\right]\int_0^L\Psi_1\cos\frac{k\pi x}{L}dx\right\},
\end{aligned}$$

and (102)

$$\begin{aligned}
C_3 = &-\frac{2L}{(k\pi)^2\phi^*}\left\{\left[\chi_k\phi^*\left(\frac{k\pi}{L}\right)^2 + G_u^*\right]\int_0^L\Phi_3\cos\frac{k\pi x}{L}dx\right.\\
&\left.+\left[-D_2\left(\frac{k\pi}{L}\right)^2 + G_v^*\right]\int_0^L\Psi_3\cos\frac{k\pi x}{L}dx\right\}.
\end{aligned}$$

Plugging (38) and (96)–(100) into the equations of u and v, respectively, and equating s^2-terms, one gets

$$\begin{aligned} &D_2\Psi_1'' + G_u^*\Phi_1 + G_v^*\Psi_1 + \frac{1}{2}(G_{uu}^*Q_k^2 + 2G_{uv}^*Q_k + G_{vv}^*)\cos^2\frac{k\pi x}{L} \\ =&\chi\left[\phi^*\Phi_1'' + (\phi_u^*Q_k + \phi_v^*)\left(\cos\frac{k\pi x}{L}\cos'\frac{k\pi x}{L}\right)'\right], \\ &\text{and} \\ &D_1\Phi_3'' + F_u^*\Phi_3 + F_v^*\Psi_3 + \frac{1}{2}(F_{uu}^* + 2F_{uv}^*P_k + F_{vv}^*P_k^2)\cos^2\frac{k\pi x}{L} \\ =&-dD_1\left[(v^*\Phi_1'' + u^*\Psi_1'') + (P_k+1)\left(\cos\frac{k\pi x}{L}\cos'\frac{k\pi x}{L}\right)'\right]. \end{aligned} \tag{103}$$

By multiplying (103) by $\cos\frac{k\pi x}{L}$ and integrating from 0 to L yields

$$\left[-D_1(1+d_kv^*)\left(\frac{k\pi}{L}\right)^2 + F_u^*\right]\int_0^L \Phi_1\cos\frac{k\pi x}{L}dx + \left[-D_1d_ku^*\left(\frac{k\pi}{L}\right)^2 + F_v^*\right]\int_0^L \Psi_1\cos\frac{k\pi x}{L}dx = 0$$

and

$$\left[\chi_k\phi^*\left(\frac{k\pi}{L}\right)^2 + G_u^*\right]\int_0^L \Phi_3\cos\frac{k\pi x}{L}dx + \left[-D_2\left(\frac{k\pi}{L}\right)^2 + G_v^*\right]\int_0^L \Psi_3\cos\frac{k\pi x}{L}dx = 0. \tag{104}$$

Let us put it another way, due to $(\Phi_1, \Psi_1) \in \mathbb{W}$ as denoted in (40), one gets

$$\left[-D_1d_ku^*\left(\frac{k\pi}{L}\right)^2 + F_v^*\right]\int_0^L \Phi_1\cos\frac{k\pi x}{L}dx + \left[D_1(1+d_kv^*)\left(\frac{k\pi}{L}\right)^2 - F_u^*\right]\int_0^L \Psi_1\cos\frac{k\pi x}{L}dx = 0$$

and

$$\left[-D_2\left(\frac{k\pi}{L}\right)^2 + G_v^*\right]\int_0^L \Phi_3\cos\frac{k\pi x}{L}dx + \left[-\chi_k\phi^*\left(\frac{k\pi}{L}\right)^2 - G_u^*\right]\int_0^L \Psi_3\cos\frac{k\pi x}{L}dx = 0. \tag{105}$$

Together with (102) and (105), we obtain

$$\begin{pmatrix} -D_1(1+d_kv^*)\left(\frac{k\pi}{L}\right)^2 + F_u^* & -D_1d_ku^*\left(\frac{k\pi}{L}\right)^2 + F_v^* \\ -D_1d_ku^*\left(\frac{k\pi}{L}\right)^2 + F_v^* & D_1(1+d_kv^*)\left(\frac{k\pi}{L}\right)^2 - F_u^* \end{pmatrix}\begin{pmatrix} \int_0^L \Phi_1\cos\frac{k\pi x}{L}dx \\ \int_0^L \Psi_1\cos\frac{k\pi x}{L}dx \end{pmatrix} = \begin{pmatrix} 0 \\ 0 \end{pmatrix} \tag{106}$$

and

$$\begin{pmatrix} \chi_k\phi^*\left(\frac{k\pi}{L}\right)^2+G_u^* & -D_2\left(\frac{k\pi}{L}\right)^2+G_v^* \\ -D_2\left(\frac{k\pi}{L}\right)^2+G_v^* & -\chi_k\phi^*\left(\frac{k\pi}{L}\right)^2-G_u^* \end{pmatrix}\begin{pmatrix} \int_0^L \Phi_3\cos\frac{k\pi x}{L}dx \\ \int_0^L \Psi_3\cos\frac{k\pi x}{L}dx \end{pmatrix}=\begin{pmatrix} 0 \\ 0 \end{pmatrix}. \tag{107}$$

Clearly, Two coefficient matrices in (106) and (107) are not singular. Then we have

$$\int_0^L \Phi_1\cos\frac{k\pi x}{L}dx=\int_0^L \Psi_1\cos\frac{k\pi x}{L}dx=\int_0^L \Phi_3\cos\frac{k\pi x}{L}dx=\int_0^L \Psi_3\cos\frac{k\pi x}{L}dx=0. \tag{108}$$

In view of (102) and (108), we see at once that $C_1=C_3=0$. Consequently, Two bifurcation branches $\Upsilon_{d_k}(s)$ and $\Upsilon_{\chi_k}(s)$ around (u^*,v^*,d_k) and (u^*,v^*,χ_k), respectively, have pitchfork type. ■

Rotational direction of $\Upsilon_{d_k}(s)$ (or $\Upsilon_{\chi_k}(s)$) with $s=0$ together with wave mode number k determine the stability of the local branch around (u^*,v^*,d_k) (or (u^*,v^*,χ_k)).

Next, we introduce another main theorem of this work, which offers some criteria to guarantee the stability of bifurcation solutions derived in Theorem 1.

Theorem 4. *Postulate that hypotheses (**H1**)–(**H3**) hold, and all the assumptions of Theorem 1 are satisfied.*

(1) *Suppose that $\phi^*<\frac{-D_2v^*}{u^*\chi}$ and $\chi<0$. Denote Υ_{d_k} as a bifurcating branch of (20) deduced from Theorem 1. Postulate that $d_{k_0}=\min\limits_{k\in\mathbb{N}_+} d_k$. Then $\Upsilon_{d_{k_0}}(s)$, $s\in(-\epsilon,\epsilon)$ is stable for $C_2>0$, and it is unstable for $C_2<0$. In addition, for any $k\neq k_0$, $\Upsilon_{d_k}(s)$, $s\in(-\epsilon,\epsilon)$, is always unstable;*

(2) *Suppose that $\phi^*<\frac{-D_2v^*}{u^*\chi}$ and $\chi>0$. Denote Υ_{d_k} as a bifurcating branch of (20) deduced from Theorem 1. Postulate that $d_{k_0}=\max\limits_{k\in\mathbb{N}_+} d_k$. Then, $\Upsilon_{d_{k_0}}(s)$, $s\in(-\epsilon,\epsilon)$ is stable for $C_2<0$, and it is unstable for $C_2>0$ and $(D_2v^*+u^*\chi\phi^*)(\frac{\pi}{L})^2<(v^*G_v^*-u^*G_u^*)$. In addition, for any $k\neq k_0$, $\Upsilon_{d_k}(s)$, $s\in(-\epsilon,\epsilon)$, is always unstable.*

Proof. The proof is similar to that of Theorem 3.2 in Ref. 55. We only need to change $d>0$ to $d\neq 0$. Hence, it is omitted. ■

The prey-taxis term ϕ is termed repulsive for $\phi^*<0$, otherwise it is called attractive ($\phi^*>0$). We can obtain at once the following corollary.

Corollary 1. *Postulate that hypotheses (**H1**)–(**H3**) hold, and all the assumptions of Theorem 1 are satisfied.*

(1) *Postulate that $\phi^*>\frac{-D_2v^*}{u^*\chi}$, $\chi<0$, and $d_{k_0}=\max\limits_{k\in\mathbb{N}_+} d_k$. Then $\Upsilon_{d_{k_0}}(s)$, $s\in(-\epsilon,\epsilon)$ is stable for $C_2<0$, and it is unstable for $C_2>0$ and $(D_2v^*+u^*\chi\phi^*)(\frac{\pi}{L})^2<(v^*G_v^*-u^*G_u^*)$. In addition, for any $k\neq k_0$, $\Upsilon_{d_k}(s)$, $s\in(-\epsilon,\epsilon)$, is always unstable;*

(2) *Postulate that* $\phi^* > \frac{-D_2 v^*}{u^* \chi}$, $\chi > 0$, *and* $d_{k_0} = \min_{k \in \mathbb{N}_+} d_k$. *Then* $\Upsilon_{d_{k_0}}(s)$, $s \in (-\epsilon, \epsilon)$ *is stable for* $C_2 > 0$, *and it is unstable for* $C_2 < 0$. *In addition, for any* $k \neq k_0$, $\Upsilon_{d_k}(s)$, $s \in (-\epsilon, \epsilon)$, *is always unstable.*

Remark 3. The bifurcation solution corresponding to $\Upsilon_{d_k}(s)$ can be treated as an equilibrium of (1) due to the stability of this bifurcation branch. In Section 6, we propose more detailed mathematical calculations for evaluating C_2 in light of model coefficients.

For prey-taxis parameter χ, we also have the following theorem and corollary.

Theorem 5. *Postulate that hypotheses (***H1***)–(***H3***) hold, and all the assumptions of Theorem 1 are satisfied.*

(1) *Suppose that* $\phi^* < 0$ *and* $d > 0$. *Denote* Υ_{χ_k} *as a bifurcating branch of (20) deduced from Theorem 1. Postulate that* $\chi_{k_0} = \min_{k \in \mathbb{N}_+} \chi_k$. *Then,* $\Upsilon_{\chi_{k_0}}(s)$, $s \in (-\epsilon, \epsilon)$ *is stable for* $C_4 > 0$, *and it is unstable for* $C_4 < 0$. *In addition, for any* $k \neq k_0$, $\Upsilon_{\chi_k}(s)$, $s \in (-\epsilon, \epsilon)$, *is always unstable;*

(2) *Suppose that* $\phi^* < 0$ *and* $d < 0$. *Denote* Υ_{χ_k} *as a bifurcating branch of (20) deduced from Theorem 1. Postulate that* $\chi_{k_0} = \max_{k \in \mathbb{N}_+} \chi_k$. *Then,* $\Upsilon_{\chi_{k_0}}(s)$, $s \in (-\epsilon, \epsilon)$ *is stable for* $C_4 < 0$, *and it is unstable for* $C_4 > 0$. *In addition, for any* $k \neq k_0$, $\Upsilon_{\chi_k}(s)$, $s \in (-\epsilon, \epsilon)$, *is always unstable.*

Corollary 2. *Postulate that hypotheses (***H1***)–(***H3***) hold, and all the assumptions of Theorem 1 are satisfied.*

(1) *Postulate that* $\phi^* > 0$, $d > 0$ *and* $\chi_{k_0} = \max_{k \in \mathbb{N}_+} \chi_k$. *Then* $\Upsilon_{\chi_{k_0}}(s)$, $s \in (-\epsilon, \epsilon)$ *is stable for* $C_4 < 0$, *and it is unstable for* $C_4 > 0$. *In addition, for any* $k \neq k_0$, $\Upsilon_{\chi_k}(s)$, $s \in (-\epsilon, \epsilon)$, *is always unstable;*

(2) *Postulate that* $\phi^* > 0$, $d < 0$ *and* $\chi_{k_0} = \min_{k \in \mathbb{N}_+} \chi_k$. *Then* $\Upsilon_{\chi_{k_0}}(s)$, $s \in (-\epsilon, \epsilon)$ *is stable for* $C_4 > 0$, *and it is unstable for* $C_4 < 0$. *In addition, for any* $k \neq k_0$, $\Upsilon_{\chi_k}(s)$, $s \in (-\epsilon, \epsilon)$, *is always unstable;*

In light of Theorems 4–5 and Corollaries 1–2, one can obtain the choice mechanism of stable wave patterns for other predator–prey systems with cross-diffusion effect and prey-taxis interaction. When the spatial mode $(u_k(s,x), v_k(s,x))$ possesses stability, the wave number k of this pattern must be the positive integer that maximizes (or minimizes) the bifurcating value d_k (or χ_k) if the cross-diffusion rate $d \neq 0$ (or the prey-taxis $\chi \neq 0$). Accordingly, a local bifurcating branch Υ_{d_k} (or Υ_{χ_k}) must be the largest one on the d-axis (or χ-axis) and shifts to the bottom at (u^*, v^*, d_k) (or (u^*, v^*, χ_k)), or vice versa, if it is stable. The other branches are meaningless due to the loss of stability at least for the neighborhood of the bifurcating point. The visualized description of stability analysis from Theorems 4–5 and Corollaries 1–2 can be performed by Figure 1 in detail.

Thanks to Lemmas 1–2, Theorems 4–5, and Corollaries 1–2, we conclude that the positive equilibrium (u^*, v^*) will lose stability to stable wave pattern $\cos \frac{k_0 \pi x}{L}$ by the bifurcation of steady state if d (or χ) goes beyond the marginal value $\max_{k \in \mathbb{N}_+} d_k$ (or $\max_{k \in \mathbb{N}_+} \chi_k$) under the predator (or prey) attractive circumstance and the threshold lines $\min_{k \in \mathbb{N}_+} d_k$ (or $\min_{k \in \mathbb{N}_+} \chi_k$) under the predator (or prey) repulsive situation.

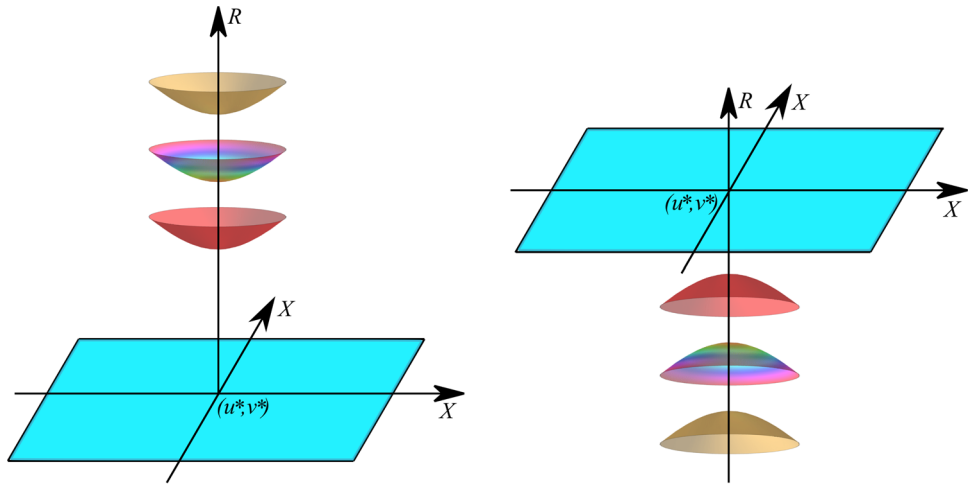

(a) *Case 1.* (b) *Case 2.*

FIGURE 1 Case 1: (1) $d_{k_0} = \min_{k\in\mathbb{N}_+} d_k$ when $\phi^* < \frac{-D_2 v^*}{u^*\chi}$ and $\chi < 0$; (2) $d_{k_0} = \min_{k\in\mathbb{N}_+} d_k$ when $\phi^* > \frac{-D_2 v^*}{u^*\chi}$ and $\chi > 0$; (3) $\chi_{k_0} = \min_{k\in\mathbb{N}_+} \chi_k$ when $\phi^* < 0$ and $d > 0$; (4) $\chi_{k_0} = \min_{k\in\mathbb{N}_+} \chi_k$ when $\phi^* > 0$ and $d < 0$. Case 2: (1) $d_{k_0} = \max_{k\in\mathbb{N}_+} d_k$ when $\phi^* < \frac{-D_2 v^*}{u^*\chi}$ and $\chi > 0$; (2) $d_{k_0} = \max_{k\in\mathbb{N}_+} d_k$ when $\phi^* > \frac{-D_2 v^*}{u^*\chi}$ and $\chi < 0$; (3) $\chi_{k_0} = \max_{k\in\mathbb{N}_+} \chi_k$ when $\phi^* < 0$ and $d < 0$; (4) $\chi_{k_0} = \max_{k\in\mathbb{N}_+} \chi_k$ when $\phi^* > 0$ and $d > 0$.

Remark 4. As a general case, determining such marginal wave value k_0 by the model coefficients is impossible since the traditional Crandall–Rabinowitz bifurcation theory has limitations. Actually, it holds

$$\begin{aligned}
\lim_{k\to\infty,k\in\mathbb{N}_+} d_k &= \lim_{k\to\infty,k\in\mathbb{N}_+} \frac{-D_1D_2\left(\frac{k\pi}{L}\right)^4 + (D_1G_v^* + D_2F_u^* + \chi\phi^*F_v^*)\left(\frac{k\pi}{L}\right)^2 - (F_u^*G_v^* - F_v^*G_u^*)}{(D_1D_2v^* + D_1u^*\chi\phi^*)\left(\frac{k\pi}{L}\right)^4 - (D_1v^*G_v^* - D_1u^*G_u^*)\left(\frac{k\pi}{L}\right)^2} \\
&= \frac{-D_2}{D_2v^* + u^*\chi\phi^*} = \lim_{L\to 0^+} d_k, \\
\lim_{k\to\infty,k\in\mathbb{N}_+} \chi_k &= \lim_{k\to\infty,k\in\mathbb{N}_+} \frac{\left(D_1(1+dv^*)\left(\frac{k\pi}{L}\right)^2 - F_u^*\right)\left(D_2\left(\frac{k\pi}{L}\right)^2 - G_v^*\right) + \left(D_1du^*\left(\frac{k\pi}{L}\right)^2 - F_v^*\right)G_u^*}{\left(F_v^* - D_1du^*\left(\frac{k\pi}{L}\right)^2\right)\phi^*\left(\frac{k\pi}{L}\right)^2} \\
&= \frac{D_2(1+dv^*)}{-du^*\phi^*} = \lim_{L\to 0^+} \chi_k.
\end{aligned} \tag{109}$$

In other words, if the interval length L is sufficient small, d_k (or χ_k) for any given k is an approximation of $\frac{-D_2}{D_2v^*+u^*\chi\phi^*}$ (or $\frac{D_2(1+dv^*)}{-du^*\phi^*}$). If the effect of the prey-taxis vanishes, that is, $\chi = 0$, then for any given k, $d_k \approx -\frac{1}{v^*}$ for small L. Conversely, when the impact of cross-diffusion disappears, that is, $d = 0$, then $\chi \approx \frac{D_1D_2(\frac{k\pi}{L})^2}{F_v^*\phi^*}$, which means that $\chi_1 = \max_{k\in\mathbb{N}_+} \chi_k$ for $\phi^* > 0$ and $\chi_1 = \min_{k\in\mathbb{N}_+} \chi_k$ for $\phi^* < 0$. For determining such marginal wave value k_0 by the model coefficients, the traditional

Crandall–Rabinowitz bifurcation theory can be only applied to the case of reaction–diffusion model with prey-taxis based on a sufficient small L. Fortunately, the user-friendly version of this bifurcation theory proposed by Shi and Wang[57] can remedy this deficiency. We can easily understand that the monotone solution does not have to be the only stable mode for each case. In addition, we can obviously discover that k_0, with respect to L, is nondecreasing, even increasing.

Remark 5. By giving a monotone solution of (20) in $(0, L)$, we can establish the corresponding nonmonotone steady states in a sufficient long interval via periodic extension and symmetry of monotone steady state at $\cdots, -3L, -2L, -L, 0, L, 2L, 3L, \cdots$.

In Theorems 4–5, the signs of C_2 and C_4 determine the stability of marginal bifurcating branch. Actually, similar to the computation in (102) for C_1 and C_3, we can exactly obtain the representation of C_2 and C_4, which are postponed to the Appendix due to the direct but tedious computations.

5 | NUMERICAL SIMULATIONS

Numerical examples can verify these theoretical results. In this section, we need to describe and check our main results via numerical simulations of (1). At first, we need to illustrate the effects of cross-diffusion rate d and prey-taxis coefficient χ for the local stability of cross-diffusion model with prey-taxis.

5.1 | Numerical examples for choosing d as a bifurcation parameter

Without loss of generality, we select the Beddington–DeAngelis and Tanner kinetic functions given by (3). Even if the initial data are chosen as a perturbation of homogeneous equilibrium, our mathematical experiments can also demonstrate that prey-taxis model with Beddington–DeAngelis and Tanner functional responses can occur miscellaneous remarkable spatiotemporal patterns with interesting structures. In following, we take

$$\phi(u, v) = uv(M - u) \tag{110}$$

as a sensitivity function, which means that the species of prey can protect themselves, or even attack predator species ($d < 0$) in a group if the density value of population exceeded the threshold level M.

For two kinetic functions $F(u, v)$ and $G(u, v)$, model coefficients in (3) are selected to be $r_1 = 2$, $b = 1, \delta = 1, \alpha = 1, \beta = 1, r_2 = 2$, and $\gamma = 2$. It is obvious via a simple computation that (1) exists a unique interior equilibrium

$$\begin{aligned} &(u^*, v^*) = \left(\frac{5 + \sqrt{65}}{10}, \frac{10 + 2\sqrt{65}}{5}\right) \approx (1.3062, 5.2249), \\ &F_u^*(u^*, v^*) = -1.1858, \ \ F_v^*(u^*, v^*) = -0.0531, \ \ G_u^*(u^*, v^*) = 8, \ \ G_v^*(u^*, v^*) = -2. \end{aligned} \tag{111}$$

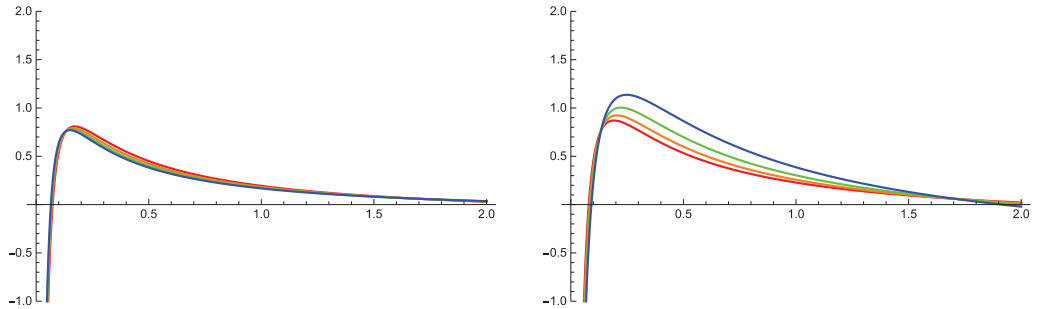

(a) $\chi > 0$. (b) $\chi < 0$.

FIGURE 2 The graph of d_k with respect to λ_k

Meanwhile, the swarm defense threshold in (110) is chosen to be $M = 0.5$, which implies $\phi^* \approx -5.5021$.

In light of the basic theory of elliptic equations, the eigenvalue problem

$$\begin{cases} -\varphi'' = \lambda\varphi, & x \in (0, L), \\ \varphi' = 0, & x = 0, L, \end{cases} \tag{112}$$

has a simple eigenvalue sequence $\lambda_k = (\frac{k\pi}{L})^2$, $k = 0, 1, 2, \ldots$. The corresponding normalized eigenfunctions can be performed by

$$\begin{cases} \varphi_k(x) = \dfrac{1}{\sqrt{L}}, & k = 0, \\ \varphi_k(x) = \sqrt{\dfrac{2}{L}} \cos\left(\dfrac{k\pi x}{L}\right), & k > 0. \end{cases} \tag{113}$$

Setting $D_1 = 0.4$, $D_2 = 40$, and plugging them into the formula of d_k and χ_k lead us to

$$\begin{aligned} d_k =& \frac{-D_1 D_2 \lambda_k^2 + (D_1 G_v^* + D_2 F_u^* + \chi\phi^* F_v^*)\lambda_k - (F_u^* G_v^* - F_v^* G_u^*)}{(D_1 D_2 v^* + D_1 u^* \chi\phi^*)\lambda_k^2 - (D_1 v^* G_v^* - D_1 u^* G_u^*)\lambda_k} \\ =& \frac{-16\lambda_k^2 - (48.2320 + 0.2922\chi)\lambda_k - 2.7964}{(83.5984 + 2.8747\chi)\lambda_k^2 + 8.3598\lambda_k}, \quad k \in \mathbb{N}_+. \end{aligned} \tag{114}$$

By setting $\chi = 5$ (red), 10 (orange), 15 (green), and 20 (blue), respectively, we obtain Figure 2A. By setting $\chi = -5$ (red), -10 (orange), -15 (green), and -20 (blue), respectively, we obtain Figure 2B.

We can also choose two Beddington–DeAngelis kinetic functions described by (3). System parameters in (3) are chosen as $\alpha = \frac{1}{15}$, $\beta = \frac{1}{10}$, $c = 6$, and $d = 2$. It is clear by a direct calculation that (1) exists a unique interior equilibrium

$$\begin{aligned} &(u^*, v^*) \approx (0.4154, 0.7285), \\ &F_u^*(u^*, v^*) = -0.4024, \ F_v^*(u^*, v^*) = -0.2749, \ G_u^*(u^*, v^*) = 3.4294, \ G_v^*(u^*, v^*) = -0.3506. \end{aligned} \tag{115}$$

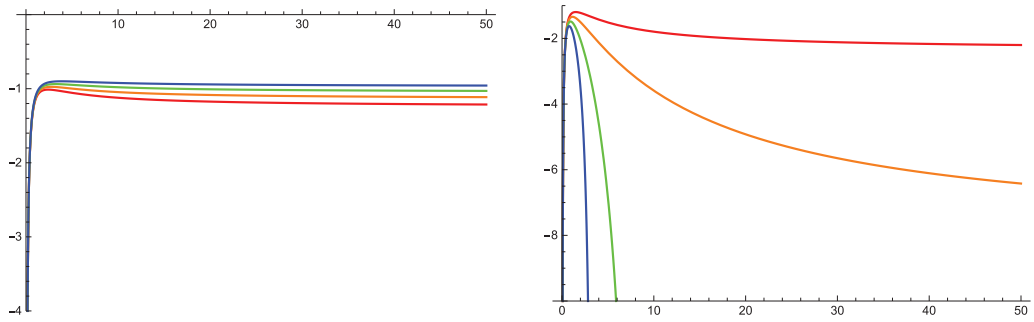

(a) $\chi > 0$. (b) $\chi < 0$.

FIGURE 3 The graph of d_k with respect to λ_k

Meanwhile, the swarm defense threshold in (110) is chosen to be $M = 2.8227$, which implies $\phi^* \approx 0.7285$. Setting $D_1 = 1$, $D_2 = 1$, and plugging them into the formula of d_k lead us to

$$\begin{aligned} d_k =& \frac{-D_1D_2\lambda_k^2 + (D_1G_v^* + D_2F_u^* + \chi\phi^*F_v^*)\lambda_k - (F_u^*G_v^* - F_v^*G_u^*)}{(D_1D_2v^* + D_1u^*\chi\phi^*)\lambda_k^2 - (D_1v^*G_v^* - D_1u^*G_u^*)\lambda_k} \\ =& \frac{-\lambda_k^2 - (0.7530 + 0.2003\chi)\lambda_k - 1.0838}{(0.7285 + 0.3026\chi)\lambda_k^2 + 1.6800\lambda_k}, \quad k \in \mathbb{N}_+. \end{aligned} \tag{116}$$

By setting $\chi = 0.25$ (red), 0.5 (orange), 0.75 (green), and 1 (blue), respectively, we obtain Figure 3A. By setting $\chi = -1$ (red), -2 (orange), -3 (green), and -4 (blue), respectively, we obtain Figure 3B.

For the last two types of functional responses, we can easily deduce the following remark.

Remark 6. We can obtain the impact of χ by studying the formulas of d_k. The conclusions are as follow:

(1) When $d_{k_0} = \max\limits_{k\in\mathbb{N}_+} d_k > 0$ and $\chi > 0$ (or $\chi < 0$), the value of $d_{k_0} = \max\limits_{k\in\mathbb{N}_+} d_k$ and the corresponding k_0 will be reduced by increasing the value of χ;
(2) When $d_{k_0} = \max\limits_{k\in\mathbb{N}_+} d_k < 0$ and $\chi > 0$ (or $\chi < 0$), the value of $d_{k_0} = \max\limits_{k\in\mathbb{N}_+} d_k$ and the corresponding k_0 will be increased by increasing the value of χ.

5.2 | Numerical examples for choosing χ as a bifurcation parameter

Setting $D_1 = 0.4$, $D_2 = 40$, and plugging them into the formula of χ_k lead us to

$$\begin{aligned} \chi_k =& \frac{D_1D_2(1 + dv^*)\lambda_k^2 - [D_1G_v^*(1 + dv^*) + D_2F_u^* - D_1u^*G_u^*d]\lambda_k + (F_u^*G_v^* - F_v^*G_u^*)}{-D_1du^*\phi^*\lambda_k^2 + F_v^*\phi^*\lambda_k} \\ =& \frac{16(1 + 5.2249d)\lambda_k^2 - (48.2320 - 8.3598d)\lambda_k + 2.7964}{-2.8747d\lambda_k^2 - 0.2922\lambda_k}, \quad k \in \mathbb{N}_+. \end{aligned} \tag{117}$$

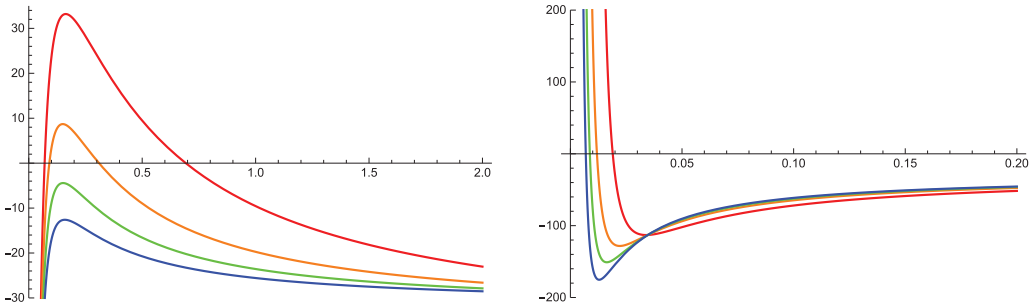

(a) $d > 0$. (b) $d < 0$.

FIGURE 4 The graph of χ_k with respect to λ_k

By setting $d = 0.5$ (red), 1 (orange), 1.5 (green), and 2 (blue), respectively, we obtain Figure 4A. By setting $d = -10$ (red), -20 (orange), -30 (green), and -40 (blue), respectively, we obtain Figure 4B.

Remark 7. We can obtain the impact of d by studying the formulas of χ_k. The conclusions are as follow:

(1) When $\chi_{k_0} = \max_{k\in\mathbb{N}_+} \chi_k > 0$ and $d > 0$, the value of $\chi_{k_0} = \max_{k\in\mathbb{N}_+} \chi_k$ and the corresponding k_0 will be decreased by increasing the value of d;
(2) When $\chi_{k_0} = \max_{k\in\mathbb{N}_+} \chi_k < 0$ and $d > 0$, the value of $\chi_{k_0} = \max_{k\in\mathbb{N}_+} \chi_k$ and the corresponding k_0 will be increased by decreasing the value of d.

For double Beddington–DeAngelis functional responses, we plug the same coefficients in (115) into the formula of χ_k and obtain

$$\begin{aligned}\chi_k =& \frac{D_1D_2(1+dv^*)\lambda_k^2 - [D_1G_v^*(1+dv^*) + D_2F_u^* - D_1u^*G_u^*d]\lambda_k + (F_u^*G_v^* - F_v^*G_u^*)}{-D_1du^*\phi^*\lambda_k^2 + F_v^*\phi^*\lambda_k} \\ =& \frac{(1+0.7285d)\lambda_k^2 + (0.7530+1.6800d)\lambda_k + 1.0838}{-0.3026d\lambda_k^2 - 0.2003\lambda_k}, \quad k \in \mathbb{N}_+.\end{aligned} \tag{118}$$

By setting $d = 0.1$ (red), 0.2 (orange), 0.3 (green), and 0.4 (blue), respectively, we obtain Figure 5A. By setting $d = -1$ (red), -2 (orange), -3 (green), and -4 (blue), respectively, we obtain Figure 5B.

Remark 8. We can also obtain the impact of d by studying the formulas of χ_k. The conclusions are as follow:

(1) When $\chi_{k_0} = \max_{k\in\mathbb{N}_+} \chi_k < 0$ and $d > 0$, the value of $\chi_{k_0} = \max_{k\in\mathbb{N}_+} \chi_k$ and the corresponding k_0 will be increased by increasing the value of d;
(2) When $\chi_{k_0} = \max_{k\in\mathbb{N}_+} \chi_k < 0$ (or $\chi_{k_0} = \min_{k\in\mathbb{N}_+} \chi_k < 0$) and $d < 0$, the value of $\chi_{k_0} = \max_{k\in\mathbb{N}_+} \chi_k$ (or $\chi_{k_0} = \min_{k\in\mathbb{N}_+} \chi_k$) and the corresponding k_0 will be increased by increasing the value of d.

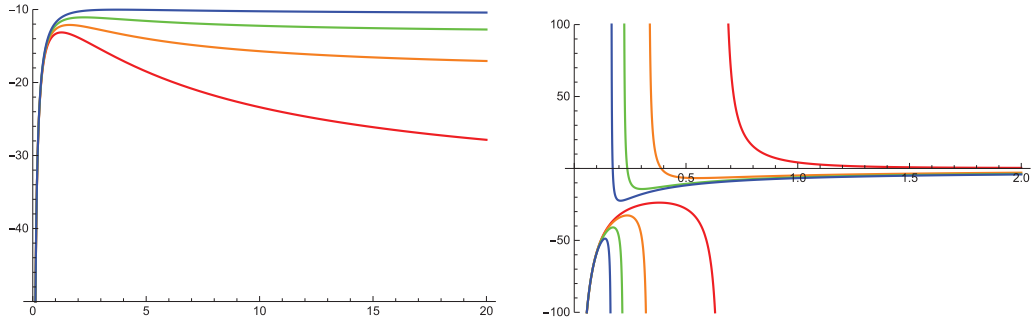

(a) $d > 0$. (b) $d < 0$.

FIGURE 5 The graph of χ_k with respect to λ_k

In terms of Remarks 7 and 8, we see that the pattern formations of system (4) not only depend on the signs of d or χ but also on the functional responses ($F(u, v)$ and $G(u, v)$) and the diffusion rates (D_1 and D_2).

Meanwhile, Figure 5B shows an interesting phenomenon that the maximal and the minimal values of χ_k can coexist with the different positive integers $\overline{k}$ and $\underline{k}$ in a same model. In other words, the local stability interval for χ is $[\min_{\underline{k}\in\mathbb{N}_+} \chi_{\underline{k}}, \max_{\overline{k}\in\mathbb{N}_+} \chi_{\overline{k}}]$ if we treat χ as a bifurcation parameter. In addition, this interval will tend to 0 when we increase the value of d ($d < 0$).

Remark 9. From the above experimental results, we verify that the local stability might appear in the following four cases, **(1)** $d > 0$, $\chi > 0$; **(2)** $d > 0$, $\chi < 0$; **(3)** $d < 0$, $\chi > 0$; **(4)** $d < 0$, $\chi < 0$, which are meaningful in the modeling.

5.3 | Numerical examples for nonconstant steady states: *d* is a bifurcation parameter

We choose the same system parameters in Section 5.1. In Figure 6, we draw the numerical solutions of (1) with double Beddington–DeAnglis functional responses and (110) under the spatial area (0,300) and the initial condition $(u_0(x), v_0(x)) = (u^*, v^*) + 0.001\cos 4\pi x$, which are small disturbances of positive equilibrium. We can easily calculate via (116) to obtain that $\max_{k\in\mathbb{N}_+} d_k = d_{72} \approx -1.58$. Hence, -1.58 can be regarded as a critical bifurcation value and $k_0 = 72$ can be treated as a positive stable wave integer. Meanwhile, $\cos\frac{72\pi x}{300} = \cos\frac{6\pi x}{25}$ represents the pattern of stable wave which implies that the homogeneous equilibrium (u^*, v^*) loses its stability. We need to notice that the initial conditions possess the profiles of space by involving perturbations $\cos 4\pi x$; but, the patterns formate in terms of the mode of stable wave $\cos\frac{6\pi x}{25}$. These figures verify our main theoretical results in the stability of bifurcating branches.

Furthermore, we offer a detailed illustration on the impacts of cross-diffusion rate d for spatial-temporal patterns in (1) with double Beddington–DeAnglis functional responses. Since $M > u^*$ implies $\phi^* > 0$, a smaller cross-diffusion rate d is conducive to the congregation and spatial heterogeneity of prey in (1). Our experimental results demonstrate that population densities evolve into spiculate functions if d is smaller than a certain threshold. We can also discover that cross-diffusion models contain a control mechanism about population densities, that is, the max-

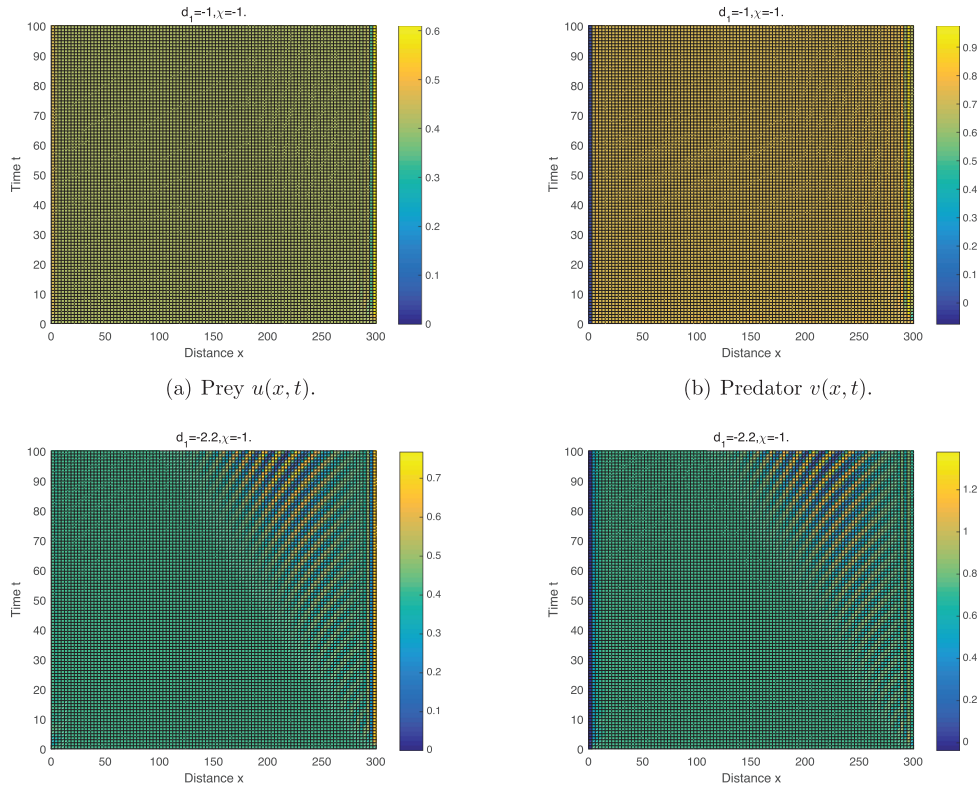

(a) Prey $u(x,t)$. (b) Predator $v(x,t)$.

(c) Prey $u(x,t)$. (d) Predator $v(x,t)$.

FIGURE 6 Spatiotemporal pattern formations of positive nonconstant steady states of (1) with Beddington–DeAnglis and Tanner functional responses and (110) over $\Omega = (0, 300)$. Model coefficients are selected the same as Section 5.1. Initial conditions are selected $(u_0(x), v_0(x)) = (u^*, v^*) + 0.001 \cos 4\pi x$.

imum value of congregation densities are maintained below some threshold values despite the cross-diffusion rate d is getting smaller.

5.4 | Numerical examples for nonconstant steady states: χ is a bifurcation parameter

We choose the same system parameters in Section 5.1. In Figure 7, we draw the numerical solutions of (1) with Beddington–DeAnglis and Tanner functional responses and (110) under the spatial area (0,400) and the initial condition $(u_0(x), v_0(x)) = (u^*, v^*) + 0.001 \cos 4\pi x$, which are small disturbances of positive equilibrium. We can easily calculate via (117) to obtain that $\max_{k\in\mathbb{N}_+} \chi_k = \chi_{49} \approx -4.43$. Thus, the related discussion similar to Figure 6 can be derived. At the same time, Figure 7E,F shows that the appearance of time-periodic modes over (0,400).

In Figure 8, we focus on the impact of spatial region length on the positive stable wave integer if χ has been selected nearby the critical value of bifurcation. Model coefficients and initial conditions are chosen to be the same as those for Section 5.1 and Figure 7, respectively. The spatial region length L are selected to be 300, 400, 500, and 600. In light of (16), we can easily

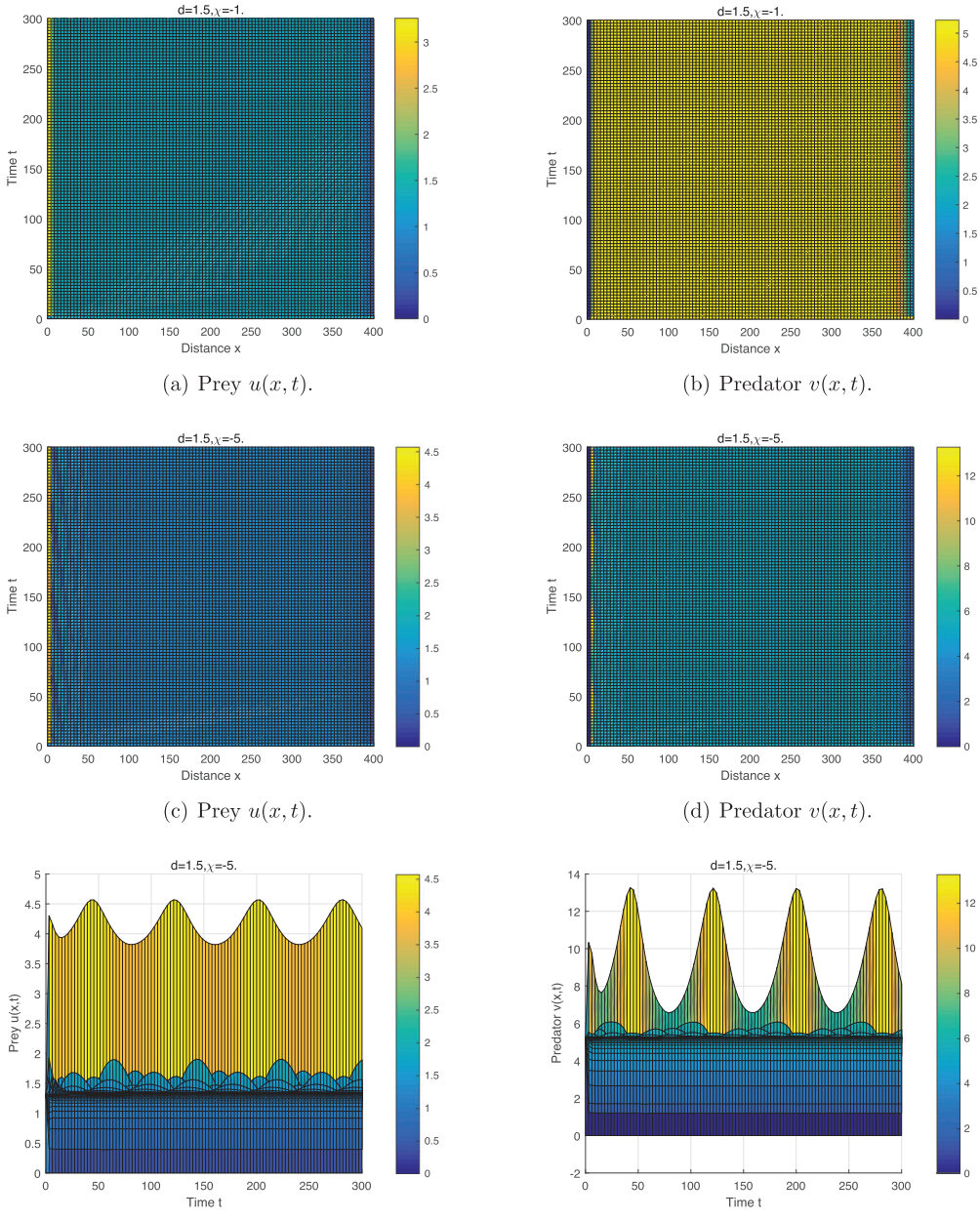

(a) Prey $u(x,t)$. (b) Predator $v(x,t)$.

(c) Prey $u(x,t)$. (d) Predator $v(x,t)$.

(e) Prey $u(x,t)$. (f) Predator $v(x,t)$.

FIGURE 7 Spatiotemporal pattern formations of nonconstant steady states of (1) with Beddington–DeAnglis and Tanner functional responses and (110) over $\Omega = (0, 400)$. Model coefficients are selected the same as Section 5.1. Initial conditions are selected $(u_0(x), v_0(x)) = (u^*, v^*) + 0.001 \cos 4\pi x$.

obtain the critical value of bifurcation via a simple calculation, that is, $\chi_{37} \approx -4.4300\,(\lambda \approx 0.1501)$, $\chi_{49} \approx -4.4375\,(\lambda \approx 0.1481)$, $\chi_{62} \approx -4.4292\,(\lambda \approx 0.1518)$, and $\chi_{74} \approx -4.4300\,(\lambda \approx 0.1501)$. Consequently, in terms of Corollary 2, (u^*, v^*) is unstable to the pattern of stable wave $\cos\frac{37\pi x}{300}$, $\cos\frac{49\pi x}{400}$, $\cos\frac{62\pi x}{500}$, and $\cos\frac{74\pi x}{600}$, respectively. Figure 8 has demonstrated these numerical verifications. By

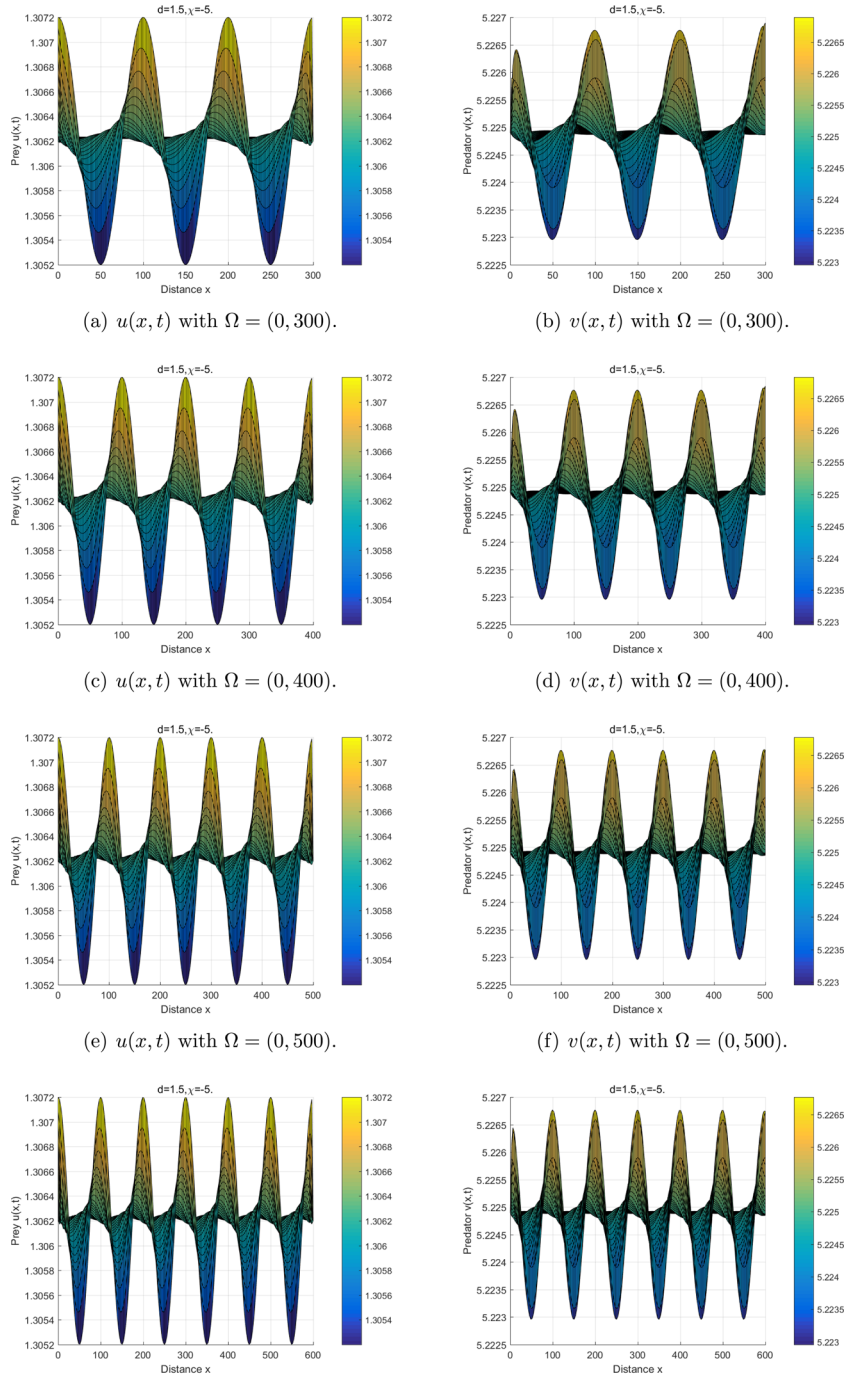

(a) $u(x,t)$ with $\Omega = (0, 300)$. (b) $v(x,t)$ with $\Omega = (0, 300)$.

(c) $u(x,t)$ with $\Omega = (0, 400)$. (d) $v(x,t)$ with $\Omega = (0, 400)$.

(e) $u(x,t)$ with $\Omega = (0, 500)$. (f) $v(x,t)$ with $\Omega = (0, 500)$.

(g) $u(x,t)$ with $\Omega = (0, 600)$. (h) $v(x,t)$ with $\Omega = (0, 600)$.

FIGURE 8 Stabilization and pattern formation of nonconstant steady states with perturbations of (u^*, v^*). Model coefficients are selected the same as Section 5.1. Actually the simulations are done in the time-dependent case and the pictures we proposed are the projections of all the graphs for $t = 0$ to $t = 100$. Initial conditions are selected $(u_0(x), v_0(x)) = (u^*, v^*) + 0.001 \cos 4\pi x$. These graphs admirably describe the stable wave pattern choice mechanism. Furthermore, a larger spatial region length can lead to more aggregations than a smaller one.

increasing the length of spatial region, the positive stable wave integer will also grow. In addition, a larger spatial region length can lead to more aggregations than a smaller one. The work introduced by Painter and Hillen[45] has investigated the influence of the spatial region length L on the stable wave pattern of Keller–Segel systems involving logistic growth by numerical experiments. However, it is not explicitly shown how to find out the positive stable wave integer and the corresponding profile via model coefficients. The current work gives a complete version of the formulation in (16) and (18).

In Figure 8, one can observe that chaotic patterns turn to stationary patterns if the spatial region length L increases. Rigorous mathematical discussion of this interesting phenomenon is out of the scope of our research direction.

6 | CONCLUSION AND DISCUSSION

In this work, the existence and stability of positive nonconstant steady states of general cross-diffusion models with prey-taxis are studied. The main conclusions can be summarized in the following four aspects:

- The results of this work are not only new but also include some previous works. When $d = 0$, model (1) will reduce to a reaction–advection–diffusion system with taxis interaction, chemotaxis model, or competition model. It depends on two kinetic functions $F(u, v)$ and $G(u, v)$. When $\chi = 0$, model (1) will reduce to a cross-diffusion model with prey cross-diffusion effect.
- We can discover that both cross-diffusion rate d and prey-taxis parameter χ can be viewed as two bifurcation parameters. Both of them have separate formulas (16) and (18), that is, d_k and χ_k, to obtain the critical values of bifurcations.
- $d < 0$ describes the aggregation effects among the species. Therefore, we should not exclude this case since nonconstant steady states can also obtain when $d < 0$.
- Small domain can guarantee the critical value of χ_k or d_k, and can be maintained at a nonzero value. It means that the coexistence of cross-diffusion effect and taxis interaction also has opportunity to obtain the local stability of (u^*, v^*), even $d < 0$.

We need to point out that our theoretical framework is not restricted to predator–prey systems. We claim that it might also be applied in competition model, symbiosis system, and so on. For instance, Wang et al[55] have introduced three interesting competition models in bounded domain with homogeneous Neumann boundary condition and initial data

$$\begin{cases} u_t = \nabla \cdot (D_1 \nabla u + \chi u \phi(v) \nabla v) + (a_1 - b_1 u - c_1 v)u, \\ \tau v_t = D_2 \Delta v + (a_2 - b_2 u - c_2 v)v, \end{cases} \tag{119}$$

$$\begin{cases} u_t = \Delta[(D_1 + \rho_{11} u + \rho_{12} v)u] + (a_1 - b_1 u - c_1 v)u, \\ v_t = \Delta[(D_2 + \rho_{21} u + \rho_{22} v)v] + (a_2 - b_2 u - c_2 v)v, \end{cases} \tag{120}$$

and

$$\begin{cases} u_t = \nabla \cdot (D_1 \nabla u + \chi \Phi_1(u, v) \nabla v) + (a_1 - b_1 u - c_1 v)u, \\ v_t = \nabla \cdot (D_2 \nabla v + \chi \Phi_2(u, v) \nabla u) + (a_1 - b_1 u - c_1 v)u. \end{cases} \tag{121}$$

It is easy to check by a simple computation that system (125) has a unique positive equilibrium

$$(u^*, v^*) = \left(\frac{a_1c_2 - a_2c_1}{b_1c_2 - b_2c_1}, \frac{a_2b_1 - a_1b_2}{b_1c_2 - b_2c_1} \right) \tag{122}$$

when and only when

$$\frac{c_1}{c_2} < \frac{a_1}{a_2} < \frac{b_1}{b_2} \text{ or } \frac{b_1}{b_2} < \frac{a_1}{a_2} < \frac{c_1}{c_2}. \tag{123}$$

In addition, the signs of F_u^*, F_v^*, G_u^*, and G_v^* should be reconsidered. Thus we have

$$\begin{aligned} F_u^* &= a_1 - 2b_1u^* - c_1v^* = \frac{b_1(a_2c_1 - a_1c_2)}{b_1c_2 - b_2c_1} < 0, \\ F_v^* &= -c_1u^* < 0, \\ G_u^* &= -b_2v^* < 0, \\ G_v^* &= a_2 - b_2u^* - 2c_2v^* = \frac{c_2(a_1b_2 - a_2b_1)}{b_1c_2 - b_2c_1} < 0 \end{aligned} \tag{124}$$

when and only when $\frac{c_1}{c_2} < \frac{a_1}{a_2} < \frac{b_1}{b_2}$ or $\frac{b_1}{b_2} < \frac{a_1}{a_2} < \frac{c_1}{c_2}$.

In the Lotka–Volterra kinetic functions $F(u, v) = (a_1 - b_1u - c_1v)u$ and $G(u, v) = (a_2 - b_2u - c_2v)v$, we can derive the following cross-diffusion model:

$$\begin{cases} \partial_t u = D_1\partial_{xx}(u + duv) + (a_1 - b_1u - c_1v)u, \\ \partial_t v = \partial_x(D_2\partial_x v - \chi\phi(u, v)\partial_x u) + (a_2 - b_2u - c_2v)v. \end{cases} \tag{125}$$

ACKNOWLEDGMENTS

Open access funding enabled and organized by Projekt DEAL.

CONFLICTS OF INTEREST

The authors declare that there is no conflict of interest that could be perceived as prejudicing the impartiality of the research reported.

CREDIT AUTHORSHIP CONTRIBUTION STATEMENT

Demou Luo: Investigation, Writing-original draft, Software. **Qiru Wang**: Writing-review and editing. **Li Chen**: Writing-review and editing.

DATA AVAILABILITY STATEMENT

Data sharing not applicable to this article as no data sets were generated or analyzed during the current study.

ORCID

Demou Luo https://orcid.org/0000-0002-1444-1777

REFERENCES

1. Beddington JR. Mutual interference between parasites or predators and its effect on searching efficiency. *J Anim Ecol*. 1975;44:331-340.
2. DeAngelis DL, Goldstein RA, O'Neill RV. A model for tropic interaction. *Ecology*. 1975;56:881-892.
3. Tanner JT. The stability and the intrinsic growth rates of prey and predator populations. *Ecology*. 1975;56:855-867.
4. Luo D. The study of global stability of a periodic Beddington–DeAngelis and Tanner predator–prey model. *Results Math*. 2019;74(3):1-18.
5. Hsu S, Huang T. Global stability for a class of predator–prey systems. *SIAM J Appl Math*. 1995;55:763-783.
6. Luo D. Global stability of solutions in a reaction–diffusion system of predator–prey model. *Filomat*. 2018;32:4665-4672.
7. Sáez E, González-Olivares E. Dynamics of a predator–prey model. *SIAM J Appl Math*. 1999;59:1867-1878.
8. Wollkind DJ, Collings JB, Logan J. Metastability in a temperature-dependent model system for predator–prey mite outbreak interactions on fruit trees. *Bull Math Biol*. 1988;50:379-409.
9. Pal PJ, Mandal PK. Bifurcation analysis of a modified Leslie–Gower predator–prey model with Beddington–DeAngelis functional response and strong Allee effect. *Math Comput Simul*. 2014;97:123-146.
10. Luo D, Wang Q. Global bifurcation and pattern formation for a reaction–diffusion predator–prey model with prey-taxis and double Beddington–DeAngelis functional responses. *Nonlinear Anal Real World Appl*. 2022;67:103638.
11. Peng R, Wang MX. Positive steady states of the Holling–Tanner prey–predator model with diffusion. *Proc R Soc Edinb A*. 2005;135:149-164.
12. Qi Y, Zhu Y. The study of global stability of a diffusive Holling–Tanner predator–prey model. *Appl Math Lett*. 2016;57:132-138.
13. Li X, Jiang WH, Shi JP. Hopf bifurcation and turing instability in the reaction–diffusion Holling–Tanner predator–prey model. *IMA J Appl Math*. 2013;78:287-306.
14. Ma ZP, Li WT. Bifurcation analysis on a diffusive Holling–Tanner predator–prey model. *Appl Math Model*. 2013;37:4371-4384.
15. Ghazaryan A, Manukian V, Schecter S. Travelling waves in the Holling–Tanner model with weak diffusion. *Proc R Soc Lond A*. 2015;471:20150045.
16. Shigesada N, Kawasaki K, Teramoto E. Spatial segregation of interacting species. *J Theor Biol*. 1979;79:83-89.
17. Li C. On global bifurcation for a cross-diffusion predator–prey system with prey-taxis. *Comput Math Appl*. 2018;76:1014-1025.
18. Tuôc PV. Global existence of solutions to Shigesada–Kawasaki–Teramoto cross-diffusion systems on domains of arbitrary dimensions. *Proc Am Math Soc*. 2007;135:3933-3941.
19. Kuto K. Full cross-diffusion limit in the stationary Shigesada–Kawasaki–Teramoto model. *Ann Inst Henri Poincaré C, Anal non lineaire*. 2021;38:1943-1959.
20. Kuto K. Global structure of steady-states to the full cross-diffusion limit in the Shigesada-Kawasaki-Teramoto model. Preprint, 2021. https://doi.org/10.48550/arXiv.2106.02060
21. Chen L, Jüngel A. Analysis of a multi-dimensional parabolic population model with strong cross-diffusion. *SIAM J Math Anal*. 2004;36:301-322.
22. Chen L, Jüngel A. Analysis of a parabolic cross-diffusion population model without self-diffusion. *J Differ Equ*. 2006;224:39-59.
23. Bie Q, Wang Q, Yao Z. Cross-diffusion induced instability and pattern formation for a Holling type-II predator–prey model. *Appl Math Comput*. 2014;247:1-12.
24. Chen L, Daus ES, Holzinger A, Jüngel A. Rigorous derivation of population cross-diffusion systems from moderately interacting particle systems. *J Nonlinear Sci*. 2021;31(94):1-38.
25. Kareiva P, Odell G. Swarms of predators exhibit "preytaxis" if individual predators use area-restricted search. *Am Nat*. 1987;130:233-270.
26. Sapoukhina N, Tyutyunov Y, Arditi R. The role of prey taxis in biological control: a spatial theoretical model. *Am Nat*. 2003;162:61-76.
27. Ainseba BE, Bendahmane M, Noussair A. A reaction–diffusion system modeling predator–prey with prey-taxis. *Nonlinear Anal Real World Appl*. 2008;9:2086-2105.

28. He X, Zheng S. Global boundedness of solutions in a reaction–diffusion system of predator–prey model with prey-taxis. *Appl Math Lett*. 2015;49:73-77.
29. Lee JM, Hilllen T, Lewis MA. Continuous traveling waves for prey-taxis. *Bull Math Biol*. 2008;70:654-676.
30. Lee JM, Hilllen T, Lewis MA. Pattern formation in prey-taxis systems. *J Biol Dyn*. 2009;3:551-573.
31. Tao Y. Global existence of classical solutions to a predator–prey model with nonlinear prey-taxis. *Nonlinear Anal Real World Appl*. 2010;11:2056-2064.
32. Wang K, Wang Q, Yu F. Stationary and time-periodic patterns of two-predator and one-prey systems with prey-taxis. *Discrete Contin Dyn Syst*. 2017;37:505-543.
33. Kuto K. Stability of steady-state solutions to a prey–predator system with cross-diffusion. *J Differ Equ*. 2004;197:293-314.
34. Kuto K, Yamada Y. Multiple coexistence states for a prey–predator system with cross-diffusion. *J Differ Equ*. 2004;197:315-348.
35. Peng R, Wang MX, Yang GY. Stationary patterns of the Holling–Tanner prey–predator model with diffusion and cross-diffusion. *Appl Math Comput*. 2008;196:570-577.
36. Wang YX, Li WT. Spatial patterns of the Holling–Tanner predator–prey model with nonlinear diffusion effects. *Appl Anal*. 2013;92:2168-2181.
37. Zhou J, Kim CG, Shi J. Positive steady state solutions of a diffusive Leslie–Gower predator–prey model with Holling type II functional response and cross-diffusion. *Discrete Contin Dyn Syst*. 2014;34:3875-3899.
38. Tello JI, Winkler M. Stabilization in a two-species chemotaxis system with a logistic source. *Nonlinearity*. 2012;25:1413-1425.
39. Wang Q, Yang J, Zhang L. Time periodic and stable patterns of a two-competing-species Keller–Segel chemotaxis model effect of cellular growth. *Discrete Contin Dyn Syst Ser B*. 2017;22:3547-3574.
40. Wang Q, Zhang L, Yang J, Hu J. Global existence and steady states of a two competing species Keller–Segel chemotaxis model. *Kinet Relat Model*. 2015;8:777-807.
41. Hsiao L, De Mottoni P. Persistence in reacting–diffusing systems: interaction of two predators and one prey. *Nonlinear Anal Theory Methods Appl*. 1987;11:367-536.
42. Lin JJ, Wang W, Zhao C, Yang TH. Global dynamics and traveling wave solutions of two predators-one prey models. *Discrete Contin Dyn Syst Ser B*. 2015;20:1135-1154.
43. Loladze I, Kuang Y, Elser JJ, Fagan WF. Competition and stoichiometry: coexistence of two predators on one prey. *Theor Popul Biol*. 2004;65:1-15.
44. Ton T, Hieu N. Dynamics of species in a model with two predators and one prey. *Nonlinear Anal Theory Methods Appl*. 2011;74:4868-4881.
45. Painter K, Hillen T. Spatio-temporal chaos in a chemotaxis model. *Physica D*. 2011;240:363-375.
46. Potapov AB, Hillen T. Metastability in chemotaxis models. *J Dyn Differ Equ*. 2005;17:293-330.
47. Hillen T, Painter KJ. A user's guidance to PDE models for chemotaxis. *J Math Biol*. 2009;58:183-217.
48. Horstmann D. From 1970 until now: the Keller–Segel model in chemotaxis and its consequences i. *Jahresber. Dtsch. Math.-Ver*. 2003;105:103-165.
49. Wang Q, Song Y, Shao L. Nonconstant positive steady states and pattern formation of 1D prey-taxis systems. *J Nonlinear Sci*. 2017;27:71-97.
50. Hillen T, Painter KJ. Global existence for a parabolic chemotaxis model with prevention of overcrowding. *Adv Appl Math*. 2001;26:280-301.
51. Painter KJ, Hillen T. Volume–filling and quorum-sensing in models for chemosensitive movement. *Can Appl Math Q*. 2002;10:501-543.
52. Jin H, Wang ZA. Global stability of prey-taxis systems. *J. Differ Equ*. 2017;262(3):1257-1290.
53. Abrams P, Matsuda H. Effects of adaptive predatory and anti-predator behaviour in a two-prey-one-predator system. *Evol Ecol*. 1993;7:312-326.
54. Gliwicz ZM, Maszczyk P, Jablonski J, Wrzosek D. Patch exploitation by planktivorous fish and the concept of aggregation as an antipredation defense in zooplankton. *Limnol Oceanogr*. 2013;58:1621-1639.
55. Wang Q, Gai C, Yan J. Qualitative analysis of a Lotka–Volterra competition system with advection. *Discrete Contin Dyn Syst*. 2015;35:1239-1284.
56. Crandall MG, Rabinowitz PH. Bifurcation from simple eigenvalues. *J Funct Anal*. 1971;8:321-340.
57. Shi J, Wang X. On global bifurcation for quasilinear elliptic systems on bounded domains. *J Differ Equ*. 2009;246:2788-2812.

58. Crandall MG, Rabinowitz PH. Bifurcation, perturbation of simple eigenvalues, and linearized stability. *Arch Ration Mech Anal*. 1973;52:161-180.
59. Luo D, Wang Q. Global bifurcation for a generalized reaction–diffusion predator–prey system with prey-taxis. Submitted for publication. https://www.researchgate.net/publication/358571645
60. Kareiva P, Odell GT. Swarms of predators exhibit prey-taxis if individual predators use area-restricted search. *Am Nat*. 1987;130:233-270.

How to cite this article: Luo D, Wang Q, Chen L. Nonconstant steady states and pattern formations of generalized 1D cross-diffusion systems with prey-taxis. *Stud Appl Math*. 2023;1-60. https://doi.org/10.1111/sapm.12560

APPENDIX A: ADDITIONAL MATERIALS

We obtain the orientations of the pitchfork bifurcations $\mathrm{Y}_{d_k}(s)$ and $\mathrm{Y}_{\chi_k}(s)$ of model (20) with generalized kinetic functions F and G. In light of Theorems 4–5 and Corollaries 1–2, the unique local stable branch has to be $\mathrm{Y}_{d_{k_0}}(s)$ (or $\mathrm{Y}_{\chi_{k_0}}(s)$), $s \in (-\epsilon, \epsilon)$. Meanwhile, the stability of $\mathrm{Y}_{d_{k_0}}(s)$ (or $\mathrm{Y}_{\chi_{k_0}}(s)$) is confirmed via the rotational direction, and all the others are always unstable. When $\mathcal{C}_2 < 0$ (or $\mathcal{C}_4 < 0$), each bifurcation branch $\mathrm{Y}_{d_k}(s)$ (or $\mathrm{Y}_{\chi_k}(s)$) is moving down. When $\mathcal{C}_2 > 0$ (or $\mathcal{C}_4 > 0$), each bifurcation branch $\mathrm{Y}_{d_k}(s)$ (or $\mathrm{Y}_{\chi_k}(s)$) is moving up. Accordingly, we must confirm the sign of $\mathcal{C}_2$ (or $\mathcal{C}_4$) for the stability of the stationary solutions of model (1).

A.1 | The expression of $\mathcal{C}_2$

Our computations can be applied for each positive integer k. For evaluating $\mathcal{C}_2$, the whole derivation process are as follow. Plugging the asymptotic expansions (96)–(99) into the first equation of (20), and equating s^3-terms, one gets

$$\begin{aligned}
&D_1\Phi_2'' + F_u^*\Phi_2 + F_v^*\Psi_2 + (F_{uu}^*Q_k + F_{uv}^*)\Phi_1\cos\frac{k\pi x}{L} + (F_{uv}^*Q_k + F_{vv}^*)\Psi_1\cos\frac{k\pi x}{L}\\
&+ \frac{1}{6}(F_{uuu}^*Q_k^3 + 3F_{uuv}^*Q_k^2 + 3F_{uvv}^*Q_k + F_{vvv}^*)\cos^3\frac{k\pi x}{L}\\
=&-d_kD_1\left[v^*\Phi_2'' + Q_k\left(\Phi_1'\cos\frac{k\pi x}{L}\right)' + \left(\Psi_1\cos'\frac{k\pi x}{L}\right)' + u^*\Psi_2'' + \left(\Psi_1'\cos\frac{k\pi x}{L}\right)' + \left(\Phi_1\cos'\frac{k\pi x}{L}\right)'\right]\\
&+ \mathcal{C}_2(u^* + v^*)\cos''\frac{k\pi x}{L}.
\end{aligned} \tag{A.1}$$

We cite the following equalities which can be evidently derived via a direct computation to deduce more accurate formula of $\mathcal{C}_2$.

$$\int_0^L \Lambda_\bullet\cos^2\frac{k\pi x}{L}dx = \frac{1}{2}\int_0^L \Lambda_\bullet\left(1 + \cos\frac{2k\pi x}{L}\right)dx, \tag{A.2}$$

$$\begin{cases} \int_0^L \left(\Lambda_\bullet' \cos\frac{k\pi x}{L}\right)' \cos\frac{k\pi x}{L}dx = -\frac{k^2\pi^2}{L^2}\int_0^L \Lambda_\bullet \cos\frac{2k\pi x}{L}dx, \\ \int_0^L \left(\Lambda_\bullet \cos'\frac{k\pi x}{L}\right)' \cos\frac{k\pi x}{L}dx = \frac{1}{2}\frac{k^2\pi^2}{L^2}\int_0^L \Lambda_\bullet\left(\cos\frac{2k\pi x}{L}-1\right)dx, \end{cases} \tag{A.3}$$

where $\Lambda = \Phi$ or Ψ, $\bullet = 1, 2, 3,$ or 4, and

$$\begin{cases} \int_0^L \cos^4\frac{k\pi x}{L}dx = \frac{(\sin(4\pi k)+8\sin(2\pi k)+12\pi k)\cdot L}{32\pi k} = \frac{3}{8}L, \\ \int_0^L \left(\cos^2\frac{k\pi x}{L}\cos'\frac{k\pi x}{L}\right)' \cos\frac{k\pi x}{L}dx \\ = \frac{k^2\pi^2}{L^2}\cdot\frac{-L(\pi k\tan^4(\pi k)+\tan^3(\pi k)+2\pi k\tan^2(\pi k)+7\tan(\pi k)+\pi k)}{8\pi k(\tan^4(\pi k)+2\tan^2(\pi k)+1)} = -\frac{k^2\pi^2}{8L}. \end{cases} \tag{A.4}$$

By multiplying (A.1) by $\cos\frac{k\pi x}{L}$ and integrating from 0 to L, we obtain in light of (A.2)–(A.4) that

$$\begin{aligned} C_2 = &-\frac{2L}{(k\pi)^2[D_1(u^*+v^*)]}\left(C_{11}\int_0^L \Phi_2\cos\frac{k\pi x}{L}dx + C_{12}\int_0^L \Psi_2\cos\frac{k\pi x}{L}dx + C_{13}\int_0^L \Phi_1\cos\frac{2k\pi x}{L}dx\right. \\ &\left. + C_{14}\int_0^L \Psi_1\cos\frac{2k\pi x}{L}dx + C_{15}\int_0^L \Phi_1 dx + C_{16}\int_0^L \Psi_1 dx + C_{17}\right). \end{aligned} \tag{A.5}$$

Here,

$$\begin{aligned} &C_{11} = -D_1(1+d_k v^*)\left(\frac{k\pi}{L}\right)^2 + F_u^*,\ \ C_{12} = -d_k D_1 u^*\left(\frac{k\pi}{L}\right)^2 + F_v^*, \\ &C_{13} = -d_k D_1\left(Q_k - \frac{1}{2}\right)\left(\frac{k\pi}{L}\right)^2 + \frac{1}{2}(F_{uu}^* Q_k + F_{uv}^*),\ \ C_{14} = -\frac{1}{2}d_k D_1\left(\frac{k\pi}{L}\right)^2 + \frac{1}{2}(F_{uv}^* Q_k + F_{vv}^*), \\ &C_{15} = -\frac{1}{2}d_k D_1\left(\frac{k\pi}{L}\right)^2 + \frac{1}{2}(F_{uu}^* Q_k + F_{uv}^*),\ \ C_{16} = -\frac{1}{2}d_k D_1\left(\frac{k\pi}{L}\right)^2 + \frac{1}{2}(F_{uv}^* Q_k + F_{vv}^*), \\ &C_{17} = \frac{L}{16}(F_{uuu}^* Q_k^3 + 3F_{uuv}^* Q_k^2 + 3F_{uvv}^* Q_k + F_{vvv}^*). \end{aligned} \tag{A.6}$$

Extracting s^3-terms in the equation of υ in (20), one gets

$$\begin{aligned}
&D_2\Psi_2'' + G_u^*\Phi_2 + G_\upsilon^*\Psi_2 + (G_{uu}^*Q_k + G_{u\upsilon}^*)\Phi_1\cos\frac{k\pi x}{L} + (G_{u\upsilon}^*Q_k + G_{\upsilon\upsilon}^*)\Psi_1\cos\frac{k\pi x}{L}\\
&+\frac{1}{6}(G_{uuu}^*Q_k^3 + 3G_{uu\upsilon}^*Q_k^2 + 3G_{u\upsilon\upsilon}^*Q_k + G_{\upsilon\upsilon\upsilon}^*)\cos^3\frac{k\pi x}{L}\\
=&\chi\left[\phi^*\Phi_2'' + (\phi_u^*Q_k + \phi_\upsilon^*)\left(\Phi_1'\cos\frac{k\pi x}{L}\right)' + \phi_u^*\left(\Phi_1\cos'\frac{k\pi x}{L}\right)' + \phi_\upsilon^*\left(\Psi_1\cos'\frac{k\pi x}{L}\right)'\right.\\
&\left.+\frac{1}{2}(\phi_{uu}^*Q_k^2 + 2\phi_{u\upsilon}^*Q_k + \phi_{\upsilon\upsilon}^*)\left(\cos^2\frac{k\pi x}{L}\cos'\frac{k\pi x}{L}\right)'\right].
\end{aligned} \tag{A.7}$$

By multiplying (A.7) by $\cos\frac{k\pi x}{L}$ and integrating from 0 to L, we obtain in light of (A.2)–(A.4) that

$$\left(\chi\phi^*\left(\frac{k\pi}{L}\right)^2 + G_u^*\right)\int_0^L \Phi_2\cos\frac{k\pi x}{L}dx + \left(-D_2\left(\frac{k\pi}{L}\right)^2 + G_\upsilon^*\right)\int_0^L \Psi_2\cos\frac{k\pi x}{L}dx = C_{18}, \tag{A.8}$$

where

$$\begin{aligned}
C_{18} =& -\left(\chi\left(\phi_u^*Q_k + \frac{1}{2}\phi_\upsilon^*\right)\left(\frac{k\pi}{L}\right)^2 + \frac{1}{2}(G_{uu}^*Q_k + G_{u\upsilon}^*)\right)\int_0^L \Phi_1\cos\frac{2k\pi x}{L}dx\\
&-\left(-\frac{1}{2}\chi\phi_\upsilon^*\left(\frac{k\pi}{L}\right)^2 + \frac{1}{2}(G_{u\upsilon}^*Q_k + G_{\upsilon\upsilon}^*)\right)\int_0^L \Psi_1\cos\frac{2k\pi x}{L}dx\\
&-\left(\frac{1}{2}\chi\phi_u^*\left(\frac{k\pi}{L}\right)^2 + \frac{1}{2}(G_{uu}^*Q_k + G_{u\upsilon}^*)\right)\int_0^L \Phi_1 dx\\
&-\left(\frac{1}{2}\chi\phi_\upsilon^*\left(\frac{k\pi}{L}\right)^2 + \frac{1}{2}(G_{u\upsilon}^*Q_k + G_{\upsilon\upsilon}^*)\right)\int_0^L \Psi_1 dx\\
&-\left(\chi(\phi_{uu}^*Q_k^2 + 2\phi_{u\upsilon}^*Q_k + \phi_{\upsilon\upsilon}^*)\left(\frac{k\pi}{L}\right)^2 + (G_{uuu}^*Q_k^3 + 3G_{uu\upsilon}^*Q_k^2 + 3G_{u\upsilon\upsilon}^*Q_k + G_{\upsilon\upsilon\upsilon}^*)\right)\frac{L}{16}.
\end{aligned} \tag{A.9}$$

Meanwhile, due to $(\Phi_2, \Psi_2) \in \mathbb{W}$ as denoted by (40), we obtain that

$$\left(D_2\left(\frac{k\pi}{L}\right)^2 - G_\upsilon^*\right)\int_0^L \Phi_2\cos\frac{k\pi x}{L}dx + \left(\chi\phi^*\left(\frac{k\pi}{L}\right)^2 + G_u^*\right)\int_0^L \Psi_2\cos\frac{k\pi x}{L}dx = 0. \tag{A.10}$$

In light of (A.8) and (A.10), we have

$$\begin{pmatrix} \chi\phi^*\left(\frac{k\pi}{L}\right)^2 + G_u^* & -D_2\left(\frac{k\pi}{L}\right)^2 + G_v^* \\ D_2\left(\frac{k\pi}{L}\right)^2 - G_v^* & \chi\phi^*\left(\frac{k\pi}{L}\right)^2 + G_u^* \end{pmatrix} \begin{pmatrix} \int_0^L \Phi_2 \cos\frac{k\pi x}{L} dx \\ \int_0^L \Psi_2 \cos\frac{k\pi x}{L} dx \end{pmatrix} = \begin{pmatrix} C_{18} \\ 0 \end{pmatrix}. \tag{A.11}$$

Solving the last matrix equation yields

$$\int_0^L \Phi_2 \cos\frac{k\pi x}{L} dx = \frac{A_{11}}{A_{10}}, \quad \int_0^L \Psi_2 \cos\frac{k\pi x}{L} dx = \frac{A_{12}}{A_{10}}, \tag{A.12}$$

where

$$\begin{aligned} A_{10} &= \left(D_2\left(\frac{k\pi}{L}\right)^2 - G_v^*\right)^2 + \left(\chi\phi^*\left(\frac{k\pi}{L}\right)^2 + G_u^*\right)^2, \quad A_{11} = C_{18}\left(\chi\phi^*\left(\frac{k\pi}{L}\right)^2 + G_u^*\right), \\ A_{12} &= C_{18}\left(-D_2\left(\frac{k\pi}{L}\right)^2 + G_v^*\right). \end{aligned} \tag{A.13}$$

The final step will evaluate $\int_0^L \Phi_1 \cos\frac{2k\pi x}{L} dx$, $\int_0^L \Psi_1 \cos\frac{2k\pi x}{L} dx$, $\int_0^L \Phi_1 dx$, and $\int_0^L \Psi_1 dx$. By integrating (101) and (103) from 0 to L, we derive that

$$\begin{pmatrix} F_u^* & F_v^* \\ G_u^* & G_v^* \end{pmatrix} \begin{pmatrix} \int_0^L \Phi_1 dx \\ \int_0^L \Psi_1 dx \end{pmatrix} = \begin{pmatrix} -\frac{L(F_{uu}^* Q_k^2 + 2F_{uv}^* Q_k + F_{vv}^*)}{4} \\ -\frac{L(G_{uu}^* Q_k^2 + 2G_{uv}^* Q_k + G_{vv}^*)}{4} \end{pmatrix}. \tag{A.14}$$

Solving the last matrix equation yields

$$\int_0^L \Phi_1 dx = \frac{B_{11}}{B_{10}}, \quad \int_0^L \Psi_1 dx = \frac{B_{12}}{B_{10}}, \tag{A.15}$$

where

$$\begin{aligned} B_{10} &= F_u^* G_v^* - F_v^* G_u^*, \quad B_{11} = -\frac{L[(F_{uu}^* Q_k^2 + 2F_{uv}^* Q_k + F_{vv}^*)G_v^* - (G_{uu}^* Q_k^2 + 2G_{uv}^* Q_k + G_{vv}^*)F_v^*]}{4}, \\ B_{12} &= \frac{L[(F_{uu}^* Q_k^2 + 2F_{uv}^* Q_k + F_{vv}^*)G_u^* - (G_{uu}^* Q_k^2 + 2G_{uv}^* Q_k + G_{vv}^*)F_u^*]}{4}. \end{aligned} \tag{A.16}$$

Multiplying (101) and (103) by $\cos\frac{2k\pi x}{L}$ and integrating from 0 to L lead us to

$$\begin{pmatrix} -D_1(1+dv^*)\left(\frac{2k\pi}{L}\right)^2 + F_u^* & -D_1du^*\left(\frac{2k\pi}{L}\right)^2 + F_v^* \\ \chi\phi^*\left(\frac{2k\pi}{L}\right)^2 + G_u^* & -D_2\left(\frac{2k\pi}{L}\right)^2 + G_v^* \end{pmatrix} \begin{pmatrix} \int_0^L \Phi_1 \cos\frac{2k\pi x}{L}dx \\ \int_0^L \Psi_1 \cos\frac{2k\pi x}{L}dx \end{pmatrix} = \begin{pmatrix} B_{13} \\ B_{14} \end{pmatrix}, \tag{A.17}$$

where

$$\begin{aligned} B_{13} &= -\frac{L(F_{uu}^*Q_k^2 + 2F_{uv}^*Q_k + F_{vv}^*)}{8} + \frac{k^2\pi^2}{2L}d_kD_1Q_k, \\ B_{14} &= -\frac{L(G_{uu}^*Q_k^2 + 2G_{uv}^*Q_k + G_{vv}^*)}{8} + \frac{k^2\pi^2}{2L}d_kD_1. \end{aligned} \tag{A.18}$$

Solving the last matrix equation yields

$$\int_L^0 \Phi_1 \cos\frac{2k\pi x}{L}dx = \frac{E_{11}}{E_{10}}, \quad \int_L^0 \Psi_1 \cos\frac{2k\pi x}{L}dx = \frac{E_{12}}{E_{10}}, \tag{A.19}$$

where

$$\begin{aligned} E_{10} =& \left(D_1(1+dv^*)\left(\frac{2k\pi}{L}\right)^2 - F_u^*\right)\left(D_2\left(\frac{2k\pi}{L}\right)^2 - G_v^*\right) \\ &+ \left(D_1du^*\left(\frac{2k\pi}{L}\right)^2 - F_v^*\right)\left(\chi\phi^*\left(\frac{2k\pi}{L}\right)^2 + G_u^*\right), \\ E_{11} =& B_{13}\left(-D_2\left(\frac{2k\pi}{L}\right)^2 + G_v^*\right) - B_{14}\left(-D_1du^*\left(\frac{2k\pi}{L}\right)^2 + F_v^*\right), \\ E_{12} =& B_{14}\left(-D_1(1+dv^*)\left(\frac{2k\pi}{L}\right)^2 + F_u^*\right) - B_{13}\left(\chi\phi^*\left(\frac{2k\pi}{L}\right)^2 + G_u^*\right). \end{aligned} \tag{A.20}$$

In view of (36), we indicate that E_{10} is always nonzero. Together with (A.12), (A.15), and (A.19), C_2 in (A.5) can be represented in light of model coefficients.

A.2 | The expression of C_4

Our computations can be utilized for each positive integer k. For evaluating C_4, the whole derivation process are as follow. Plugging the asymptotic expansions (96)–(98) and (100) into the second

equation of (20), and equating s^3-terms, we obtain

$$\begin{aligned}
&D_2\Psi_4''(x)+G_u^*\Phi_4+G_v^*\Psi_4+(G_{uu}^*+G_{uv}^*P_k)\Phi_3\cos\frac{k\pi x}{L}+(G_{uv}^*+G_{vv}^*P_k)\Psi_3\cos\frac{k\pi x}{L}\\
&+\frac{1}{6}(G_{uuu}^*+3G_{uuv}^*P_k+3G_{uvv}^*P_k^2+G_{vvv}^*P_k^3)\cos^3\frac{k\pi x}{L}\\
=&\chi_k\left[\phi^*\Phi_4''+(\phi_u^*+\phi_v^*P_k)\left(\Phi_3'\cos\frac{k\pi x}{L}\right)'+\phi_u^*\left(\Phi_3\cos'\frac{k\pi x}{L}\right)'+\phi_v^*\left(\Psi_3\cos'\frac{k\pi x}{L}\right)'\right.\\
&\left.+\frac{1}{2}(\phi_{uu}^*+2\phi_{uv}^*P_k+\phi_{vv}^*P_k^2)\left(\cos^2\frac{k\pi x}{L}\cos'\frac{k\pi x}{L}\right)'\right]+C_4\phi^*\cos''\frac{k\pi x}{L}.
\end{aligned}\tag{A.21}$$

By multiplying (A.21) by $\cos\frac{k\pi x}{L}$ and integrating from 0 to L, we obtain in light of (A.2)–(A.4) that

$$\begin{aligned}
C_4=&-\frac{2L}{(k\pi)^2\phi^*}\left(C_{21}\int_0^L\Phi_4\cos\frac{k\pi x}{L}dx+C_{22}\int_0^L\Psi_4\cos\frac{k\pi x}{L}dx+C_{23}\int_0^L\Phi_3\cos\frac{2k\pi x}{L}dx\right.\\
&\left.+C_{24}\int_0^L\Psi_3\cos\frac{2k\pi x}{L}dx+C_{25}\int_0^L\Phi_3dx+C_{26}\int_0^L\Psi_3dx+C_{27}\right).
\end{aligned}\tag{A.22}$$

Here,

$$\begin{aligned}
&C_{21}=\chi_k\phi^*\left(\frac{k\pi}{L}\right)^2+G_u^*,\quad C_{22}=-D_2\left(\frac{k\pi}{L}\right)^2+G_v^*,\\
&C_{23}=\chi_k\left(\frac{1}{2}\phi_u^*+\phi_v^*P_k\right)\left(\frac{k\pi}{L}\right)^2+\frac{1}{2}(G_{uu}^*+G_{uv}^*P_k),\quad C_{24}=-\frac{1}{2}\chi_k\phi_v^*\left(\frac{k\pi}{L}\right)^2+\frac{1}{2}(G_{uv}^*+G_{vv}^*P_k),\\
&C_{25}=\frac{1}{2}\chi_k\phi_u^*\left(\frac{k\pi}{L}\right)^2+\frac{1}{2}(G_{uu}^*+G_{uv}^*P_k),\quad C_{26}=\frac{1}{2}\chi_k\phi_v^*\left(\frac{k\pi}{L}\right)^2+\frac{1}{2}(G_{uv}^*+G_{vv}^*P_k),\\
&C_{27}=\left[\chi_k(\phi_{uu}^*+2\phi_{uv}^*P_k+\phi_{vv}^*P_k^2)\left(\frac{k\pi}{L}\right)^2+(G_{uuu}^*+3G_{uuv}^*P_k+3G_{uvv}^*P_k^2+G_{vvv}^*P_k^3)\right]\frac{L}{16}.
\end{aligned}\tag{A.23}$$

Extracting s^3-terms in the equation of u in (20), one gets

$$\begin{aligned}
&D_1\Phi_4''+F_u^*\Phi_4+F_v^*\Psi_4+(F_{uu}^*+F_{uv}^*P_k)\Phi_3\cos\frac{k\pi x}{L}+(F_{uv}^*+F_{vv}^*P_k)\Psi_3\cos\frac{k\pi x}{L}\\
&+\frac{1}{6}(F_{uuu}^*+3F_{uuv}^*P_k+3F_{uvv}^*P_k^2+F_{vvv}^*P_k^3)\cos^3\frac{k\pi x}{L}\\
=&-d_kD_1\left[v^*\Phi_4''+\left(\Phi_3'\cos\frac{k\pi x}{L}\right)'+\left(\Psi_3\cos'\frac{k\pi x}{L}\right)'+u^*\Psi_4''+P_k\left(\Psi_3'\cos\frac{k\pi x}{L}\right)'+\left(\Phi_3\cos'\frac{k\pi x}{L}\right)'\right].
\end{aligned}\tag{A.24}$$

Multiplying the last equality by $\cos\frac{k\pi x}{L}$ and integrating from 0 to L, one gets

$$\left(-D_1(1+dv^*)\left(\frac{k\pi}{L}\right)^2+F_u^*\right)\int_0^L \Phi_4\cos\frac{k\pi x}{L}dx+\left(-D_1du^*\left(\frac{2k\pi}{L}\right)^2+F_v^*\right)\int_0^L \Psi_4\cos\frac{k\pi x}{L}dx=C_{28}, \tag{A.25}$$

where

$$\begin{aligned}C_{28}=&\left(-\frac{1}{2}d_kD_1\left(\frac{k\pi}{L}\right)^2+\left(P_k-\frac{1}{2}\right)(F_{uu}^*+F_{uv}^*P_k)\right)\int_0^L \Phi_3\cos\frac{2k\pi x}{L}dx\\&+\left(-\frac{1}{2}d_kD_1\left(\frac{k\pi}{L}\right)^2+\frac{1}{2}(F_{uv}^*+F_{vv}^*P_k)\right)\int_0^L \Psi_3\cos\frac{2k\pi x}{L}dx\\&+\left(-\frac{1}{2}d_kD_1\left(\frac{k\pi}{L}\right)^2+\frac{1}{2}(F_{uu}^*+F_{uv}^*P_k)\right)\int_0^L \Phi_3dx\\&+\left(-\frac{1}{2}d_kD_1\left(\frac{k\pi}{L}\right)^2+\frac{1}{2}(F_{uv}^*+F_{vv}^*P_k)\right)\int_0^L \Psi_3dx\\&+\frac{L}{16}(F_{uuu}^*+3F_{uuv}^*P_k+3F_{uvv}^*P_k^2+F_{vvv}^*P_k^3).\end{aligned} \tag{A.26}$$

Meanwhile, due to $(\Phi_4,\Psi_4)\in\mathbb{W}$ as denoted by (40), we obtain that

$$\left(-D_1du^*\left(\frac{2k\pi}{L}\right)^2+F_v^*\right)\int_0^L \Phi_4\cos\frac{k\pi x}{L}dx+\left(D_1(1+dv^*)\left(\frac{k\pi}{L}\right)^2-F_u^*\right)\int_0^L \Psi_4\cos\frac{k\pi x}{L}dx=0. \tag{A.27}$$

In view of (A.25) and (A.27), one gets

$$\begin{pmatrix}-D_1(1+dv^*)\left(\frac{k\pi}{L}\right)^2+F_u^* & -D_1du^*\left(\frac{2k\pi}{L}\right)^2+F_v^*\\ -D_1du^*\left(\frac{2k\pi}{L}\right)^2+F_v^* & D_1(1+dv^*)\left(\frac{k\pi}{L}\right)^2-F_u^*\end{pmatrix}\begin{pmatrix}\int_0^L \Phi_4\cos\frac{k\pi x}{L}dx\\ \int_0^L \Psi_4\cos\frac{k\pi x}{L}dx\end{pmatrix}=\begin{pmatrix}C_{28}\\0\end{pmatrix}. \tag{A.28}$$

Solving the last matrix equation yields

$$\int_0^L \Phi_4\cos\frac{k\pi x}{L}dx=\frac{A_{21}}{A_{20}},\quad \int_0^L \Psi_4\cos\frac{k\pi x}{L}dx=\frac{A_{22}}{A_{20}}, \tag{A.29}$$

where

$$A_{20} = -\left(D_1(1+dv^*)\left(\frac{k\pi}{L}\right)^2 - F_u^*\right)^2 - \left(-D_1 du^*\left(\frac{2k\pi}{L}\right)^2 + F_v^*\right)^2,$$
$$A_{21} = C_{28}\left(-D_1 du^*\left(\frac{2k\pi}{L}\right)^2 + F_v^*\right), \tag{A.30}$$
$$A_{22} = C_{28}\left(D_1 du^*\left(\frac{2k\pi}{L}\right)^2 - F_v^*\right).$$

The final step will evaluate $\int_0^L \Phi_3 \cos\frac{2k\pi x}{L}dx$, $\int_0^L \Psi_3 \cos\frac{2k\pi x}{L}dx$, $\int_0^L \Phi_3 dx$, and $\int_0^L \Psi_3 dx$. By integrating (101) and (103) from 0 to L, we derive that

$$\begin{pmatrix} F_u^* & F_v^* \\ G_u^* & G_v^* \end{pmatrix}\begin{pmatrix} \int_0^L \Phi_3 dx \\ \int_0^L \Psi_3 dx \end{pmatrix} = \begin{pmatrix} -\frac{L(F_{uu}^* + 2F_{uv}^* P_k + F_{vv}^* P_k^2)}{4} \\ -\frac{L(G_{uu}^* + 2G_{uv}^* P_k + G_{vv}^* P_k^2)}{4} \end{pmatrix}. \tag{A.31}$$

Solving the last matrix equation yields

$$\int_0^L \Phi_3 dx = \frac{B_{21}}{B_{20}}, \quad \int_0^L \Psi_3 dx = \frac{B_{22}}{B_{20}}, \tag{A.32}$$

where

$$B_{20} = F_u^* G_v^* - F_v^* G_u^*, \quad B_{21} = -\frac{L[(F_{uu}^* + 2F_{uv}^* P_k + F_{vv}^* P_k^2)G_v^* - (G_{uu}^* + 2G_{uv}^* P_k + G_{vv}^* P_k^2)F_v^*]}{4},$$
$$B_{22} = \frac{L[(F_{uu}^* + 2F_{uv}^* P_k + F_{vv}^* P_k^2)G_u^* - (G_{uu}^* + 2G_{uv}^* P_k + G_{vv}^* P_k^2)F_u^*]}{4}. \tag{A.33}$$

Multiplying (101) and (103) by $\cos\frac{2k\pi x}{L}$ and integrating from 0 to L lead us to

$$\begin{pmatrix} -D_1(1+dv^*)\left(\frac{2k\pi}{L}\right)^2 + F_u^* & -D_1 du^*\left(\frac{2k\pi}{L}\right)^2 + F_v^* \\ \chi\phi^*\left(\frac{2k\pi}{L}\right)^2 + G_u^* & -D_2\left(\frac{2k\pi}{L}\right)^2 + G_v^* \end{pmatrix}\begin{pmatrix} \int_0^L \Phi_3 \cos\frac{2k\pi x}{L}dx \\ \int_0^L \Psi_3 \cos\frac{2k\pi x}{L}dx \end{pmatrix} = \begin{pmatrix} B_{23} \\ B_{24} \end{pmatrix}, \tag{A.34}$$

where

$$B_{23} = -\frac{L(F_{uu}^* + 2F_{uv}^* P_k + F_{vv}^* P_k^2)}{8} - \frac{k^2\pi^2}{2L}\chi_k\phi^*,$$
$$B_{24} = -\frac{L(G_{uu}^* + 2G_{uv}^* P_k + G_{vv}^* P_k^2)}{8} - \frac{k^2\pi^2}{2L}\chi_k\phi^* P_k. \tag{A.35}$$

Solving the last matrix equation yields

$$\int_0^L \Phi_3 \cos\frac{2k\pi x}{L}dx = \frac{E_{21}}{E_{20}}, \quad \int_0^L \Psi_3 \cos\frac{2k\pi x}{L}dx = \frac{E_{22}}{E_{20}}, \tag{A.36}$$

where

$$\begin{aligned} E_{20} =& \left(D_1(1+dv^*)\left(\frac{2k\pi}{L}\right)^2 - F_u^*\right)\left(D_2\left(\frac{2k\pi}{L}\right)^2 - G_v^*\right) \\ &+ \left(D_1 du^*\left(\frac{2k\pi}{L}\right)^2 - F_v^*\right)\left(\chi\phi^*\left(\frac{2k\pi}{L}\right)^2 + G_u^*\right), \\ E_{21} =& B_{23}\left(-D_2\left(\frac{2k\pi}{L}\right)^2 + G_v^*\right) - B_{24}\left(-D_1 du^*\left(\frac{2k\pi}{L}\right)^2 + F_v^*\right), \\ E_{22} =& B_{24}\left(-D_1(1+dv^*)\left(\frac{2k\pi}{L}\right)^2 + F_u^*\right) - B_{23}\left(\chi\phi^*\left(\frac{2k\pi}{L}\right)^2 + G_u^*\right). \end{aligned} \tag{A.37}$$

In view of (36), we indicate that E_{20} is always nonzero. Together with (A.29), (A.32), and (A.36), C_2 in (A.22) can be represented in light of model coefficients.

A.3 | Example

In this example, we select the Holling-II and Tanner kinetic functions given by (3). It means that $\beta = 0$. For the sake of simplicity, we set $D_1 = 1, D_2 = 1, r_1 = 2, r_2 = 1, b = 1, \delta = 1, \alpha = 1, \gamma = 1$, and $L = 2$. We choose $d = 0$ and χ as a bifurcation parameter. It is easy to see that

$$(u^*, v^*) = \left(\frac{(r_1\alpha - b - r_2\gamma\delta) + \sqrt{(r_1\alpha - b - r_2\gamma\delta)^2 + 4br_1\alpha}}{2b\alpha}, r_2\gamma u^*\right) = (\sqrt{2}, \sqrt{2}). \tag{A.38}$$

Based on the above constant steady state, we obtain

$$F_u^* = \frac{-2-3\sqrt{2}}{(1+\sqrt{2})^2}, \quad F_v^* = -\frac{\sqrt{2}}{1+\sqrt{2}}, \quad G_u^* = 1, \quad G_v^* = -1,$$

$$F_{uu}^* = \frac{-14-8\sqrt{2}}{(1+\sqrt{2})^3}, \quad F_{uv}^* = -\frac{1}{(1+\sqrt{2})^2}, \quad F_{vv}^* = 0,$$

$$G_{uu}^* = -\sqrt{2}, \quad G_{uv}^* = \sqrt{2}, \quad G_{vv}^* = -\sqrt{2}, \quad G_{uuu}^* = 3, \quad G_{uuv}^* = -2, \quad G_{uvv}^* = 1, \quad G_{vvv}^* = 0,$$

$$P_k = \frac{D_1\left(\frac{k\pi}{L}\right)^2 - F_u^*}{F_v^*} = \frac{(1+\sqrt{2})^2\left(\frac{k\pi}{L}\right)^2 + (2+3\sqrt{2})}{-(2+\sqrt{2})},$$

$$\chi_k = \frac{\left[D_1\left(\frac{k\pi}{L}\right)^2 - F_u^*\right]\left[D_2\left(\frac{k\pi}{L}\right)^2 - G_v^*\right] - F_v^* G_u^*}{F_v^*\phi^*\left(\frac{k\pi}{L}\right)^2} = \frac{\left[\left(\frac{k\pi}{L}\right)^2 + \frac{2+3\sqrt{2}}{(1+\sqrt{2})^2}\right]\left[\left(\frac{k\pi}{L}\right)^2 + 1\right] + \frac{\sqrt{2}}{1+\sqrt{2}}}{-\frac{\sqrt{2}}{1+\sqrt{2}}\cdot 2\sqrt{2}\cdot\left(\frac{k\pi}{L}\right)^2}. \tag{A.39}$$

In the following, we take

$$\phi(u,v) = uv(M-u) \tag{A.40}$$

as a sensitivity function. If $M = 2\sqrt{2}$, we have

$$\phi^* = 2\sqrt{2},\ \ \phi^*_u = 0,\ \ \phi^*_v = 2,\ \ \phi^*_{uu} = -2\sqrt{2},\ \ \phi^*_{uv} = 0,\ \ \phi^*_{vv} = 0. \tag{A.41}$$

Therefore, if we denote $(\frac{k\pi}{L})^2 = \lambda$, we have

$$C_{21} = \frac{\left[\left(\frac{k\pi}{L}\right)^2 + \frac{2+3\sqrt{2}}{(1+\sqrt{2})^2}\right]\left[\left(\frac{k\pi}{L}\right)^2 + 1\right] + \frac{\sqrt{2}}{1+\sqrt{2}}}{-\frac{\sqrt{2}}{1+\sqrt{2}}} + 1 \approx \frac{(\lambda+1.0711)(\lambda+1)}{-0.5858} \approx -1.7071\lambda^2 - 3.5355\lambda - 1.8284, \tag{A.42}$$

$$C_{22} = -\left(\frac{k\pi}{L}\right)^2 - 1 = -\lambda - 1, \tag{A.43}$$

$$\begin{aligned} C_{23} =& \frac{\left[\left(\frac{k\pi}{L}\right)^2 + \frac{2+3\sqrt{2}}{(1+\sqrt{2})^2}\right]\left[\left(\frac{k\pi}{L}\right)^2 + 1\right] + \frac{\sqrt{2}}{1+\sqrt{2}}}{-\frac{2}{1+\sqrt{2}}} \cdot \frac{(1+\sqrt{2})^2\left(\frac{k\pi}{L}\right)^2 + (2+3\sqrt{2})}{-(2+\sqrt{2})} \\ &+ \frac{1}{2}\left(-\sqrt{2} - \frac{(1+\sqrt{2})^2\left(\frac{k\pi}{L}\right)^2 + (2+3\sqrt{2})}{1+\sqrt{2}}\right) \\ \approx& \left(\frac{(\lambda+1.0711)(\lambda+1)}{-0.8284} - 0.7071\right)\left(\frac{5.8284\lambda + 6.2426}{-3.4142}\right) + 0.5(-2.4142\lambda - 4) \\ =& (1.2071\lambda^2 + 2.5\lambda + 2)(1.8537\lambda + 1.8284) - 1.2071\lambda - 2 \\ =& 2.2376\lambda^3 + 6.8413\lambda^2 + 7.0713\lambda + 1.6568, \end{aligned} \tag{A.44}$$

$$\begin{aligned} C_{24} =& \frac{\left[\left(\frac{k\pi}{L}\right)^2 + \frac{2+3\sqrt{2}}{(1+\sqrt{2})^2}\right]\left[\left(\frac{k\pi}{L}\right)^2 + 1\right] + \frac{\sqrt{2}}{1+\sqrt{2}}}{\frac{\sqrt{2}}{1+\sqrt{2}} \cdot 2\sqrt{2}} + \frac{1}{2}\left(\sqrt{2} + \frac{(1+\sqrt{2})^2\left(\frac{k\pi}{L}\right)^2 + (2+3\sqrt{2})}{1+\sqrt{2}}\right) \\ \approx& \left(\frac{(\lambda+1.0711)(\lambda+1)}{1.6569} + 0.3536\right) + 0.5(2.4142\lambda + 4) \\ =& 0.6035\lambda^2 + 2.4570\lambda + 3, \end{aligned} \tag{A.45}$$

$$C_{25} = \frac{1}{2}\left(-\sqrt{2} + \frac{(1+\sqrt{2})^2\left(\frac{k\pi}{L}\right)^2 + (2+3\sqrt{2})}{-(1+\sqrt{2})}\right) \approx 0.5(-2.4142\lambda - 4) = -1.2071\lambda - 2, \tag{A.46}$$

$$C_{26}=\frac{\left[\left(\frac{k\pi}{L}\right)^2+\frac{2+3\sqrt{2}}{(1+\sqrt{2})^2}\right]\left[\left(\frac{k\pi}{L}\right)^2+1\right]+\frac{\sqrt{2}}{1+\sqrt{2}}}{-\frac{\sqrt{2}}{1+\sqrt{2}}\cdot 2\sqrt{2}}+\frac{1}{2}\left(\sqrt{2}+\frac{(1+\sqrt{2})^2\left(\frac{k\pi}{L}\right)^2+(2+3\sqrt{2})}{1+\sqrt{2}}\right)$$

$$\approx-\left(\frac{(\lambda+1.0711)(\lambda+1)}{1.6569}+0.3536\right)+0.5(2.4142\lambda+4)$$

$$=-0.6035\lambda^2-0.0428\lambda+1, \tag{A.47}$$

$$C_{27}=\frac{\left[\left(\frac{k\pi}{L}\right)^2+\frac{2+3\sqrt{2}}{(1+\sqrt{2})^2}\right]\left[\left(\frac{k\pi}{L}\right)^2+1\right]+\frac{\sqrt{2}}{1+\sqrt{2}}}{\frac{\sqrt{2}}{1+\sqrt{2}}}\frac{L}{16}$$

$$+\left[6-6\frac{(1+\sqrt{2})^2\left(\frac{k\pi}{L}\right)^2+(2+3\sqrt{2})}{-(2+\sqrt{2})}+3\left(\frac{(1+\sqrt{2})^2\left(\frac{k\pi}{L}\right)^2+(2+3\sqrt{2})}{-(2+\sqrt{2})}\right)^2\right]\frac{L}{16}$$

$$\approx\left(\frac{(\lambda+1.0711)(\lambda+1)}{4.6863}+0.125\right)+0.125\left[\left(6+\frac{34.9706\lambda+37.4558}{3.4142}\right)+3\left(\frac{5.8284\lambda+6.2426}{-3.4142}\right)^2\right]$$

$$=1.3062\lambda^2+4.0633\lambda+3.7286, \tag{A.48}$$

$$\int_0^L\Phi_4\cos\frac{k\pi x}{L}dx$$

$$=\frac{\left(\left(P_k-\frac{1}{2}\right)(F^*_{uu}+F^*_{uv}P_k)\int_0^L\Phi_3\cos\frac{2k\pi x}{L}dx+\frac{1}{2}(F^*_{uv}+F^*_{vv}P_k)\int_0^L\Psi_3\cos\frac{2k\pi x}{L}dx\right)F^*_v}{-\left(D_1\left(\frac{k\pi}{L}\right)^2-F^*_u\right)^2-(F^*_v)^2}$$

$$+\frac{\left(\frac{1}{2}(F^*_{uu}+F^*_{uv}P_k)\int_0^L\Phi_3dx+\frac{1}{2}(F^*_{uv}+F^*_{vv}P_k)\int_0^L\Psi_3dx\right)F^*_v}{-\left(D_1\left(\frac{k\pi}{L}\right)^2-F^*_u\right)^2-(F^*_v)^2}$$

$$+\frac{\frac{L}{16}(F^*_{uuu}+3F^*_{uuv}P_k+3F^*_{uvv}P_k^2+F^*_{vvv}P_k^3)F^*_v}{-\left(D_1\left(\frac{k\pi}{L}\right)^2-F^*_u\right)^2-(F^*_v)^2}=-\int_0^L\Psi_4\cos\frac{k\pi x}{L}dx$$

$$\approx\frac{(-1.7071\lambda-2.3284)[-1.7990+0.1716(1.7071\lambda+2.8284)]\left(\frac{-4.49383-20.4793\lambda-20.0239\lambda^2-8.5355\lambda^3}{12\lambda^2-2.6274}\right)(-0.5858)}{-(\lambda+1.0711)^2-0.3431}$$

$$+\frac{0.5\cdot 0.1716\left(\frac{22.2154+83.3482\lambda+120.238\lambda^2+82.9109\lambda^3+23.3135\lambda^4}{12\lambda^2-2.6274}\right)(-0.5858)}{-(\lambda+1.0711)^2-0.3431}$$

$$+\frac{0.5[-1.7990+0.1716(1.7071\lambda+2.8284)]\left(2.05356+2.59098\lambda+0.728548\lambda^2\right)(-0.5858)}{-(\lambda+1.0711)^2-0.3431}$$

$$+\frac{0.5\cdot 0.1716(-0.260083-1.11603\lambda-1.33208\lambda^2)(-0.5858)}{-(\lambda+1.0711)^2-0.3431}$$

$$+\frac{0.125[-0.2498-0.4263(1.7071\lambda+2.8284)](-0.5858)}{-(\lambda+1.0711)^2-0.3431}$$

$$=\frac{4.54499+34.1693\lambda+57.8283\lambda^2+34.7568\lambda^3+2.2643\lambda^4-3.25055\lambda^5}{3.91576+5.62842\lambda-15.2569\lambda^2-25.7064\lambda^3-12\lambda^4}, \tag{A.49}$$

$$\int_0^L \Phi_3\cos\frac{2k\pi x}{L}dx=\frac{\left(\frac{L(F^*_{uu}+2F^*_{uv}P_k+F^*_{vv}P_k^2)}{8}+\frac{k^2\pi^2}{2L}\chi_k\phi^*\right)\left(D_2\left(\frac{2k\pi}{L}\right)^2-G^*_v\right)}{\left(D_1\left(\frac{2k\pi}{L}\right)^2-F^*_u\right)\left(D_2\left(\frac{2k\pi}{L}\right)^2-G^*_v\right)-F^*_v\left(\chi_k\phi^*\left(\frac{2k\pi}{L}\right)^2+G^*_u\right)}$$

$$+\frac{\left(\frac{L(G^*_{uu}+2G^*_{uv}P_k+G^*_{vv}P_k^2)}{8}+\frac{k^2\pi^2}{2L}\chi_k\phi^*P_k\right)F^*_v}{\left(D_1\left(\frac{2k\pi}{L}\right)^2-F^*_u\right)\left(D_2\left(\frac{2k\pi}{L}\right)^2-G^*_v\right)-F^*_v\left(\chi_k\phi^*\left(\frac{2k\pi}{L}\right)^2+G^*_u\right)}$$

$$=\frac{\left[\frac{1}{4}\left(\frac{-14-8\sqrt{2}}{(1+\sqrt{2})^3}-\frac{2}{(1+\sqrt{2})^2}\frac{(1+\sqrt{2})^2\lambda+(2+3\sqrt{2})}{-(2+\sqrt{2})}\right)+2\sqrt{2}\lambda\frac{\left(\lambda+\frac{2+3\sqrt{2}}{(1+\sqrt{2})^2}\right)(\lambda+1)+\frac{\sqrt{2}}{1+\sqrt{2}}}{-\frac{\sqrt{2}}{1+\sqrt{2}}\cdot 2\sqrt{2}\cdot\lambda}\right](4\lambda+1)}{\left(4\lambda+\frac{2+3\sqrt{2}}{(1+\sqrt{2})^2}\right)(4\lambda+1)+\frac{\sqrt{2}}{1+\sqrt{2}}\left(8\sqrt{2}\lambda\frac{\left(\lambda+\frac{2+3\sqrt{2}}{(1+\sqrt{2})^2}\right)(\lambda+1)+\frac{\sqrt{2}}{1+\sqrt{2}}}{-\frac{\sqrt{2}}{1+\sqrt{2}}\cdot 2\sqrt{2}\cdot\lambda}+1\right)}$$

$$+\frac{\frac{1}{4}\left(-\sqrt{2}+2\sqrt{2}\frac{(1+\sqrt{2})^2\lambda+(2+3\sqrt{2})}{-(2+\sqrt{2})}-\sqrt{2}\left(\frac{(1+\sqrt{2})^2\lambda+(2+3\sqrt{2})}{-(2+\sqrt{2})}\right)^2\right)\left(-\frac{\sqrt{2}}{1+\sqrt{2}}\right)}{\left(4\lambda+\frac{2+3\sqrt{2}}{(1+\sqrt{2})^2}\right)(4\lambda+1)+\frac{\sqrt{2}}{1+\sqrt{2}}\left(8\sqrt{2}\lambda\frac{\left(\lambda+\frac{2+3\sqrt{2}}{(1+\sqrt{2})^2}\right)(\lambda+1)+\frac{\sqrt{2}}{1+\sqrt{2}}}{-\frac{\sqrt{2}}{1+\sqrt{2}}\cdot 2\sqrt{2}\cdot\lambda}+1\right)}$$

$$+\frac{2\sqrt{2}\lambda\left(\frac{\left(\lambda+\frac{2+3\sqrt{2}}{(1+\sqrt{2})^2}\right)(\lambda+1)+\frac{\sqrt{2}}{1+\sqrt{2}}}{-\frac{\sqrt{2}}{1+\sqrt{2}}\cdot 2\sqrt{2}\cdot\lambda}\right)\left(\frac{(1+\sqrt{2})^2\lambda+(2+3\sqrt{2})}{-(2+\sqrt{2})}\right)\left(-\frac{\sqrt{2}}{1+\sqrt{2}}\right)}{\left(4\lambda+\frac{2+3\sqrt{2}}{(1+\sqrt{2})^2}\right)(4\lambda+1)+\frac{\sqrt{2}}{1+\sqrt{2}}\left(8\sqrt{2}\lambda\frac{\left(\lambda+\frac{2+3\sqrt{2}}{(1+\sqrt{2})^2}\right)(\lambda+1)+\frac{\sqrt{2}}{1+\sqrt{2}}}{-\frac{\sqrt{2}}{1+\sqrt{2}}\cdot 2\sqrt{2}\cdot\lambda}+1\right)}$$

$$\approx\frac{-4.49383-20.4793\lambda-20.0239\lambda^2-8.5355\lambda^3}{12\lambda^2-2.6274}, \tag{A.50}$$

$$\int_0^L \Psi_3 \cos\frac{2k\pi x}{L}dx = \frac{\left(\frac{L(G^*_{uu}+2G^*_{uv}P_k+G^*_{vv}P_k^2)}{8}+\frac{k^2\pi^2}{2L}\chi_k\phi^*P_k\right)\left(D_1\left(\frac{2k\pi}{L}\right)^2-F^*_u\right)}{\left(D_1\left(\frac{2k\pi}{L}\right)^2-F^*_u\right)\left(D_2\left(\frac{2k\pi}{L}\right)^2-G^*_v\right)-F^*_v\left(\chi_k\phi^*\left(\frac{2k\pi}{L}\right)^2+G^*_u\right)}$$

$$+\frac{\left(\frac{L(F^*_{uu}+2F^*_{uv}P_k+F^*_{vv}P_k^2)}{8}+\frac{k^2\pi^2}{2L}\chi_k\phi^*\right)\left(\chi_k\phi^*\left(\frac{2k\pi}{L}\right)^2+G^*_u\right)}{\left(D_1\left(\frac{2k\pi}{L}\right)^2-F^*_u\right)\left(D_2\left(\frac{2k\pi}{L}\right)^2-G^*_v\right)-F^*_v\left(\chi_k\phi^*\left(\frac{2k\pi}{L}\right)^2+G^*_u\right)}$$

$$=\frac{\frac{1}{4}\left(-\sqrt{2}+2\sqrt{2}\frac{(1+\sqrt{2})^2\lambda+(2+3\sqrt{2})}{-(2+\sqrt{2})}-\sqrt{2}\left(\frac{(1+\sqrt{2})^2\lambda+(2+3\sqrt{2})}{-(2+\sqrt{2})}\right)^2\right)\left(4\lambda+\frac{2+3\sqrt{2}}{(1+\sqrt{2})^2}\right)}{\left(4\lambda+\frac{2+3\sqrt{2}}{(1+\sqrt{2})^2}\right)(4\lambda+1)+\frac{\sqrt{2}}{1+\sqrt{2}}\left(8\sqrt{2}\lambda\frac{\left(\lambda+\frac{2+3\sqrt{2}}{(1+\sqrt{2})^2}\right)(\lambda+1)+\frac{\sqrt{2}}{1+\sqrt{2}}}{-\frac{\sqrt{2}}{1+\sqrt{2}}\cdot 2\sqrt{2}\cdot\lambda}+1\right)}$$

$$+\frac{2\sqrt{2}\lambda\left(\frac{\left(\lambda+\frac{2+3\sqrt{2}}{(1+\sqrt{2})^2}\right)(\lambda+1)+\frac{\sqrt{2}}{1+\sqrt{2}}}{-\frac{\sqrt{2}}{1+\sqrt{2}}\cdot 2\sqrt{2}\cdot\lambda}\right)\left(\frac{(1+\sqrt{2})^2\lambda+(2+3\sqrt{2})}{-(2+\sqrt{2})}\right)\left(4\lambda+\frac{2+3\sqrt{2}}{(1+\sqrt{2})^2}\right)}{\left(4\lambda+\frac{2+3\sqrt{2}}{(1+\sqrt{2})^2}\right)(4\lambda+1)+\frac{\sqrt{2}}{1+\sqrt{2}}\left(8\sqrt{2}\lambda\frac{\left(\lambda+\frac{2+3\sqrt{2}}{(1+\sqrt{2})^2}\right)(\lambda+1)+\frac{\sqrt{2}}{1+\sqrt{2}}}{-\frac{\sqrt{2}}{1+\sqrt{2}}\cdot 2\sqrt{2}\cdot\lambda}+1\right)}$$

$$+\frac{\frac{1}{4}\left(\frac{-14-8\sqrt{2}}{(1+\sqrt{2})^3}-\frac{2}{(1+\sqrt{2})^2}\frac{(1+\sqrt{2})^2\lambda+(2+3\sqrt{2})}{-(2+\sqrt{2})}\right)\left(8\sqrt{2}\lambda\frac{\left(\lambda+\frac{2+3\sqrt{2}}{(1+\sqrt{2})^2}\right)(\lambda+1)+\frac{\sqrt{2}}{1+\sqrt{2}}}{-\frac{\sqrt{2}}{1+\sqrt{2}}\cdot 2\sqrt{2}\cdot\lambda}+1\right)}{\left(4\lambda+\frac{2+3\sqrt{2}}{(1+\sqrt{2})^2}\right)(4\lambda+1)+\frac{\sqrt{2}}{1+\sqrt{2}}\left(8\sqrt{2}\lambda\frac{\left(\lambda+\frac{2+3\sqrt{2}}{(1+\sqrt{2})^2}\right)(\lambda+1)+\frac{\sqrt{2}}{1+\sqrt{2}}}{-\frac{\sqrt{2}}{1+\sqrt{2}}\cdot 2\sqrt{2}\cdot\lambda}+1\right)}$$

$$+\frac{\left(2\sqrt{2}\lambda\frac{\left(\lambda+\frac{2+3\sqrt{2}}{(1+\sqrt{2})^2}\right)(\lambda+1)+\frac{\sqrt{2}}{1+\sqrt{2}}}{-\frac{\sqrt{2}}{1+\sqrt{2}}\cdot 2\sqrt{2}\cdot\lambda}\right)\left(8\sqrt{2}\lambda\frac{\left(\lambda+\frac{2+3\sqrt{2}}{(1+\sqrt{2})^2}\right)(\lambda+1)+\frac{\sqrt{2}}{1+\sqrt{2}}}{-\frac{\sqrt{2}}{1+\sqrt{2}}\cdot 2\sqrt{2}\cdot\lambda}+1\right)}{\left(4\lambda+\frac{2+3\sqrt{2}}{(1+\sqrt{2})^2}\right)(4\lambda+1)+\frac{\sqrt{2}}{1+\sqrt{2}}\left(8\sqrt{2}\lambda\frac{\left(\lambda+\frac{2+3\sqrt{2}}{(1+\sqrt{2})^2}\right)(\lambda+1)+\frac{\sqrt{2}}{1+\sqrt{2}}}{-\frac{\sqrt{2}}{1+\sqrt{2}}\cdot 2\sqrt{2}\cdot\lambda}+1\right)}$$

$$\approx\frac{22.2154+83.3482\lambda+120.238\lambda^2+82.9109\lambda^3+23.3135\lambda^4}{12\lambda^2-2.6274}, \tag{A.51}$$

$$\int_0^L \Phi_3 dx = -\frac{L[(F^*_{uu}+2F^*_{uv}P_k+F^*_{vv}P_k^2)G^*_v-(G^*_{uu}+2G^*_{uv}P_k+G^*_{vv}P_k^2)F^*_v]}{4(F^*_uG^*_v-F^*_vG^*_u)}$$

$$=\frac{\left(\frac{-14-8\sqrt{2}}{(1+\sqrt{2})^3}-\frac{2}{(1+\sqrt{2})^2}\frac{(1+\sqrt{2})^2\left(\frac{k\pi}{L}\right)^2+(2+3\sqrt{2})}{-(2+\sqrt{2})}\right)}{\frac{8}{1+\sqrt{2}}}$$

$$+\frac{\left(-\sqrt{2}+2\sqrt{2}\frac{(1+\sqrt{2})^2\left(\frac{k\pi}{L}\right)^2+(2+3\sqrt{2})}{-(2+\sqrt{2})}-\sqrt{2}\left(\frac{(1+\sqrt{2})^2\left(\frac{k\pi}{L}\right)^2+(2+3\sqrt{2})}{-(2+\sqrt{2})}\right)^2\right)\frac{-\sqrt{2}}{1+\sqrt{2}}}{\frac{8}{1+\sqrt{2}}} \tag{A.52}$$

$$\approx 0.1768\lambda+0.0536+0.25+0.5(1.7071\lambda+1.8284)+0.25(1.7071\lambda+1.8284)^2$$

$$=2.05356+2.59098\lambda+0.728548\lambda^2,$$

$$\int_0^L \Psi_3 dx = \frac{L[(F^*_{uu}+2F^*_{uv}P_k+F^*_{vv}P_k^2)G^*_u-(G^*_{uu}+2G^*_{uv}P_k+G^*_{vv}P_k^2)F^*_u]}{4(F^*_uG^*_v-F^*_vG^*_u)}$$

$$=\frac{\left(\frac{-14-8\sqrt{2}}{(1+\sqrt{2})^3}-\frac{2}{(1+\sqrt{2})^2}\frac{(1+\sqrt{2})^2\left(\frac{k\pi}{L}\right)^2+(2+3\sqrt{2})}{-(2+\sqrt{2})}\right)}{\frac{8}{1+\sqrt{2}}}$$

$$-\frac{\left(-\sqrt{2}+2\sqrt{2}\frac{(1+\sqrt{2})^2\left(\frac{k\pi}{L}\right)^2+(2+3\sqrt{2})}{-(2+\sqrt{2})}-\sqrt{2}\left(\frac{(1+\sqrt{2})^2\left(\frac{k\pi}{L}\right)^2+(2+3\sqrt{2})}{-(2+\sqrt{2})}\right)^2\right)\frac{-2-3\sqrt{2}}{(1+\sqrt{2})^2}}{\frac{8}{1+\sqrt{2}}}$$

$$\approx 0.1768\lambda+0.0536-0.4571+0.9142(1.7071\lambda+1.8284)-0.4571(1.7071\lambda+1.8284)^2$$

$$=-0.260083-1.11603\lambda-1.33208\lambda^2. \tag{A.53}$$

It means that

$$C_4$$

$$=-\frac{2L}{(k\pi)^2\phi^*}\left(C_{21}\int_0^L \Phi_4\cos\frac{k\pi x}{L}dx+C_{22}\int_0^L \Psi_4\cos\frac{k\pi x}{L}dx+C_{23}\int_0^L \Phi_3\cos\frac{2k\pi x}{L}dx\right.$$

$$\left.+C_{24}\int_0^L \Psi_3\cos\frac{2k\pi x}{L}dx+C_{25}\int_0^L \Phi_3 dx+C_{26}\int_0^L \Psi_3 dx+C_{27}\right)$$

$$\approx -\frac{1}{2.8284\lambda}\left[\left(-1.7071\lambda^2-3.5355\lambda-1.8284\right)\right.$$

$$
\begin{aligned}
&\times \frac{4.54499 + 34.1693\lambda + 57.8283\lambda^2 + 34.7568\lambda^3 + 2.2643\lambda^4 - 3.25055\lambda^5}{3.91576 + 5.62842\lambda - 15.2569\lambda^2 - 25.7064\lambda^3 - 12\lambda^4} \\
&+ (\lambda + 1)\frac{4.54499 + 34.1693\lambda + 57.8283\lambda^2 + 34.7568\lambda^3 + 2.2643\lambda^4 - 3.25055\lambda^5}{3.91576 + 5.62842\lambda - 15.2569\lambda^2 - 25.7064\lambda^3 - 12\lambda^4} \\
&+ (2.2376\lambda^3 + 6.8413\lambda^2 + 7.0713\lambda + 1.6568)\frac{-4.49383 - 20.4793\lambda - 20.0239\lambda^2 - 8.5355\lambda^3}{12\lambda^2 - 2.6274} \\
&+ (0.6035\lambda^2 + 2.4570\lambda + 3)\frac{22.2154 + 83.3482\lambda + 120.238\lambda^2 + 82.9109\lambda^3 + 23.3135\lambda^4}{12\lambda^2 - 2.6274} \\
&+ (-1.2071\lambda - 2)(2.05356 + 2.59098\lambda + 0.728548\lambda^2) \\
&+ (-0.6035\lambda^2 - 0.0428\lambda + 1)(-0.260083 - 1.11603\lambda - 1.33208\lambda^2) \\
&+ (1.3062\lambda^2 + 4.0633\lambda + 3.7286)\Big] \\
= &\frac{-94.4959 - 544.734\lambda - 1277.91\lambda^2 - 1533.76\lambda^3 - 1022.33\lambda^4 - 417.894\lambda^5 - 170.169\lambda^6 - 86.8835\lambda^7 - 23.7166\lambda^8}{-11.0753\lambda - 15.9194\lambda^2 + 43.1526\lambda^3 + 72.708\lambda^4 + 33.9408\lambda^5}.
\end{aligned}
\tag{A.54}
$$